# Sparse Decompositions for Ventricular and Atrial Activity Separation

**Javier Molinero Hernández**

ETSETB
Universitat Politècnica de Catalunya

Signal Processing Institute,
Ecole Polytechnique Fédérale de Lausanne (EPFL)

MASTER'S THESIS

Assistants: Dr. Òscar Divorra Escoda
Mr. Lorenzo Granai
Mr. Mathieu Lemay
Supervisors: Prof. Pierre Vandergheynst
Dr. Jean-Marc Vesin

February 2005 - August 2005

# Acknowledgements

En primer lugar quiero dar las gracias, de una forma especial, a mis padres, Juan José y Nati, por sus consejos y su apoyo incondicional. Gracias por todo lo que me habeis dado.

A mi hermano Ignacio, quiero agradecerle su dedicación siempre que lo he necesitado. Siempre has sido y serás mi referencia.

También quiero dar las gracias a Cristina por haber estado a mi lado en todo momento.

Of course, I would like to thank Dr. Òscar Divorra Escoda, Lorenzo Granai and Mathieu Lemay for guiding me during these months. I have learnt a lot with you. Thank you very much!

I am also grateful to Prof. Pierre Vandergheynst and Dr. Jean-Marc Vesin for giving me the possibility to do my master's thesis at EPFL.

Thanks also to all my colleagues and friends in LTS for sharing with me these unforgettable months: Bruno, David Bayona, David Marimón, Mireia, Roger, Thomas,...

Many thanks to my roommates: Álex, Catalina, Daniel, Eric and Martin. I will never forget this time with you!

To all of you, thanks a lot!

# Contents

# List of Figures

# List of Tables

# Abstract

Atrial fibrillation (AF) is the most common type of human arrhythmia. Beside its clinical description as absolute arrhythmia, its diagnosis has been assessed for years by visual inspection of the surface electrocardiogram (ECG). Due to the much higher amplitude of the electrical ventricular activity, the analysis of atrial fibrillation requires the previous isolation of the atrial activity component.

In this work, an approach to separate atrial and ventricular signal components, decomposing the signal over a redundant multi-component dictionary, is explored. This idea requires a careful dictionary design, taking into account the signal structures and characteristics. Being the dictionary overcomplete, more than one decomposition of a given signal is possible. However, we are interested in sparse solutions. A key point in this work is also, jointly with the dictionary design, to determine the appropriate analysis technique for the best performance of the ECG components separation. Greedy Algorithms, such as Matching Pursuit, or optimization methods, such as Basis Pursuit are studied. To improve our signal separation, the *a priori* knowledge we have from the ECG signals is also used. Finally, the solution proposed is tested over an ECG database.

# Chapter 1

# Introduction

## 1.1 Situation

Atrial Fibrillation (AF) is the most common sustained cardiac arrhythmia encountered by clinicians. Approximately 0.4%-1.0% of the general population suffers from this illness. This type of arrhythmia may appear anytime, but its prevalence tends to increase along with the age (up to 10% of the population older than 80 years has been diagnosed with AF). Usually, it affects men slightly more often than women [1]. With the increase of life expectancy, the prevalence is expected to double in the next 50 years.

Neither the natural history of AF nor its response to therapy are predictable enough by clinical and echocardiographic parameters. Nowadays, AF treatment (e.g. pacemaker implementation, choice of antiarrhythmic drugs or device therapy, curative ablation) may be viewed as a trial and error. Consequently, AF has in recent years been the subject of thorough investigations for a better understanding of its mechanism and improving its management. Several studies have focused on finding algorithms able to predict AF by the analysis of surface electrocardiographic records [2, 3, 4, 5, 6]. However, further studies are still necessary in order to select and time the appropriate therapy for the individual patient.

### 1.1.1 Atrial Fibrillation Fundamentals

First of all, before explaining the mechanism and characteristics of AF, we are going to start describing the heart and its mechanical and electrical activity.

Weighing about 300g and about the size of a large man's fist, the human heart is the central organ of the circulatory system. Like all mammalian hearts, it is composed of four chambers

(see Figure 1.1):

- the upper chambers, called the left and the right atria, which receive incoming blood from the lungs and the body, respectively;

- the lower chambers, called the left and the right ventricles, which pump blood out to the systemic and pulmonary circulatory branches, respectively.

Separating these upper and lower chambers, there are valves that passively open and close to direct the flow of blood. On the left part, the mitral valve separates the left atrium from the left ventricle and, on the right part, we have the tricuspid valve that separates the right atrium from the right ventricle.

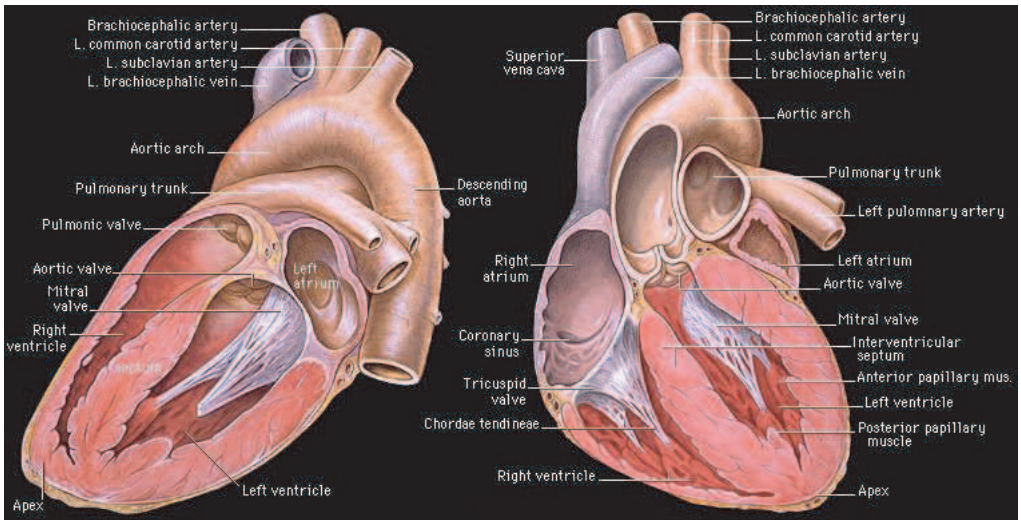


Figure 1.1: Heart anatomy

In order to pump, the heart must receive some kind of electrical stimulation which will provoke the contraction of the muscle. It starts at the top of the right atrium, in the sinoatrial node (SA node), and propagates simultaneously through the left atrium and down to the interface with the ventricles (see Figure 1.2). The atria and the ventricles are electrically insulated at this interface, except for a region known as the atrioventricular node (AV node). This last behaves like a delay line, retarding the activation signal about 100ms, that allows the atrial contraction to finish before the ventricular contraction begins.

Once the signal clears the AV node, it is carried along a specialized noncontractile conduction system, starting with the bundle of His (AV bundle), then proceeding very fast through a branching network, known as the Purkinje Fibers, to numerous sites along the inner chambers

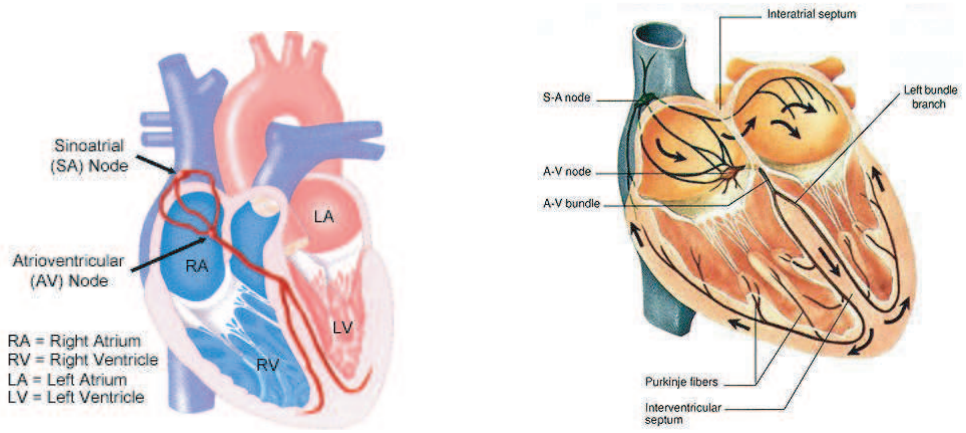


(a) (b)

Figure 1.2: Heart activation

of the ventricles. This cycle of electrical stimulation is known as normal sinus rhythm (NSR), which provokes a synchronization between the atria and the ventricles of the heart.

In these conditions, the pacemaker function of the heart is carried out by the SA node. The node cells initiate regular depolarization waves through atria and ventricles, 60-100 times per minute at rest. Doing some exercise, they can fire as fast as 180-200 times per minute.

On the other hand, the standard 12-lead Electrocardiogram (ECG) is a representation of the heart's electrical activity recorded from electrodes on the body surface. In Figure 1.3, we can see the evolution of the electrical activity during a healthy cardiac activation sequence by means of its ECG representation.

In this case, the depolarization of the atria manifests itself as the P wave, in the ECG, and the depolarization of the ventricles causes the feature known as the QRS complex. The subsequent repolarization of the ventricular mass produces the T wave and the cardiac cycle concludes. Figure 1.4 shows an schematic of the ECG waveform in NSR.

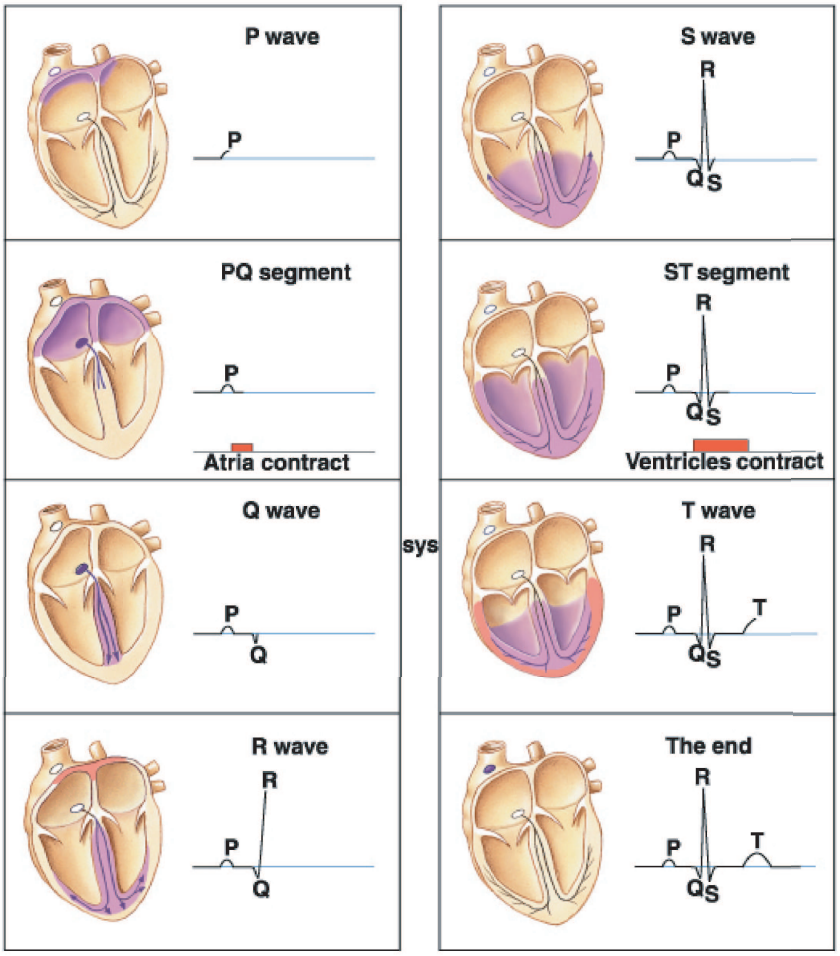


Figure 1.3: Cardiac activation sequence (left) and electrocardiogram signal (right)

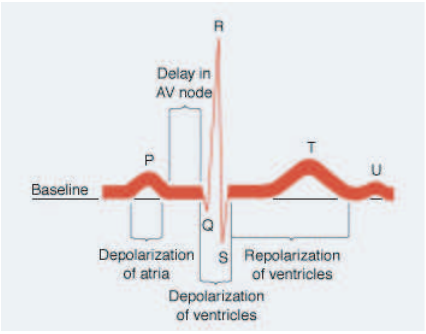


Figure 1.4: A schematic of the ECG exhibiting normal sinus rhythm

So far, we have slightly introduced the heart structure, its normal mechanical and electrical activity and the tool we have to measure this last, the ECG. Now it is time to explain in what consists the AF.

The atrial fibrillation is a supraventricular arrhythmia associated with the asynchronous

contraction of the atrial muscle fibres. Its underlying mechanism, involving self-sustained multiple reentrant waves, was discovered several decades ago. During AF, the SA node becomes the secondary pacemaker, being supplanted by the atrial myocardium, causing the upper chambers to quiver or to fibrillate at 350-600 times per minute (see Figure 1.5).

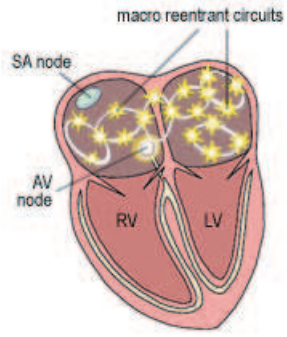


Figure 1.5: Heart in atrial fibrillation

On the ECG, AF is described by the replacement of consistent P waves by rapid oscillations or fibrillatory waves (F waves) that vary in size, shape, and timing, associated with an irregular, frequently rapid ventricular response, as we can observe in Figure 1.6.

(a) normal sinus rhythm

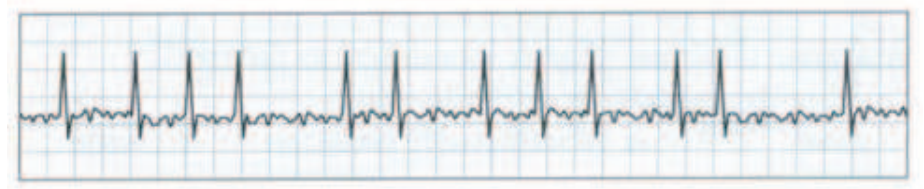

(b) atrial fibrillation

Figure 1.6: ECG signals in NSR and in AF

## 1.2 Context

The suitable analysis and characterization of atrial fibrillation from ECG recordings needs a previous isolation of the atrial activity component, due to the much higher amplitude of the electrical ventricular activity. Unfortunately, this low amplitude and the fact that both signals possess spectral distributions that notably overlap, making linear filtering solutions unsuccessful, hinder this operation.

Different methods have already been proposed to perform the isolation of the AA. One of them is the segmentation of the AA in the surface ECG. One identifies the QRST location (several QRS detection algorithms are available, see [7]) and extracts the segments where there are only atrial components, by time-oriented operations. This technique has one disadvantage, which is the loss of the information placed in the VA parts.

Another well-known technique is the QRST cancellation. The use of adaptive recurrent filtering and the average beat subtraction (ABS) are the principal methods proposed to this aim. This last approach takes advantage of the fact that AF is uncoupled to ventricular activity and, hence, the average beat is subtracted to generate a residual signal, which contains the fibrillation waveforms. M. Stridh and L. Sörnmo [2] proposed an ABS method, based on the correct spatiotemporal alignment of every complex prior to the cancellation. All these techniques rely on the assumption that the average beat can represent each one accurately. However, the morphology of the QRS often suffers slight changes caused by variations in the electrical axis of the heart. Therefore, this last effect is reflected in the QRS cancellation efficiency.

New techniques have appeared without relying on direct QRST elimination. These treat the problem as a *blind source separation* [8, 9, 10, 11, 12, 13, 14]. That is, when several signals have been mixed together and the objective is to find out what the original signals were. A classical example is the "cocktail party problem", where a number of people are talking simultaneously in a room (like a cocktail party), and one is trying to follow one of the discussions. The human brain can handle this sort of auditory source separation problem, but it is a very tricky problem in digital signal processing.

Blind source separation techniques are based on two important assumptions, which make possible the use of independent component analysis (ICA) methods. First, the assumption that there is bioelectrical independence between the atrial and ventricular regions. This allows to view the ECG signal as a weighted sum of atrial and ventricular source contributions, noise and artifacts. Second, the fact that the random distributions of the atrial and ventricular activities are less than 2 gaussians. These ICA-based methods put higher order statistical conditions

necessary to separate AA from VA [6, 15, 3, 4, 5]. Nevertheless, there are two problems with these methods. Firstly, the assumption that AA and VA are statistically independent is really dubious in AF; the electrical propagation in ventricles is still commanded by the AV node. Secondly, the sources must be point sources when ICA is used for source separation. This is not a realistic hypothesis owing to the fact that the electrical sources are strongly extended spatially in surface to be considered as point sources.

In this work, we deal with the problem as a *source separation* problem, but our methodology is really different from the techniques explained just above (ICA methods). Starting from the ECG, we aim at obtaining two different signals containing the isolated components of the ventricular activity and the atrial activity. This is a challenging problem since both components overlap in the frequency domain and are not orthogonal among them. For this purpose, more powerful approaches are needed.

During the past 10 years, many advances have been achieved by non-linear signal approximation methods, using overcomplete (non-orthogonal) sets of functions (dictionaries). In many applications, these techniques offer better performances than those based on orthonormal transforms. In this work, an approach to separate atrial and ventricular signal components decomposing the signal over a redundant Multi-component dictionary will be explored.

The first objective is to build a Multi-component dictionary [14, 16] composed of two sub-dictionaries, each one to approximate one signal. Its design must take into account the signal structures and characteristics. Being the dictionary overcomplete, more than one decomposition of a given signal are possible. However, we are interested in sparse solutions. Useful techniques for these decompositions are given, among others, by Greedy Algorithms such as Matching Pursuit or optimization methods such as Basis Pursuit. A key point in this work will be, jointly with the dictionary design, to determine the appropriate analysis technique for a best performance of the ECG components separation.

Moreover, the approach has to be evaluated by separating simulated ECG signals in atrial fibrillation (AF) and real ECG signals in AF. The first ones are more useful because we can compare the approximations with the signals used to create the simulated ECG signal.

Lastly, we apply a method which allows us to exploit the *a priori* knowledge we have about the ECG signals. This will improve the signal separation.

## 1.3 Organization

This report is structured as follows. In **Chapter 2**, the theoretical background involved in our approach is provided, jointly with a schematic description of our method. **Chapter 3** describes the full design of the dictionary. It contains firstly, the signals built to check our system and the different options we have tested until achieving the best dictionary. In **Chapter 4**, the results with the best dictionary found and the different analysis techniques are given. In **Chapter 5**, the decomposition is refined by exploiting the *a priori* knowledge about ECG signals. This allows to improve the VA and AA separation as shown by numerical examples. Finally, in **Chapter 6**, all relevant conclusions drawn from work carried out are summarized.

# Chapter 2

# Methodology Formalization

## 2.1 Theoretical Background

Over the last years, there has been an increase of interest looking for alternatives to traditional signal representations. Instead of representing signals as superpositions of sinusoids or wavelets, we now have available alternative dictionaries (union of functions called *atoms*), most of them overcomplete. This means that some elements of the dictionary have representations in terms of other elements, which causes the nonuniqueness of the decomposition of a signal $f$:

$$f = \sum_{\gamma \in \Gamma} b_\gamma g_\gamma, \tag{2.1}$$

and also of the approximate decomposition:

$$f = \sum_{k=1}^{m} b_{\gamma_k} g_{\gamma_k} + r_m f, \tag{2.2}$$

where:

- $\Gamma$ is the set of indexes, with cardinality $m$, of the basis functions used in the decomposition,
- $\Gamma \subset \Omega$, where $\Omega$ is the indexes set of all basis functions composing the dictionary $\mathcal{D} = \{g_\gamma : \gamma \in \Omega\}$,
- $b_\gamma \neq 0$, $\forall \gamma \in \Gamma$,
- We assume $f \equiv \mathbb{R}^N$ and $r_m f$ is the residue of the approximation with $m$ coefficients.

The nonuniqueness gives us the possibility of adaptation, i.e., of choosing among many representations the one which (most) fits our purposes.

On the other hand, the dictionaries $\mathcal{D}$ we are interested in are large and overcomplete. Usually, they are built by the union of $d \geq 2$ subdictionaries, each one particularly suitable for describing a certain feature of the signal:

$$\mathcal{D} = \bigcup_i \mathcal{D}_i, \quad \text{with} \quad 1 \leq i \leq d. \tag{2.3}$$

These bases sets are also called sometimes Multi-Component Dictionaries (MCD) [16]. Despite the complex problems to solve with these dictionaries, the reason why they are really appreciated is due to their capacity to bring in sparse representations and approximations. These dictionaries have a rich collection of shapes, in order to adapt better to the characteristics of the signals to represent/approximate.

With regard to the signal representations, we are really interested in these sparse decompositions. The criterion of sparseness has been studied for a long time and, in the last years, has become popular in the signal processing community [17, 18, 19]. This is because sparseness reflects the capacity of efficiently modelling and extracting the main structural components of a given signal.

The *sparsity* of a coefficient vector is the number of places where it equals zero. On the other hand, the *diversity* counts the number of places where the coefficient vector does not equal zero. The most common measure of diversity of a vector $c$ is its $l_0$ quasi-norm:

$$\|c\|_0 \triangleq |supp(c)|. \tag{2.4}$$

We use, here, $|\cdot|$ to indicate the cardinality. For any positive $p$, we can define a $p$-norm:

$$\|c\|_p \triangleq \left[\sum_{i\in\Omega} |c_i|^p\right]^{1/p}. \tag{2.5}$$

It is well known that the smallest $p$, for which Eq. (2.5) is convex, is 1.

### 2.1.1 Sparse Approximations

The exact representation of a signal $f$ on a dictionary of basis functions $\mathcal{D}$ is defined by:

$$f = D\mathbf{b}, \tag{2.6}$$

where $D$ is the synthesis matrix associated to the dictionary $\mathcal{D}$, i.e. each column of $D$ corresponds to an atom in the dictionary and $\mathbf{b} \in \mathbb{R}^{\Omega}$ is the vector of coefficients. Therefore, the sparsest exact representation of $f$ on $\mathcal{D}$ is the one with the smallest support:

$$\arg\min_{\mathbf{b}} \|\mathbf{b}\|_0 \quad \text{s.t.} \quad f = D\mathbf{b}. \tag{2.7}$$

On the other hand, when we tolerate some error between the reconstructed signal $\hat{f} = D\mathbf{b}$ and the original one $f$, the representation turns into an approximation. In such a case, the problem of finding the sparsest approximation of $f$ with a maximum of $m$ terms, such that the error norm is minimized, can be stated as:

$$\arg\min_{\mathbf{b}} \|f - D\mathbf{b}\|_2^2 \quad \text{s.t.} \quad \|\mathbf{b}\|_0 \leq m. \tag{2.8}$$

### 2.1.2 Overcomplete Dictionaries

Assuming that a non-redundant dictionary, with synthesis matrix $A$ (i.e. $D = A$ in Eq. (2.6)), is used to represent $f$, then:

$$f = A\mathbf{b}, \tag{2.9}$$

where $A$ is a $n \times n$ matrix and their columns are linearly independent. This defines a determined system and, therefore, we find the unique representation as:

$$\mathbf{b} = A^{-1}f. \tag{2.10}$$

When the atoms are mutually orthonormal, then $A^{-1} = A^T$ and the decomposition becomes very simple.

On the other hand, using redundant (overcomplete) dictionaries, the synthesis matrix is not a square matrix any more. Then, for a given synthesis matrix $B$ (i.e. $D = B$ in Eq. (2.6)),

$$f = B\mathbf{b}, \tag{2.11}$$

where $B$ is a $n \times d$ matrix with $n < d$.

In such a case, we have an under-determined system with infinite number of solutions. Consequently, in general it turns the problems stated in Eq. (2.7) and (2.8) into NP-Hard ones, implying that their complexity grows exponentially with the number of columns in the dictionary. Several alternative approaches have been proposed, in order to make computationally feasible the retrieval of a solution for **b**. In many cases, this solution may not be the sparsest one, however.

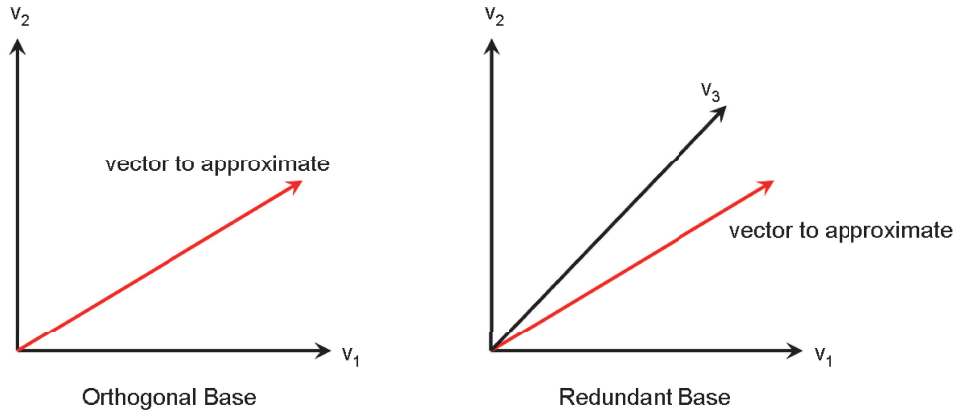


Figure 2.1: Approximation error for a vector in the orthogonal (left) and redundant (right) dictionaries

Figure 2.1 shows a graphical example where the approximation of a vector, by means of a unique vector from the basis, is searched. In the orthogonal case (left), the best approximation is obtained by projecting the vector onto $v_1$. In the redundant case (right), a better approximation is achieved by projecting the vector onto $v_3$.

In general, we can prove that for any vector belonging to $\mathbb{R}^2$, the approximation error obtained by a one term approximation is always equal or lower on the redundant base than in the orthogonal one.

### 2.1.3 Greedy Algorithms

#### Matching Pursuit

Mallat and Zhang [20, 21] introduced Matching Pursuit (MP) as a *greedy algorithm that decomposes any signal into a linear expansion of waveforms that are selected from a redundant dictionary of functions*. This expansion of waveforms refers to an iteratively extraction of vectors, one by one, from the dictionary, while optimizing the signal approximation (in terms of

energy) at each step. Although a matching pursuit is non-linear, it maintains an energy conservation that guarantees its convergence.

Let us consider $\mathcal{D} = \{g_\gamma\}_{\gamma\in\Omega}$ a dictionary where atoms belong to $\mathbb{R}^N$, and with $N$ linearly independent vectors, having a unit $\ell_2$-norm. Let $r_k f$ be the residual of a $k$ term approximation of a given signal $f \in \mathbb{R}^N$. MP is an iterative algorithm that sub-decomposes the residue $r_k f$ by projecting it on a vector of $\mathcal{D}$ that matches $r_k f$ at best.

If we consider the initial residual as $r_0 f = f$, at the first iteration Matching Pursuit begins by projecting it on a vector $g_{\gamma_0} \in \mathcal{D}$ and computing the residue $r_1 f$:

$$f = r_0 f = \langle f, g_{\gamma_0}\rangle g_{\gamma_0} + r_1 f. \tag{2.12}$$

As $r_1 f$ is orthogonal to $g_{\gamma_0}$, the module of $f$ will be:

$$\|r_0 f\|_2^2 = |\langle r_0 f, g_{\gamma_0}\rangle|^2 + \|r_1 f\|_2^2. \tag{2.13}$$

Since $\|r_1 f\|_2$ is the term that must be minimized,

$$\|r_1 f\|_2^2 = \|r_0 f\|_2^2 - |\langle r_0 f, g_{\gamma_0}\rangle|^2, \tag{2.14}$$

the atom $g_{\gamma_0} \in \mathcal{D}$ to be selected is the one which maximizes $|\langle r_0 f, g_{\gamma_0}\rangle|$, or, generalizing, $|\langle r_k f, g_{\gamma_k}\rangle|$. This is,

$$|\langle r_k f, g_{\gamma_k}\rangle| = \sup_{\gamma\in\Omega} |\langle r_k f, g_\gamma\rangle|. \tag{2.15}$$

From Eq. (2.12), we can easily see by induction that the $K$ term decomposition of $f$ is given by:

$$f = \sum_{k=0}^{K-1} \langle r_k f, g_{\gamma_k}\rangle g_{\gamma_k} + r_K f. \tag{2.16}$$

Similarly, we can also deduce from 2.13 that the $\ell_2$-norm of the signal $f$ is:

$$\|f\|^2 = \sum_{k=0}^{K-1} |\langle r_k f, g_{\gamma_k}\rangle|^2 + \|r_K f\|^2, \tag{2.17}$$

where $\|r_K f\|$ converges exponentially to 0 when $K$ tends to infinity and the number of signal dimensions is finite [20].

#### Orthogonal Matching Pursuit

The approximations of a matching pursuit can be improved by orthogonalizing the directions of projection, with a Gram-Schmidt procedure. This motivated a refinement of MP called Orthogonal Matching Pursuit (OMP) [22], a recursive algorithm to compute representations of functions with respect to nonorthogonal and possibly overcomplete dictionaries. In the latter, for every newly selected atom by the MP rule, all expansion coefficients are recalculated such that the approximation error becomes orthogonal to all the selected atoms previously (in MP, however, only the last selected atom is orthogonal to the residual).

The resulting algorithm converges with a finite number of iterations, unlike the case for a non-orthogonal pursuit. Unluckily, the important computational cost of the orthogonalization is the price to be paid.

### 2.1.4 Basis Pursuit

#### Basis Pursuit

Basis Pursuit (BP) is a principle for decomposing a signal into an optimal superposition of dictionary atoms. This paradigm was proposed by Chen, Donoho and Saunders [23] to minimize the $\ell_1$ norm of the coefficients vector, in order to avoid the *non convexity* and hard solution of Eq. (2.7):

$$\arg\min_{\mathbf{b}} \|\mathbf{b}\|_1 \;\; s.t. \;\; f = D\mathbf{b}. \tag{2.18}$$

In some cases, the solution to Eq. 2.18 will coincide with that of Eq. (2.7). The problem formulated in Eq. (2.18) can be solved by polynomial-time linear programming approaches.

#### Basis Pursuit Denoising

To adapt BP to the case of noisy data [23], a new principle appeared, called Basis Pursuit Denoisign (BPDN), which refers to the solution of:

$$\arg\min_{\mathbf{b}} \frac{1}{2}\|f - D\mathbf{b}\|_2^2 + \gamma\|\mathbf{b}\|_1, \tag{2.19}$$

where $\gamma$ is a positive real value employed as a threshold (to limit the maximum $\ell_1$ norm of $\mathbf{b}$).

BPDN can be solved using classical Quadratic Programming methods and it turned up to adapt BP to the approximation case.

### 2.1.5 Dictionary Analysis

The most fundamental measure associated with a dictionary $\mathcal{D}$ is the *coherence parameter* $\mu$ [17, 24, 25]. Assuming that the columns of $\mathcal{D} \in \mathbb{R}^{n\times d}$, where $d \geq n$, are all normalized, i.e. $\|d_k\|_2 = 1$, the coherence measure ($\mu$) equals the maximum absolute inner product between two distinct columns in the dictionary:

$$\mu \triangleq \max_{1\leq k,j\leq d,\ k\neq j} \left|d_k^T d_j\right|. \tag{2.20}$$

Roughly speaking, this quantity measures the maximum similarity between two vectors in the dictionary. Coherence is a blunt instrument because it only reflects the highest correlation. Still, it is easy to calculate and it captures the behaviour of uniform dictionaries.

Obviously, every orthonormal basis has coherence $\mu = 0$, indicating total independence between the dictionary's atoms. For overcomplete dictionaries with $d \geq n$, $\mu$ is usually non-zero, and we desire the smallest possible quantity so as to get close to the ideal independence.

As it is presented in [17]: *Orthogonal Matching Pursuit and Basis Pursuit both recover every superposition of m atoms from $\mathcal{D}$ whenever one of the following conditions is satisfied:*

$$m < \frac{1}{2}\left(\mu^{-1} + 1\right) \qquad \textit{or, more generally,} \tag{2.21}$$

$$\mu_1(m) < \frac{1}{2}, \tag{2.22}$$

where $\mu_1(m)$ is the cumulative coherence measure and $\Gamma \subset \Omega$ has cardinality $m$:

$$\mu_1(m) \triangleq \max_{|\Gamma|=m} \max_{i\in\Omega\setminus\Gamma} \sum_{\lambda\in\Gamma} \left|\langle g_i, g_\lambda\rangle\right|. \tag{2.23}$$

## 2.2 Approach investigated

In this section, the approach investigated in the project is presented. Our methodology is based on the block diagram shown in Figure 2.4.

Firstly, we must start designing a Multi-component dictionary (see Eq. (2.3)), built by the union of two sub-dictionaries. The first subdictionary would take care of the VA representation, whereas the second of the AA representation, as it shows the next figure:

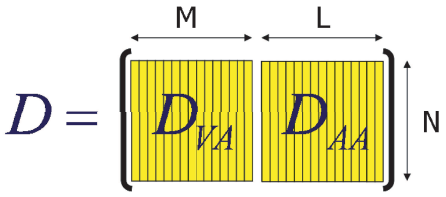


Figure 2.2: Multi-component dictionary structure to separate VA and AA signals

Subsequently, we are going to use an analysis algorithm to obtain a sparse approximation of our original signal from the ECG, with $m$ coefficients. But, there are several and we must previously check which one can better manage with our problem. The studied ones will be Orthogonal Matching Pursuit (OMP) and Basis Pursuit Denoising (BPDN). However, unless we say the contrary, all our tests will be realized by using an OMP approach.

Of course, both dictionaries must have a low correlation to achieve a successful separation of the VA and AA signals. That means, the basis functions to represent one signal should be as incorrelated as possible, with the basis functions to represent the other signal. If the dictionaries have a high correlation, the analysis algorithm could take, with more probability, atoms from the wrong dictionary to approximate some part of the signal, that should be represented by the other dictionary.

As a result of applying these analysis techniques, a coefficients vector will be obtained with the same number of elements as the dictionary size:

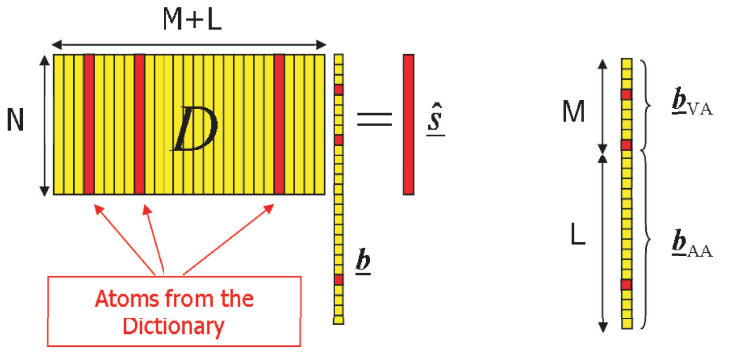


Figure 2.3: Sparse approximation technique with the MCD (left) and structure of the coefficients vector (right)

where $\mathbf{b}$ will only contain $m$ non-zero elements to approximate the original signal.

To carry out the desired separation, we must finally do a projection step over the VA and AA dictionary of the two parts which forms the $\mathbf{b}$ vector:

$$f_{VA} \simeq D_{VA} \cdot b_{VA}$$
$$f_{AA} \simeq D_{AA} \cdot b_{AA} \tag{2.24}$$

where $\mathbf{b}_{VA}$ is the part of the coefficients vector which should contain the sparse approximation of the VA signal and $\mathbf{b}_{AA}$ is the part that should contain the sparse approximation of the AA signal.

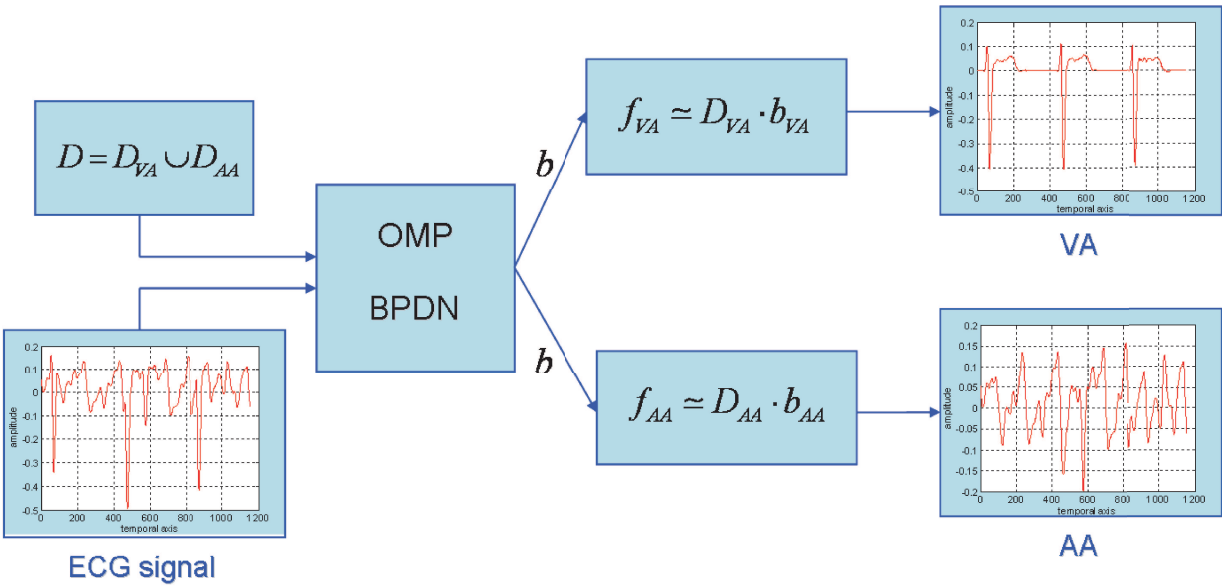


Figure 2.4: Schematic description of the followed methodology

# Chapter 3

# Dictionary design

## 3.1 Introduction

An essential requirement in our aim is to choose two appropriate dictionaries, one for the ventricular activity representation, and the other for the atrial activity representation. The union of both will set up a Multi-component dictionary (MCD) [16]:

$$\mathcal{D} = \mathcal{D}_{VA} \cup \mathcal{D}_{AA}, \tag{3.1}$$

which will be used with the analysis algorithms (OMP or BP) to extract a sparse approximation of the original signal.

The reason of using this kind of dictionary is because our ECG signals ($f_{ECG}$) are composed of the addition of two signals:

$$f_{ECG} = f_{VA} + f_{AA}, \tag{3.2}$$

where $f_{VA}$ and $f_{AA}$ are the ventricular and atrial activity signals, respectively.

Thus, we can think about building a simulated ECG signal as a result of adding two signals, which are going to behave as the originals (see Eq. (3.3), where $\hat{}$ indicates approximation). For this purpose, we are going to use ECG signals of a patient in sinus rhythm (as VA) and simulated AA in atrial fibrillation (see [26, 27, 28, 29, 30]).

$$\hat{f}_{ECG} = \hat{f}_{VA} + \hat{f}_{AA} \tag{3.3}$$

## 3.2 Ventricular Activity and Atrial Activity Signals

The means at our disposal to create the VA and AA signals are the following:

- 12 standard ECG-signals of simulated atrial activity in atrial fibrillation. Sampling frequency: 1KHz,
- 12 standard ECG-signals of a patient in sinus rhythm. Sampling frequency: 500Hz,
- The average position of the Q,R,S and T waves and the atrial activity intervals (from $AA_1$ to $AA_2$) for the 12 ECG-signals from the patient. These last are the points between the QRST complexes where there is only AA (see Figure 3.1).

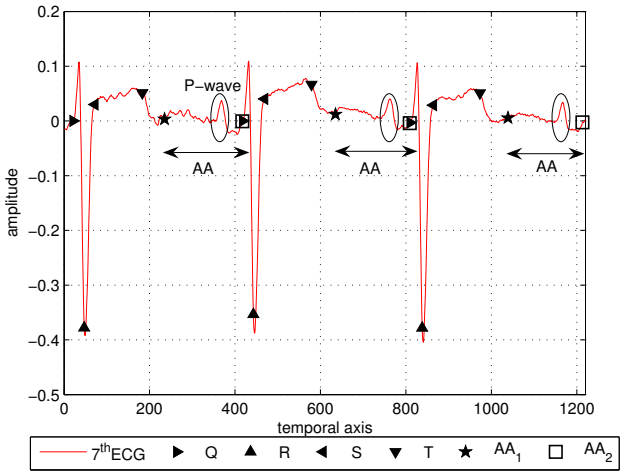


Figure 3.1: Segment of a patient in sinus rhythm (lead V1). It can be observed the P-waves inside the AA intervals

We also have some information about the structure of the VA signal, in sinus rhythm, and the AA signal, in atrial fibrillation. For the former, we know its electrical representation in terms of the QRST complex. Its frequencies interval is usually between 1 and 3 Hz. The second is represented in the ECG by numerous, irregularly spaced small deflections of varying configuration (F-waves), instead of the P-waves, which are the AA representation in sinus rhythm. For this case, the frequencies interval of the signal is placed between 3 and 10 Hz [31].

With all these, we want to get a ventricular activity signal (VA) and an atrial activity signal (AA), each one without any information from the other. Thus, we will be able to calculate the signal separation SNR (see Eq. (3.4), where $s$ is the original signal and $\hat{s}$ the approximation) and to give a visual approval of the obtained approximation.

$$SNR(dB) = 10\log\left(\frac{\|s\|_2^2}{\|s-\hat{s}\|_2^2}\right). \tag{3.4}$$

### 3.2.1 Ventricular Activity Signal

To get a ventricular activity signal, we have jointly worked with the ECG-lead segments of the patient in sinus rhythm and the $\mathrm{AA}_i (i = 1, 2)$ positions, as we can see in Figure 3.1.

The proposed model to obtain this signal is shown in the next figure:

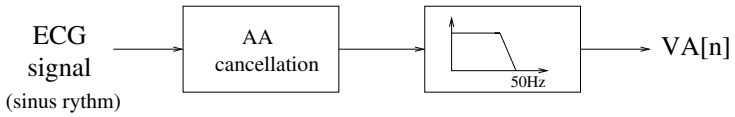


Figure 3.2: Ventricular activity model to obtain a ventricular activity signal from an ECG signal in sinus rhythm

To avoid AA in our VA signal, we have put zero value from $\mathrm{AA}_1$ to $\mathrm{AA}_2$ because there is only AA. Finally, we have introduced a low-pass filter (LPF) at 50Hz to eliminate the noise (see Figure 3.3).

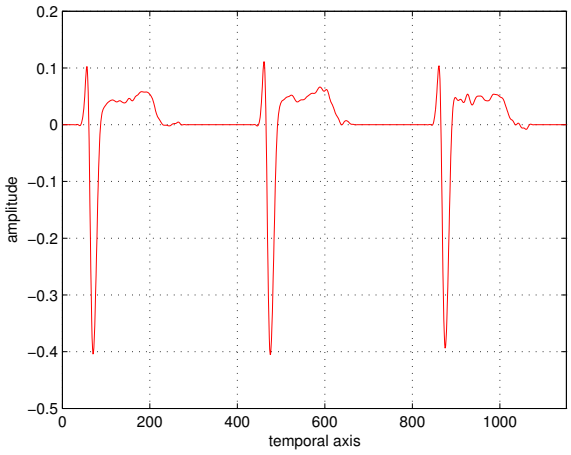


Figure 3.3: Simulated ventricular activity signal to create a simulated ECG signal in AF

### 3.2.2 Atrial Activity Signal

For the atrial activity signal, we have taken the simulated AA in atrial fibrillation [26, 27, 28, 29, 30] and we have also applied a LPF at 50Hz to eliminate the noise (see model in Figure 3.4). Because of simulated AA has been generated with a sampling frequency of 1KHz, we have

downsampled by a factor 2 to get both signals, VA and AA, with the same sampling frequency (500Hz).

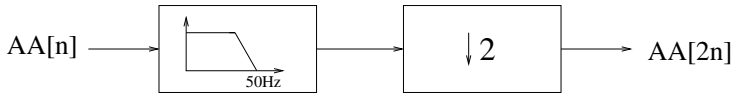


Figure 3.4: Atrial activity model to obtain an atrial activity signal in AF from simulated atrial fibrillation

In Figure 3.5 we can observe the resulting AA segment. Lastly, in Figure 3.6, the resulting simulated ECG signal in AF is shown.

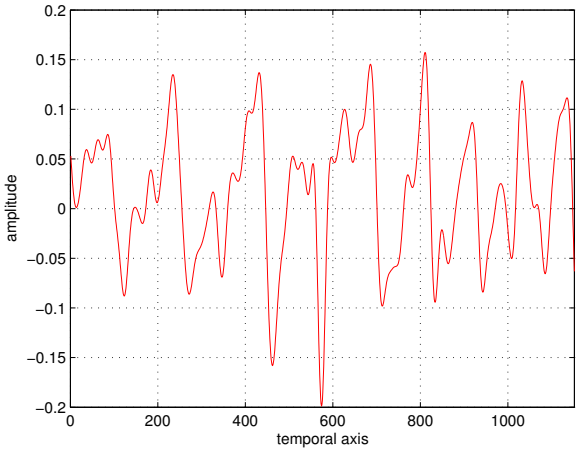


Figure 3.5: Simulated atrial activity signal in AF to create a simulated ECG signal in AF

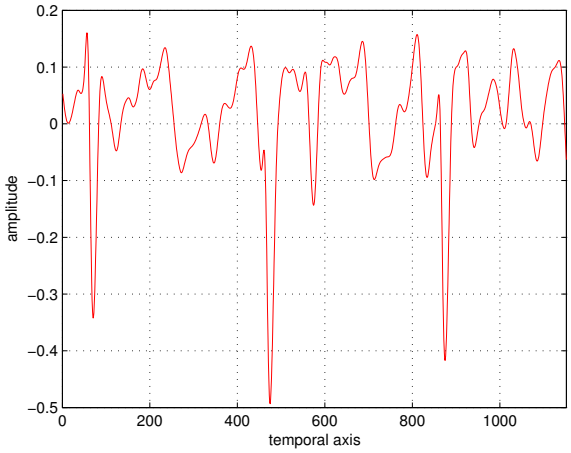


Figure 3.6: Simulated ECG signal in atrial fibrillation

## 3.3 Gaussian dictionary for VA Representation

The aim of this section is to design a dictionary to represent the ventricular activity signal. The reason for creating first the VA dictionary is that, at first sight, it seems easier to find a dictionary to approximate the VA signal than a dictionary to approximate the AA signal. This is because, in this signal, we are able to find some characteristics that can help us to find some suitable basis functions. To the contrary, in the AA signal this is very difficult to do.

According to the signal shape of VA, we have decided to check Gaussian functions to see how they perform approximating it. The results prove that, up to some degree, they are a good choice.

### 3.3.1 Gaussian Function

The VA dictionary is composed by a family of gaussian functions:

$$g_\gamma[n] = Ke^{\left(-\frac{1}{2}\left(\frac{n-p}{s}\right)^2\right)} \qquad (\gamma = (p, s)). \tag{3.5}$$

where $s$ is the scale factor, $p$ the temporal shift and $K$ a constant.

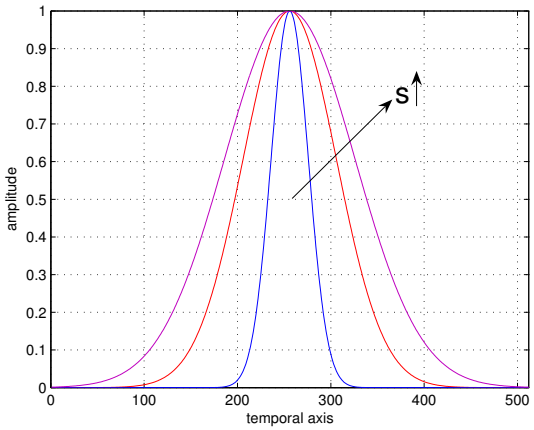


Figure 3.7: Gaussian functions with different scales

Note that a scale factor $s$ means that we have $s$ samples from the Gaussian maximum amplitude until this has fallen by $\sqrt{e}$ :

$$g_\gamma[p+s] = Ke^{\left(-\frac{1}{2}\left(\frac{p+s-p}{s}\right)^2\right)} = \frac{K}{\sqrt{e}} = 0.6065K \qquad g_\gamma[p] = K \tag{3.6}$$

### 3.3.2 Gaussian Parameters Choice

Let us start to study a VA segment to find the best parameters in our Gaussian dictionary to represent as well as possible the VA shape.

To represent the QRST complex, we have decided to approximate each of the 4 parts in which is made up, only with a Gaussian function. Even though we have seen in Figure 3.3 that the S wave is hidden behind the T-wave, this is an example and the S wave will surely be present in other cases.

The only parameter we must fix in Eq. (3.5) is the best scale to approximate the Q,R,S and T-wave, because we have put a temporal resolution of 1 sample, owing to the fact that the Q,R and S waves are very short in time.

To determine the necessary scales, we have taken the ventricular activity signal generated (lead V1) and we have studied 3 QRST complexes. We know that it is not enough to characterize a general QRST complex, because we should have done a thorough study for different leads and for different patients. Nevertheless, we have considered that for an initial contact with the problem and to design subsequently the AA dictionary, we have enough with the information obtained from one patient.

Table 3.1 illustrates the selected scales for Gaussian dictionary to approximate the ventricular activity segment we have chosen (lead V1).

| Wave | Scales |
|---|---|
| Q | 5 |
| R | 6,8 |
| T | 51,52 |

Table 3.1: Scales to represent the chosen segment of the ventricular activity signal (lead V1)

Notice that, in the previous table, there is no scale for the S wave because, as we have previously explained, in the present case it is hidden behind the T wave. However, we know that in other leads it might appear but, fortunately, with the same range of scales as the Q and R waves. So, it will be possible to approximate it too with the ones in Table 3.1.

The suggested idea of representing each peak with only one gaussian succeeds in approximating quite well the QRST complex using only three gaussians, as we can see in Figure 3.8.

However, we cannot put only these values to represent a ventricular activity segment, because they change depending on the ECG-lead and also the patient. Therefore, we must introduce a range of values, around the previous, to try to approximate all the leads as much as

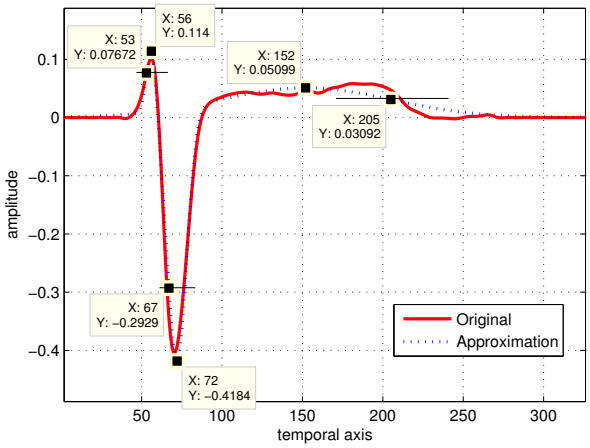


Figure 3.8: QRST(lead V1) approximation with only 3 gaussians (OMP)

possible.

After doing several tests, the appropriate set of scales to represent QRST complexes is: 4, 5, 6, 7, 51, 52, 53, 54.

### 3.3.3 VA Signal Representation

In Figure 3.9 we can see how our Gaussian dictionary is able to approximate 3 QRST complexes with only 9 gaussians. Finally, we want to obtain this approximation in the VA and AA separation.

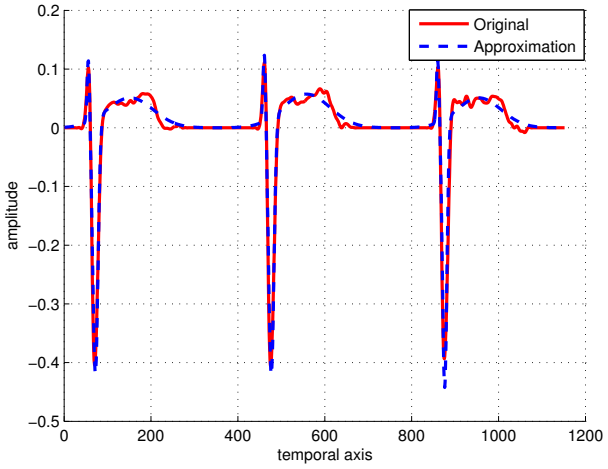


Figure 3.9: Ventricular activity approximation (lead V1) with 9 coefficients (OMP)

Figure 3.10 shows the recovery capacity of the VA dictionary. We have represented a VA

segment with 50 coefficients to give us a hint of how our dictionary is able to obtain a very accurate approximation. As we can observe, we are able to represent it practically with only 50 basis functions.

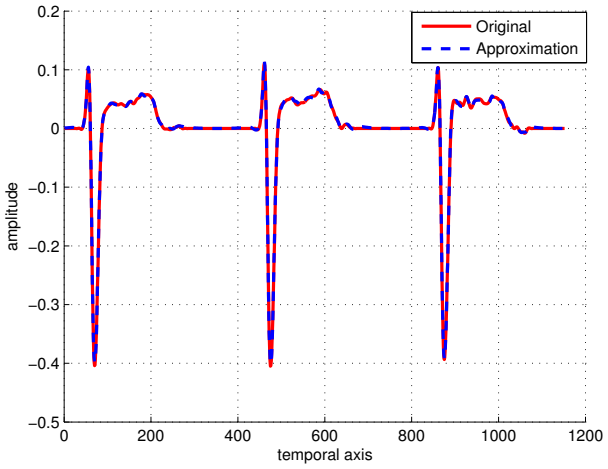


Figure 3.10: Ventricular activity approximation (lead V1) with 50 coefficients (OMP)

### 3.3.4 Discussion

The idea of approximating each wave with a gaussian function has achieved encouraging results. We can reach two objectives at the same time: a good approximation of the signal and the use of very few coefficients. As we have previously mentioned, this is really interesting to search sparse approximations to achieve good signals separation.

In addition, flexibility appears as the most important property of this dictionary. The *scale* makes it suitable for different leads and patients.

However, as we will see in Section 3.6, we can still refine it to achieve a better VA and AA separation.

## 3.4 Cosine Packet Dictionary for AA Representation

In this section we design a dictionary to approximate the atrial activity. At first sight, is seems clear that we will need some sort of sinusoidal functions to approximate it.

Hence we have studied meticulously the Cosine Packet(CP) dictionary [32]. It has some interesting properties which can give us a good approximation. These ones are the different scales and frequencies present in the dictionary, which we can tone with only one parameter.

### 3.4.1 Cosine Packet Function

The cosine packet dictionary is an overcomplete system, which was developed to meet the computational demands of digital signal processing. It is composed of the standard orthogonal Fourier dictionary and a variety of Gabor-like elements: sinusoids of various frequencies weighted by windows of various widths and locations.

We are going to use it from a computing environment called Atomizer [33]. This CP dictionary depends on two parameters: the length $N$ of the signal to be approximated and the *depth of finest time splitting*. This last controls the levels of decomposition (see Figure 3.12).

The functions we have in a time splitting of the Cosine Packet dictionary are:

$$X(k) = \sqrt{\frac{2}{M}} \sum_{n=0}^{M-1} x(n) \cdot cos\left(\frac{\pi}{M}\left(k-\frac{1}{2}\right)\left(n-\frac{1}{2}\right)\right) \qquad k = 1, ..., M \qquad M = N, \frac{N}{2}, \frac{N}{4}, ..., \tag{3.7}$$

where $x(n)$ is a smooth window, or bell, $M$ is the length of the time splitting and $k$ is the frequency index. Each function has a different frequency, which depends on $M$:

$$f(k) = \frac{1}{2M}\left(k-\frac{1}{2}\right) \qquad k = 1, ..., M. \tag{3.8}$$

In the next figure we have an example of CP function:

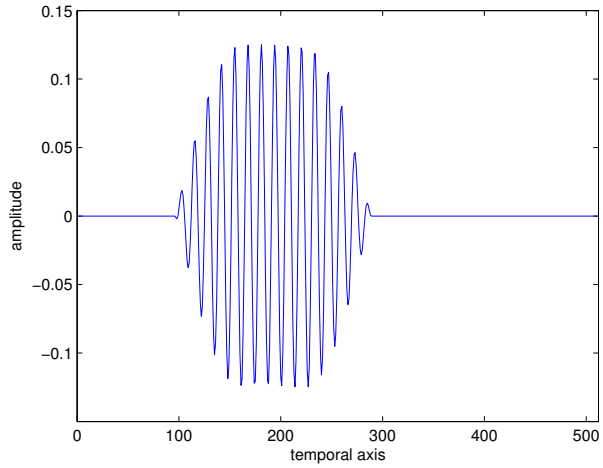


Figure 3.11: Cosine packet function

Figures 3.12 and 3.13 illustrate the AA dictionary structure:

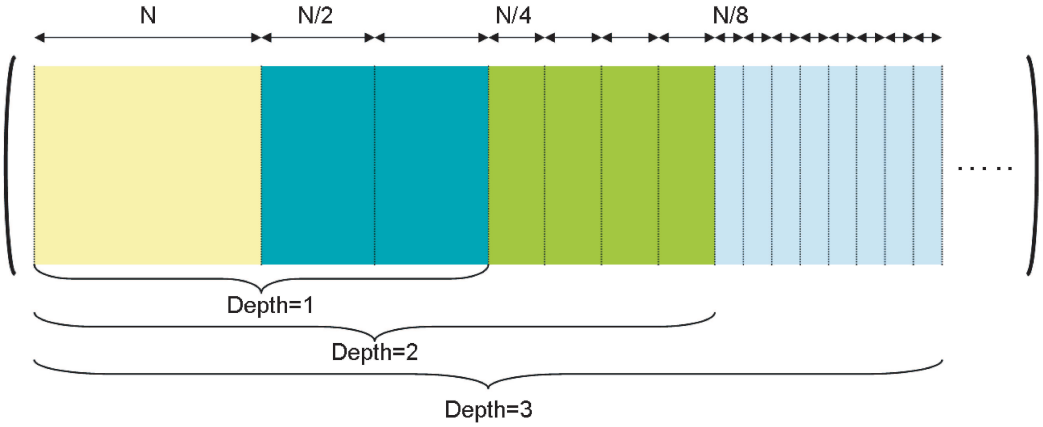


Figure 3.12: Cosine packet dictionary structure

In the first N columns, we have the first block of the CP dictionary. There, we can find basis functions with length N and from the first until the $N^{th}$ function the frequency changes according to Eq.(3.8).

In the next N columns, we have the second block. Inside it, there are two parts, the left part is made of basis functions with length $\frac{N}{2}$ and centred at $\frac{N}{4}$. The right part has functions with the same length as the others of this block, but now centred at $\frac{3N}{4}$.

Both blocks fall to *depth*=1. As the *depth* grows the levels of decomposition also increase.

The graphical representation of the dictionary matrix can be seen in Figure 3.13, where the columns are the waveforms that compose the dictionary (for N=128, depth=3).

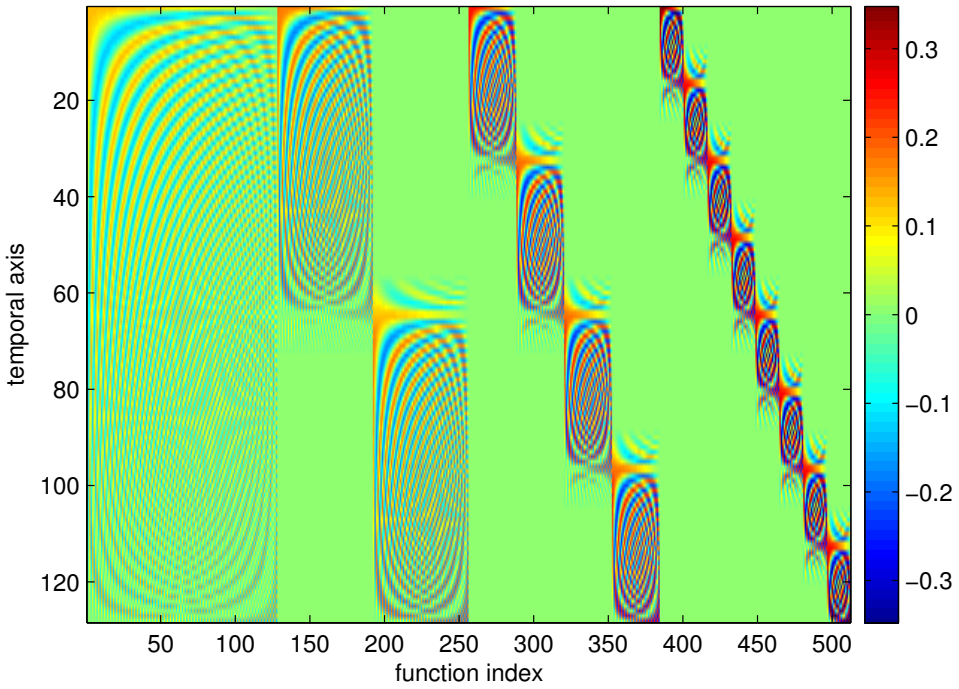


Figure 3.13: Graphical representation of a dictionary formed by CP functions, that have N=128 samples, and with depth=3. The number of base functions is N*(depth+1)=512

### 3.4.2 Correlation between Dictionaries

As we have previously mentioned, an essential requirement in our objective is to choose two appropriate dictionaries, one for the VA representation and the other for the AA representation. But we must guarantee that they will be as uncorrelated as possible to achieve a good separation between VA and AA. Otherwise, if the dictionaries contain some basis functions highly correlated, OMP and BP may select wrongly some atoms. It means that the analysis algorithm may use some basis functions from one dictionary to represent some parts of the signal, which should be represented by the other dictionary. This may lead to a wrong VA and AA separation. Therefore, the first thing that must be checked is what happens with the correlation between VA and AA dictionary, for different *depth* values of the CP dictionary.

For our research into CP dictionary, we are going to look at only *depth*=1,...,5, because higher values would bring about having functions with the same scale as Gaussian functions to represent VA and, consequently, we would have unwanted high correlation. Moreover, they

would not be very useful to represent AA features.

We must reflect on the correlation maximum that we will tolerate to avoid wrong choice of the atoms by the analysis algorithm (OMP, BP). As we have seen in Section 2.1, we can consider the maximum correlation as the maximum *coherence parameter* $\mu$ (see Eq. (2.20) and (2.21)) permitted in a redundant dictionary to achieve the optimal approximation, but this condition is highly pessimistic and it only allows a value of $\mu$ too small.

So, we have to do another analysis to decide which limit to use. Our methodology is based on studying the evolution of the VA and AA SNR, doing the signal separation (shown in Section 2.2), with respect to the maximum correlation permitted between basis functions of both dictionaries (see Figure 3.15). For this purpose, we have joined the Gaussian (studied in the previous section) and the CP dictionary to represent:

- VA (lead V1, sinus rhythm) + AA (lead V1, simulated, in AF)
- VA (lead Vr, sinus rhythm) + AA (lead Vr, simulated, in AF)

both signals try to approximate two real ECG-leads, the V1 and the Vr leads, when the patient has atrial fibrillation (see Figure 3.14). From now on, we will use the name of lead V1 and lead Vr to refer to the signals we have created to approximate the reality.

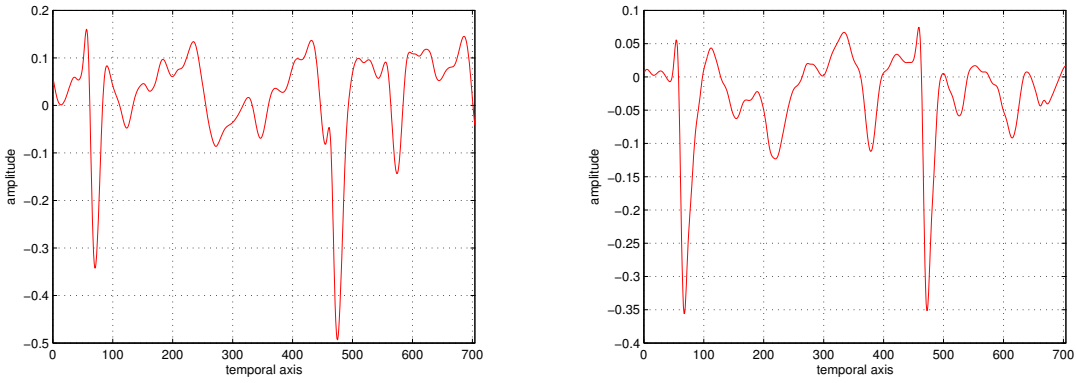


(a) lead V1 (b) lead Vr

Figure 3.14: Signals to approximate the leads V1 and Vr in atrial fibrillation

Once we have obtained the VA and AA SNR (see Figure 3.15), we can assert that the limit value must take place when the SNR starts to misbehave, that is, starting to decrease when it should increase as the number of coefficients does it. From this moment the effects of the dictionaries likeness start turning up.

Nevertheless, we cannot fix a limit for all the *depth* because, as we have checked, it changes depending on the dictionary we use. In Table 3.2 we have given the maximum correlations for all *depth* we can use, depending on the signal, and a general value to apply for all ECG-leads.

| | Limit lead V1 | Limit lead Vr | General limit |
|---|---|---|---|
| *depth*=1 | 0.4-0.65 | 0.4 | 0.4 |
| *depth*=2 | 0.6 | 0.4-0.55 | 0.5 |
| *depth*=3 | 0.5-0.65 | 0.4 | 0.5 |
| *depth*=4 | 0.4-0.5 | 0.4 | 0.5 |
| *depth*=5 | 0.5-0.7 | 0.4-0.8 | 0.6 |

Table 3.2: Maximum correlations for each *depth*

Once we know which are the maximum correlation values that we can allow between both dictionaries, we must remove the CP functions that cause higher correlation values than these maximums.

Intuitively, we can think that the problem falls on the first basis functions of each time splitting. The reason is because there, the frequencies are nearly 0 and the bell window can be really similar to the gaussians that are present in the VA dictionary. Therefore, we could think

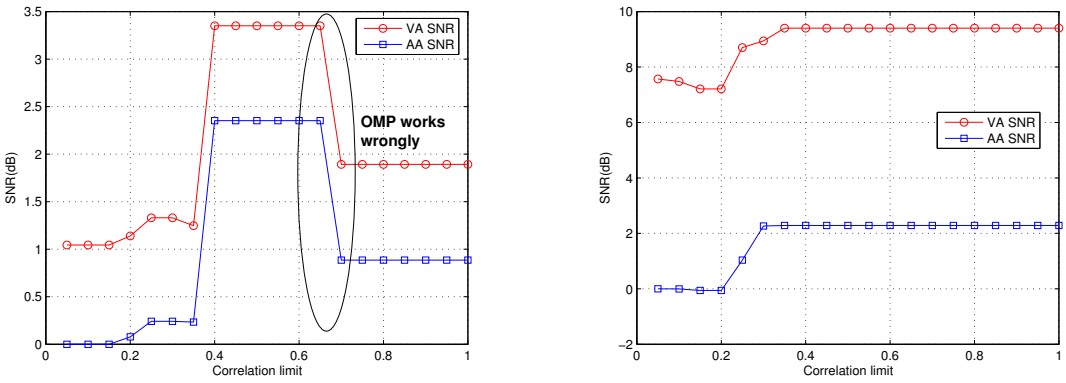


(a) lead V1/*depth*=1 (b) lead Vr/*depth*=1

Figure 3.15: Evolution of the VA and AA SNR doing the signal separation with respect to the limit of maximum allowed correlation for *depth*=1 and for the leads V1 and Vr in atrial fibrillation (OMP, 50 coefficients). The traces are increasing until OMP starts to work wrongly and then they misbehave

that, if we cut some of the first frequencies of each time splitting, our AA dictionary would probably become sufficiently uncorrelated to avoid wrong behaviour of the analysis algorithm.

As we can see in Table 3.3, our intuition was correct and we can find low correlation values, between both dictionaries, cutting some of the lowest frequencies of each block inside the CP dictionary structure (see Figure 3.16). Our methodology has consisted of cutting the first basis function of each time splitting, until we have achieved correlation values below the maximum tolerated in each case. To do this, we have considered the maximum values of correlation viewed in Table 3.2.

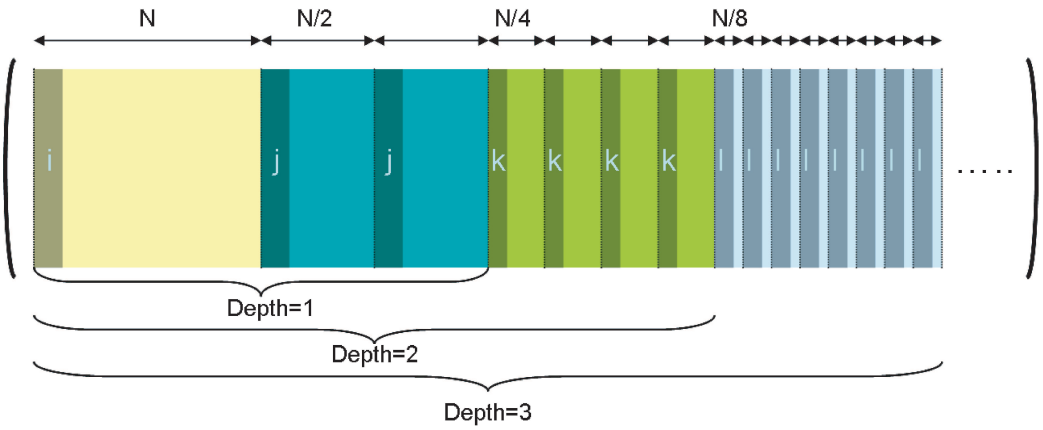


Figure 3.16: Cosine packet dictionary structure after cutting the first frequencies of each time splitting for *depth*=1,...,5. The dark blocks belong to the removed basis functions

| Dictionary | Size | Cut frequencies | | | | | | *Max Correlation* |
|---|---|---|---|---|---|---|---|---|
| | | i | j | k | l | m | n | |
| $D_{CP_{depth=1}}$ | 1408 | 0 | 0 | | | | | 0.994771 |
| | | 1 | 0 | | | | | 0.994771 |
| | | 0 | 1 | | | | | 0.951928 |
| | | 1 | 1 | | | | | 0.791709 |
| | | 2 | 1 | | | | | 0.652552 |
| | | 1 | 2 | | | | | 0.791709 |
| | | 2 | 2 | | | | | 0.567807 |
| | | 3 | 2 | | | | | 0.567807 |
| | | 2 | 3 | | | | | 0.526735 |
| | | 3 | 3 | | | | | 0.520095 |
| | | 4 | 3 | | | | | 0.520095 |
| | | 3 | 4 | | | | | 0.465735 |
| | | 4 | 4 | | | | | 0.465735 |
| | | 5 | 4 | | | | | 0.465735 |
| | | 4 | 5 | | | | | 0.430738 |
| | | 5 | 5 | | | | | 0.420536 |
| | | 6 | 5 | | | | | 0.420536 |
| | | 5 | 6 | | | | | 0.393798 |
| | | 6 | 6 | | | | | 0.387322 |
| $D_{CP_{depth=2}}$ | 2112 | 5 | 5 | 0 | | | | 0.902086 |
| | | 5 | 5 | 1 | | | | 0.771076 |
| | | 5 | 5 | 2 | | | | 0.625646 |
| | | 5 | 5 | 3 | | | | 0.526082 |
| | | 5 | 5 | 4 | | | | 0.460686 |
| $D_{CP_{depth=3}}$ | 2816 | 5 | 5 | 3 | 0 | | | 0.955894 |
| | | 5 | 5 | 3 | 1 | | | 0.807877 |
| | | 5 | 5 | 3 | 2 | | | 0.606564 |
| | | 5 | 5 | 3 | 3 | | | 0.526082 |
| | | 5 | 5 | 3 | 4 | | | 0.526082 |
| $D_{CP_{depth=4}}$ | 3520 | 5 | 5 | 3 | 3 | 0 | | 0.996226 |
| | | 5 | 5 | 3 | 3 | 1 | | 0.753548 |
| | | 5 | 5 | 3 | 3 | 2 | | 0.526082 |
| | | 5 | 5 | 3 | 3 | 3 | | 0.526082 |
| $D_{CP_{depth=5}}$ | 4224 | 5 | 5 | 3 | 3 | 2 | 0 | 0.98282 |
| | | 5 | 5 | 3 | 3 | 2 | 1 | 0.591017 |

Table 3.3: Cut frequency index for maximum allowed correlations

Finally, we have found which are the frequencies we must cut to achieve low values of correlation. Nevertheless, we must guarantee that our possible CP dictionaries (different *depth*) are able to represent AA after cutting these frequencies. To do this, we have represented an AA segment for *depth*=1,...,5 with 50 coefficients in Figure 3.17 (as we have done in Section 3.3).

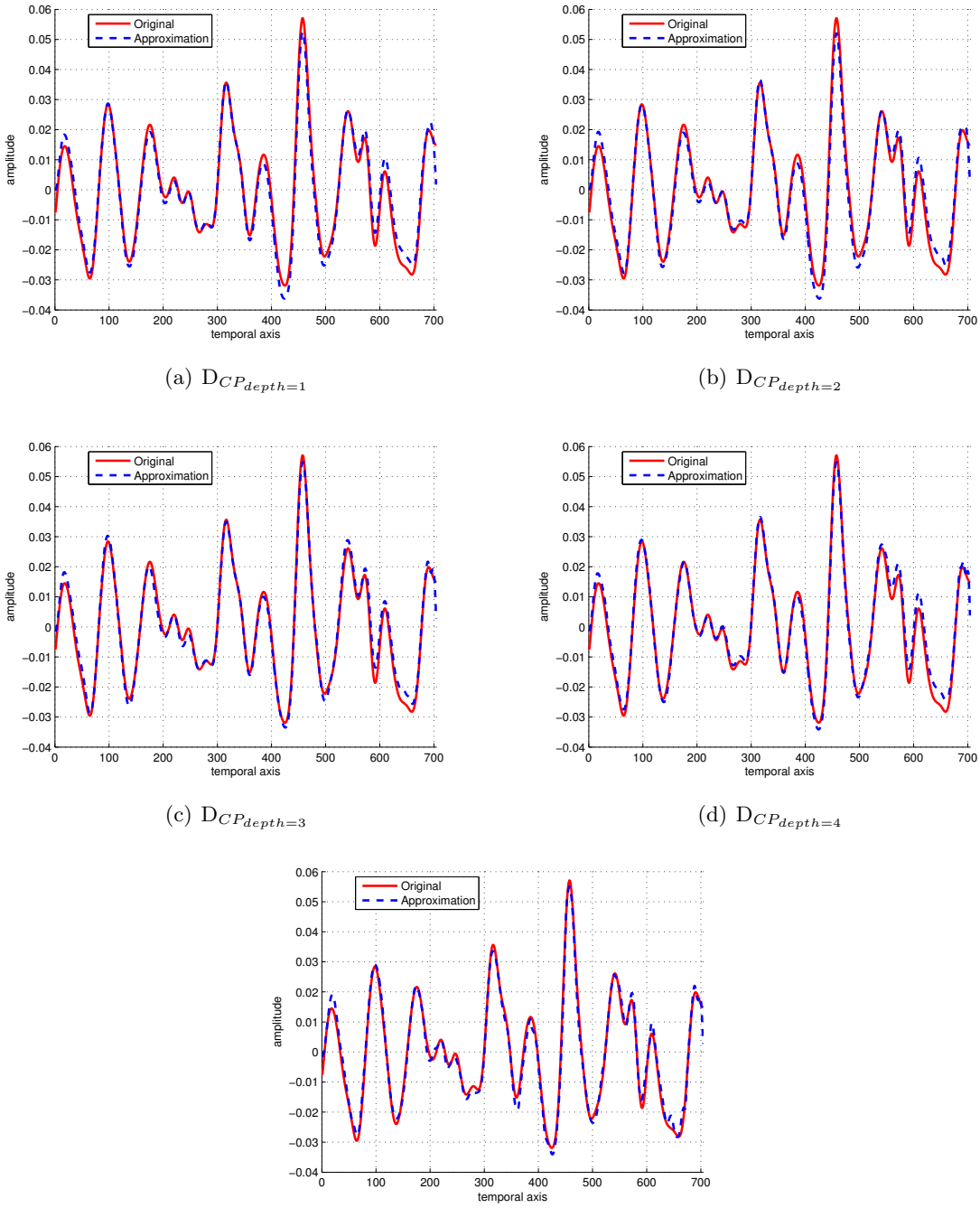


(a) $D_{CP_{depth=1}}$

(b) $D_{CP_{depth=2}}$

(c) $D_{CP_{depth=3}}$

(d) $D_{CP_{depth=4}}$

(e) $D_{CP_{depth=5}}$

Figure 3.17: Atrial activity approximations for *depth*=1,...,5 and with 50 coefficients (OMP)

We can see that the traces are overlapped. Thus, we can affirm that all the 5 dictionaries are able to approximate accurately the atrial activity segment without any problem, although we have cut some basis functions.

### 3.4.3 VA and AA Signal Separation

Previously, we have done a study about Gaussian and CP dictionary to represent VA and AA signal respectively. Now, we want to see what we are able to do in terms of VA and AA signal separation. The methodology we have followed is the one we have explained in Section 2.2.

To decide which *depth* is the most appropriate to approximate our signals, we are going to see the VA and AA SNR doing the signal separation for the 5 different *depth*. The results are shown in Figures 3.18 and 3.19.

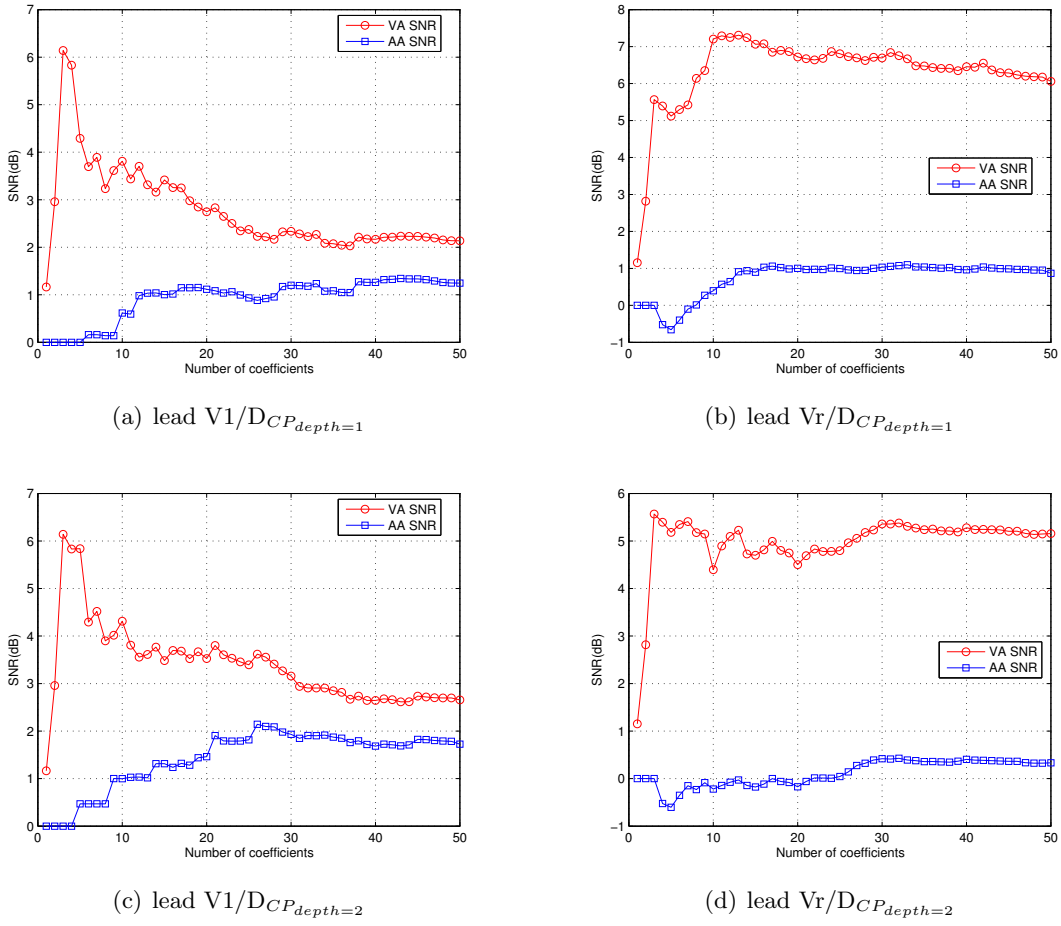


(a) lead V1/$D_{CP_{depth=1}}$

(b) lead Vr/$D_{CP_{depth=1}}$

(c) lead V1/$D_{CP_{depth=2}}$

(d) lead Vr/$D_{CP_{depth=2}}$

Figure 3.18: Evolution of the VA and AA SNR doing the signal separation with respect to the number of coefficients for *depth*=1,2 and for the leads V1 and Vr in atrial fibrillation (OMP, 50 coefficients)

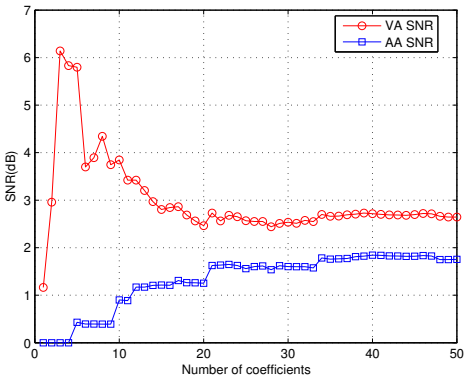


(a) lead V1/D$_{CP_{depth=3}}$

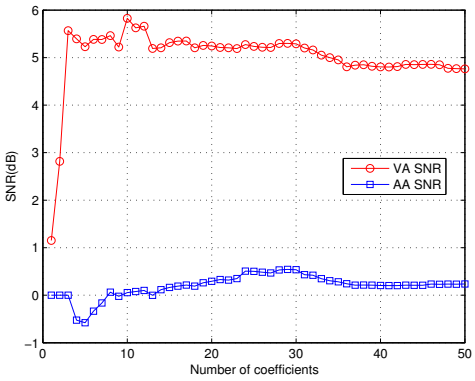


(b) lead Vr/D$_{CP_{depth=3}}$

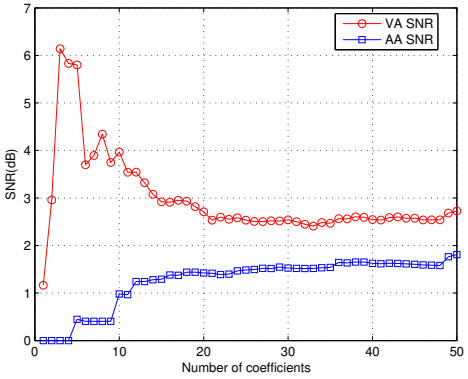


(c) lead V1/D$_{CP_{depth=4}}$

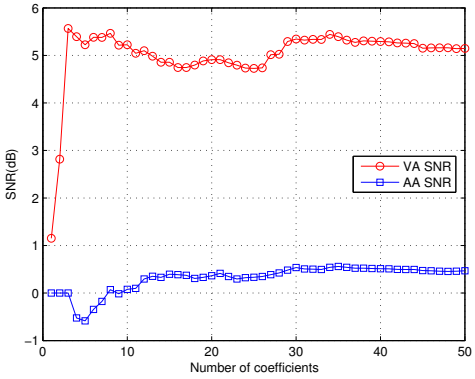


(d) lead Vr/D$_{CP_{depth=4}}$

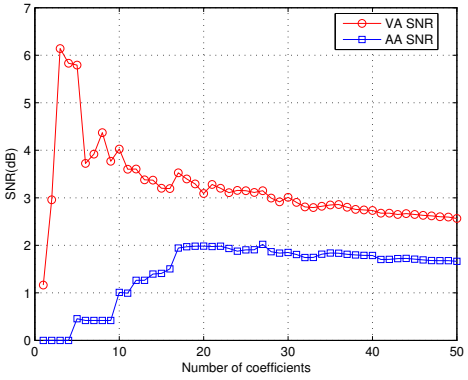


(e) lead V1/D$_{CP_{depth=5}}$

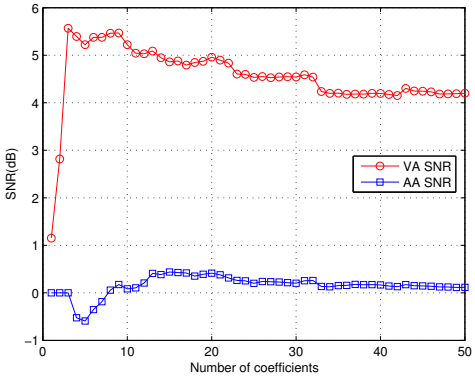


(f) lead Vr/D$_{CP_{depth=5}}$

Figure 3.19: Evolution of the VA and AA SNR doing the signal separation with respect to the number of coefficients for *depth*=3,4,5 and for the leads V1 and Vr in atrial fibrillation (OMP, 50 coefficients)

As we can observe in Figures 3.18 and 3.19, we cannot find one dictionary which best represents both signals:

- Even though for lead V1 the best is when we take *depth*=3, there are not high differences with the others, except *depth*=1 which is worse.

- For the lead Vr the best is clearly with *depth*=1.

Figure 3.20 shows the approximations for V1 and Vr leads with their best dictionary:

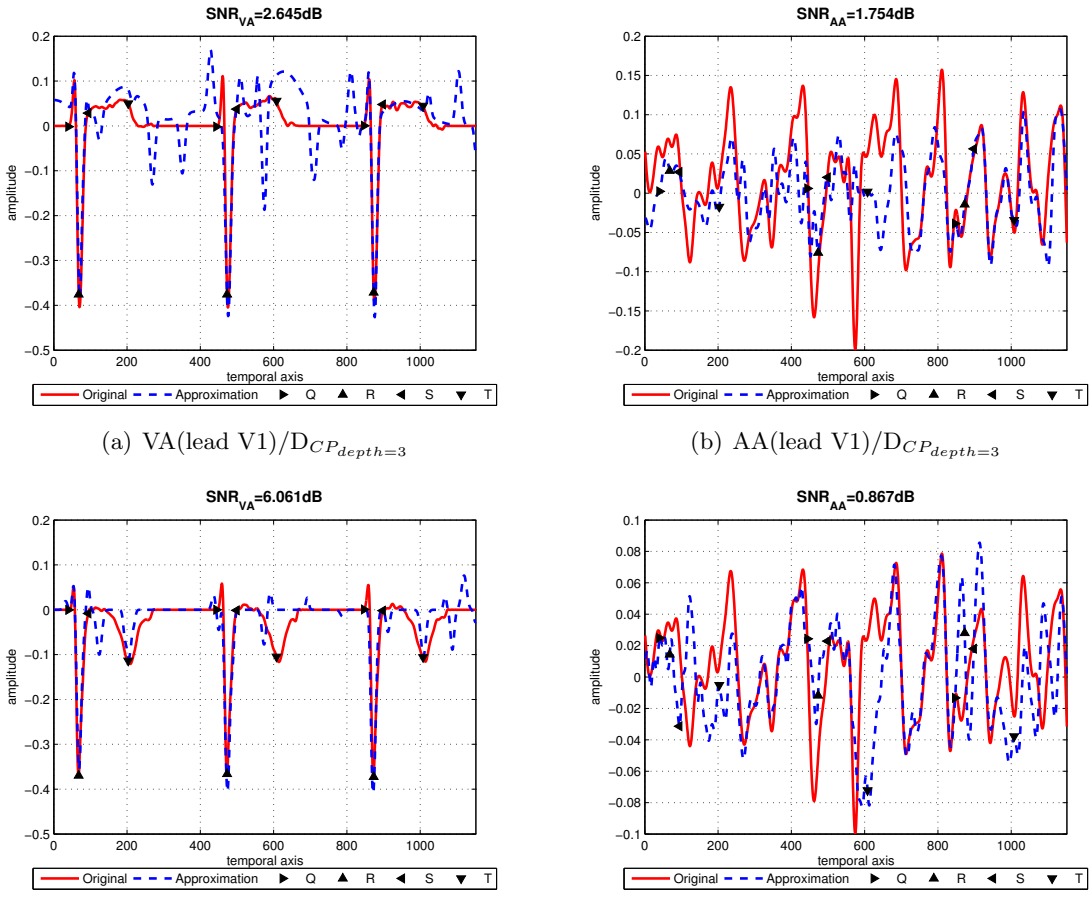


(a) VA(lead V1)/$D_{CP_{depth=3}}$

(b) AA(lead V1)/$D_{CP_{depth=3}}$

(c) VA(lead Vr)/$D_{CP_{depth=1}}$

(d) AA(lead Vr)/$D_{CP_{depth=1}}$

Figure 3.20: VA and AA separation for the leads V1 and Vr with $D_{CP_{depth=3}}$ for the first and $D_{CP_{depth=1}}$ for the second, using OMP (50 coefficients)

### 3.4.4 Discussion

In this section, we have studied the Cosine Packet dictionary to see how it deals with our problem. As we have established in the previous results, it is not the appropriate one to approximate the atrial activity signal, when we are doing the signal separation. This is clear if we regard the Figure 3.20, where the approximations are still far from the original signals. However, there are

some intervals where there is an interesting representation. That means the frequencies of our dictionary are correct but the temporal resolution is not enough.

Another interesting point of our study comes from the correlation between Gaussian and CP dictionary. We already know which frequencies must not be in our AA dictionary to avoid high values of correlation and, hence, we must cut. The correct ones and the respective scales are used to build the Gabor dictionary to represent AA signal in the next section.

## 3.5 Gabor Dictionary for AA Representation

In this section we want to improve the AA dictionary, giving it higher temporal resolution than the previous dictionary. This is the way to achieve a better AA approximation.

Hence, we will check the Gabor dictionary, taking advantage of the information about the frequencies and scales we have obtained in the CP study, because if we use these, we will not have any problem with the correlation between VA and AA dictionary.

The reason of selecting Gabor functions as another alternative to approximate AA is because, although there is no clear information from the signal which we can use to design our AA dictionary, one thing we can bear in mind is that we will need sinusoidal basis functions with different temporal windows. Consequently, we want to try with Gabor functions because they have these properties and also the wanted high temporal resolution.

At the end, we want to compare CP and Gabor dictionary, both having the same properties that they share and taking advantage of their other ones.

### 3.5.1 Gabor Function

A time and frequency translation invariant Gabor dictionary is constructed by scaling, translating and modulating a Gaussian window. This last is employed because of its optimal time and frequency energy concentration [20, 21].

Since our signals are real, we can see a Gabor funcion as (see Figure 3.21):

$$g_\gamma[n] = Ke^{\left(-\frac{1}{2}\left(\frac{n-p}{s}\right)^2\right)} cos\left(\frac{2\pi kn}{N}\right), \tag{3.9}$$

where $N$ is the signal length, $s$ the scale, $p$ the temporal shift and $\frac{k}{N}$ the normalized frequency.

The first modification we have introduced is that the cosine will also be translated in time, because our implementation of OMP makes it necessary to achieve the approximations:

$$g_\gamma[n] = Ke^{\left(-\frac{1}{2}\left(\frac{n-p}{s}\right)^2\right)} cos\left(2\pi\frac{k}{N}(n-p)\right). \tag{3.10}$$

In addition to the Gabor properties, as frequency and scale, we want to introduce also different phase values in the cosine ($\Delta\varphi$). In this way, we will have more precision representing

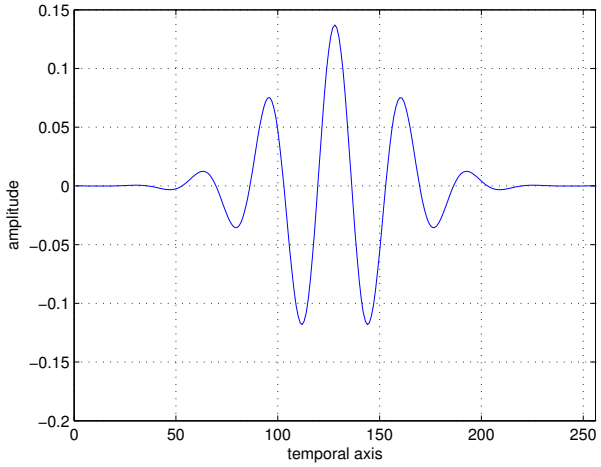


Figure 3.21: Gabor function

the present oscillations in AA signal.

To do this, we have to modify the Gabor function like this:

$$g_\gamma[n] = K \cdot e^{\left(-\frac{1}{2}\left(\frac{n-p}{s}\right)^2\right)} \cdot cos\left(2\pi\frac{k}{N}(n-p) - \Delta\varphi\right) \qquad \gamma = (p, k, s, \Delta\varphi). \tag{3.11}$$

As a result of using the following trigonometrical property:

$$cos(\alpha - \beta) = cos\alpha \cdot cos\beta + sin\alpha \cdot sin\beta, \tag{3.12}$$

we can do the equivalence between Eq.(3.11) and Eq.(3.12) as:

$$cos\left(2\pi\frac{k}{N}(n-p) - \Delta\varphi\right) = cos\left(2\pi\frac{k}{N}(n-p)\right) \cdot cos\Delta\varphi + sin\left(2\pi\frac{k}{N}(n-p)\right) \cdot sin\Delta\varphi. \tag{3.13}$$

Finally, we can see our new basis function as:

$$g_\gamma[n] = K \cdot e^{\left(-\frac{1}{2}\left(\frac{n-p}{s}\right)^2\right)} \cdot \left[cos\left(2\pi\frac{k}{N}(n-p)\right) \cdot cos\Delta\varphi + sin\left(2\pi\frac{k}{N}(n-p)\right) \cdot sin\Delta\varphi\right]. \tag{3.14}$$

### 3.5.2 Gabor Parameters Choice

Firstly, we want to fix the phase values that we are going to input. As we can see in Figure 3.22, we should be careful with the phase value of the cosine, because we can get to have identical basis functions in the dictionary but with opposite sign ($\varphi = 0$ and $\varphi = \pi$). This is absolutely unnecessary, because we want to get a dictionary as small as possible to decrease the computational complexity.

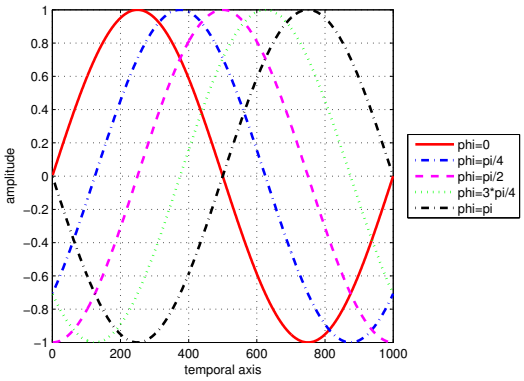


Figure 3.22: Sine evolution with different phase values

Therefore, to avoid repeated atoms in our dictionary, the phase values must be located in the interval $\Delta\varphi = [0, \pi)$. We have taken a discrete uniform distribution between this interval:

$$p(\Delta\varphi) = \begin{cases} \frac{1}{L} & \Delta\varphi = 0, \frac{\pi}{L}, \frac{2\pi}{L}, ..., \frac{(L-1)\pi}{L} \\ 0 & other \end{cases}$$

Once we have introduced the phase values and we know which we should put in our dictionary, it is likewise important to decide the other parameters of the Gabor functions: the scales and the frequencies.

To do that, we will take the knowledge that comes from CP study about frequencies and scales. It means that we are going to use the same scales and frequencies that we have taken in all CP dictionaries. So we will construct 5 dictionaries, as we have done in Section 3.4, but also introducing 16 phase values ($L = 16$) and a temporal resolution of 1 sample. As we have already seen in the previous section, we strongly need this temporal resolution.

In the next Tables we show the scales, the minimum frequencies and the number of frequencies we have obtained from CP dictionary to be able to compare both options, taking the advantages that Gabor provides:

| Gabor dictionaries | Scales |
|---|---|
| $D_{G_1}$(CP *depth*=1) | 206/412 |
| $D_{G_2}$(CP *depth*=2) | 103/206/412 |
| $D_{G_3}$(CP *depth*=3) | 52/103/206/412 |
| $D_{G_4}$(CP *depth*=4) | 26/52/103/206/412 |
| $D_{G_5}$(CP *depth*=5) | 13/26/52/103/206/412 |

Table 3.4: Scales to use in Gabor dictionary obtained from CP study

| Gabor dictionaries | Minimum frequencies for each scale |
|---|---|
| $D_{G_1}$(CP *depth*=1) | 0.0078125/0.00390625 |
| $D_{G_2}$(CP *depth*=2) | 0.009943181/0.0078125/0.00390625 |
| $D_{G_3}$(CP *depth*=3) | 0.019886363/0.009943181/0.0078125/0.00390625 |
| $D_{G_4}$(CP *depth*=4) | 0.02840909/0.019886363/0.009943181/0.0078125/0.00390625 |
| $D_{G_5}$(CP *depth*=5) | 0.034090909/0.02840909/0.019886363/0.009943181/0.0078125/0.00390625 |

Table 3.5: Minimum frequencies to use in Gabor dictionary obtained from CP study

| Gabor dictionaries | Number of frequencies for each scale |
|---|---|
| $D_{G_1}$(CP *depth*=1) | 347/699 |
| $D_{G_2}$(CP *depth*=2) | 173/347/699 |
| $D_{G_3}$(CP *depth*=3) | 85/173/347/699 |
| $D_{G_4}$(CP *depth*=4) | 42/85/173/347/699 |
| $D_{G_5}$(CP *depth*=5) | 21/42/85/173/347/699 |

Table 3.6: Number of frequencies to use in Gabor dictionary obtained from CP study

The maximum frequency normalized is $f_{max} = 0.5$, which is the one that comes from the Nyquist condition:

$$F_{sampling} \geq 2 \cdot F_{max} \longleftrightarrow f_{max} = \frac{F_{max}}{F_{sampling}} = \frac{1}{2} \tag{3.15}$$

The reason for using the information from the Section 3.4 is because we can profit the correlation study we have done there. Taking the same scales and frequencies, we will guarantee that OMP will perform correctly.

From now on, we will use the terminology introduced in the previous Tables to mention all the different Gabor dictionaries we have studied.

### 3.5.3 VA and AA Signal Separation

In the same way we have already done in CP case, we are going to separate the VA and AA signals.

First of all, we would want to compare the signal separation SNR of both possibilities for AA dictionary, CP and Gabor dictionary. After this, we will be able to decide which is the most appropriate option.

In Figure 3.23 we have the comparison between both dictionaries, by means of the signal separation SNR for the leads V1 and Vr. As we can notice, the results are clearly much better for Gabor dictionary than for CP dictionary (see Table 3.7).

| lead V1 | Gauss ∪ CP | Gauss ∪ Gabor |
|---|---|---|
| VA SNR(dB) | 2.645 | 6.589 |
| AA SNR(dB) | 1.754 | 5.737 |
| lead Vr | Gauss ∪ CP | Gauss ∪ Gabor |
| VA SNR(dB) | 6.061 | 6.431 |
| AA SNR(dB) | 0.867 | 1.115 |

Table 3.7: Signal separation SNR comparison with Gaussian functions for the VA dictionary and two options for the AA dictionary: CP functions and Gabor functions (50 coefficients, OMP)

Although the Gabor results in Figure 3.23 are much interesting than CP results, there are still better using another Gabor parameters. The best one is $D_{G_4}$ (see Tables 3.4, 3.5, 3.6), whose signal separation SNR is shown in Table 3.8 and in Figure 3.24. Figure 3.25 illustrates the VA and AA approximations.

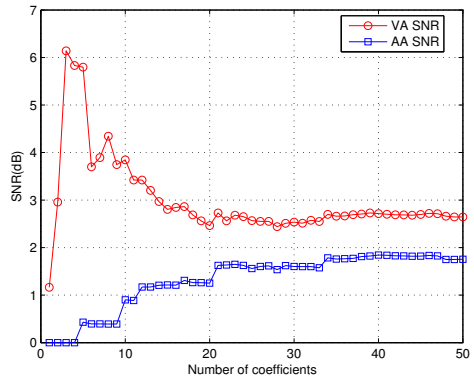


(a) lead V1/$D_{CP_{depth=3}}$

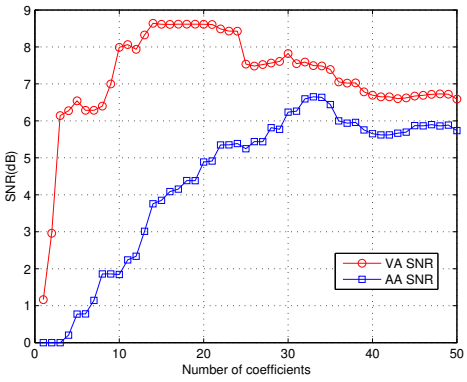


(b) lead V1/$D_{G_3}$

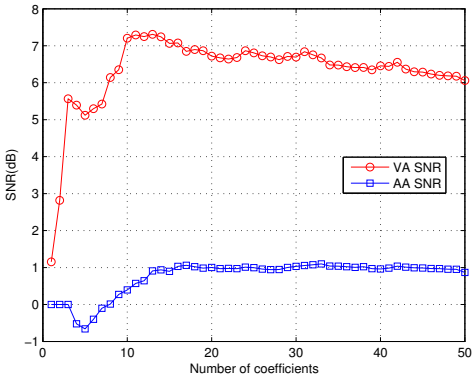


(c) lead Vr/$D_{CP_{depth=1}}$

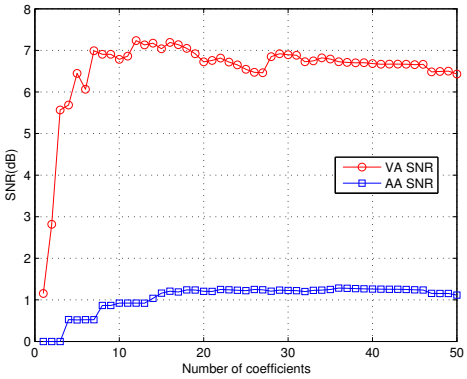


(d) lead Vr/$D_{G_1}$

Figure 3.23: Comparison between CP (left) and Gabor SNR (right) for the leads V1 and Vr, each one with its best results with CP dictionary ($D_{CP_{depth=3}}$, $D_{CP_{depth=1}}$) and their respective Gabor dictionary ($D_{G_3}$, $D_{G_1}$)

| lead V1 | Gauss ∪ Gabor |
|---|---|
| VA SNR(dB) | 7.398 |
| AA SNR(dB) | 6.327 |

| lead Vr | Gauss ∪ Gabor |
|---|---|
| VA SNR(dB) | 6.686 |
| AA SNR(dB) | 1.103 |

Table 3.8: Signal separation SNR with Gaussian functions for the VA dictionary and Gabor ones for the AA dictionary: $D_{G_4}$ (50 coefficients, OMP)

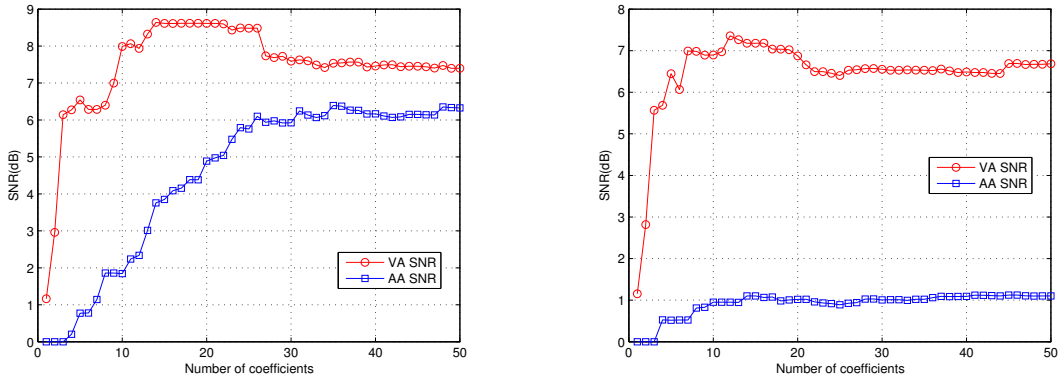


(a) lead V1 (b) lead Vr

Figure 3.24: Signal separation SNR for each signal, leads V1 and Vr, with the best Gabor dictionary to represent AA, which is $D_{G_4}$

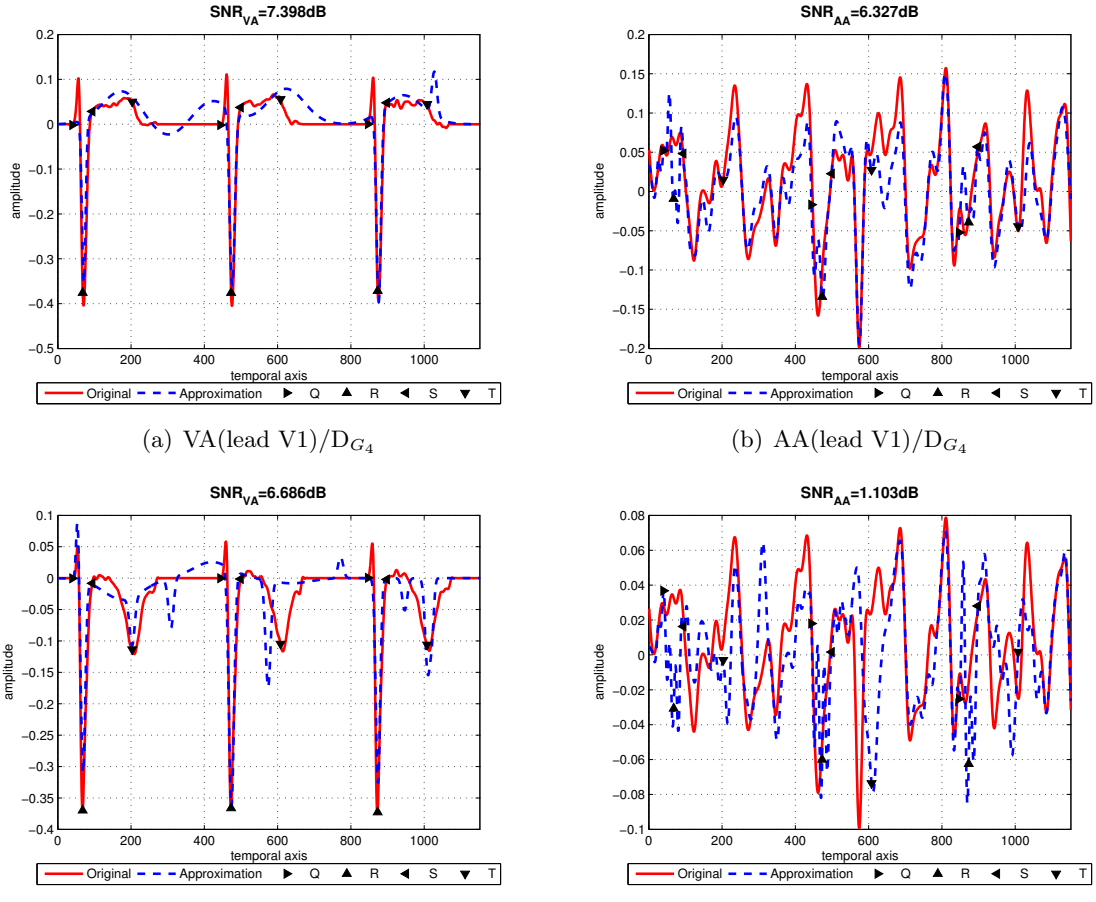


(a) VA(lead V1)/$D_{G_4}$ (b) AA(lead V1)/$D_{G_4}$

(c) VA(lead Vr)/$D_{G_4}$ (d) AA(lead Vr)/$D_{G_4}$

Figure 3.25: Gabor approximation (signal separation) for each signal, leads V1 and Vr, with the best Gabor dictionary to represent AA, which is $D_{G_4}$

### 3.5.4 Discussion

We have seen that a good approximation of the atrial activity signal can be achieved with Gabor functions. They give the opportunity to introduce the scales, the frequencies, the phase values and also, and the most important novelty, the temporal resolution of 1 sample. All these things become essential to improve the signal separation we have realized in the previous section with CP dictionary.

As we have already mentioned, the signal separation SNR is really better in this case than in CP one. We have about 4-5dB more in the lead V1 and 0.3-0.6dB more in the lead Vr. This is reflected in the approximations (see Figures 3.23, 3.24 and 3.25):

- The VA approximations start to be interesting because there are not many basis functions destined to the AA representation. Although the R waves are well approximated, they and the Q and T waves can be improved. One way to do it, with the Q and R waves, is to use the Generalized Gaussian as we will see in the next Section. For T waves is more difficult to improve the basis functions to represent them, owing to the different shapes that they have depending on the lead and the patient.

- The AA approximation is really good, except some parts which are destined for the VA representation. So, we should clearly improve the VA dictionary to achieve better results.

Thus, we can affirm that Gabor dictionary is definitely the appropriate dictionary to approximate the atrial activity.

## 3.6 Generalized Gaussian Dictionary for VA Representation

In the previous section, we have come to the conclusion that it would be necessary to refine the approximations of the Q and R waves. In order to do it, we change the Gaussian functions, from the VA dictionary, for Generalized Gaussian functions. This last modification in our MCD gives better results in the VA and AA signal separation.

### 3.6.1 Generalized Gaussian Function

The function we are going to introduce in our VA dictionary, instead of the Gaussian function, is the Generalized Gaussian(GG) function:

$$g_\gamma[n] = Ke^{\left(-\left(\frac{|n-p|}{\alpha}\right)^\beta\right)} \qquad \gamma = (p, \alpha, \beta) \tag{3.16}$$

The newness, with regard to the Gabor function, is the parameter $\beta$ that will let us to approximate with more accuracy the Q and R peaks:

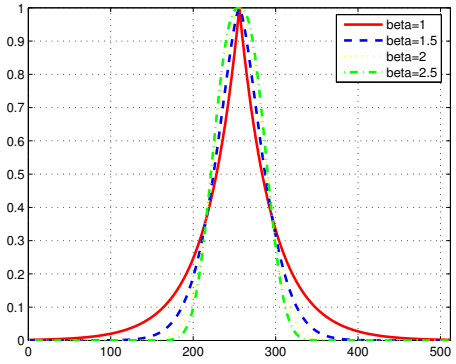


Figure 3.26: Generalized Gaussian functions with different $\beta$

In the previous figure we can observe how the GG allows to obtain two well known functions, changing only the $\beta$:

- $\beta = 2$: Gaussian function.

- $\beta = 1$: Laplacian function.

### 3.6.2 Generalized Gaussian Parameters Choice

The methodology we have followed to decide which were the best parameters of the GG to represent Q and R peaks, as we have previously done designing the Gaussian dictionary, is totally heuristic.

We have observed in Section 3.5, that the Gaussian functions are not able to approximate all the Q and R peaks, because they do not have exactly Gaussian shapes and OMP puts in their places another functions from the AA dictionary. To solve it, we think that the Generalized Gaussian could improve the VA approximations, because now we pass from one to two degrees of freedom. Therefore, we will have more accuracy representing both Q and R waves.

In the next table we show the best parameters of our new VA dictionary, that we have found after several tests:

| $D_{GG}$ | $\alpha$ | $\beta$ |
|---|---|---|
| Q, R | 3,4,5,6,7 | 1.5,1.6,...,2.2 |
| T | 49,50,51,52,53,54 | 2 |

Table 3.9: Generalized Gaussian parameters ($\alpha$, $\beta$) to improve VA approximation and consequently AA approximation

### 3.6.3 VA and AA Signal Separation

As we have done in the other cases, we are going to see if this modification is able to achieve a better signal separation than the previous. The two possibilities that we want to compare are changing the VA dictionary, not the AA one, however. The first option is composed of the Gaussian dictionary and the Gabor one for VA and AA signals respectively, and the second option consists of the Generalized Gaussian dictionary for VA and also the Gabor dictionary for AA. This last is the $D_{G_2}$ (see Section 3.5), which has given the best results jointly with the Generalized Gaussian one.

In Figure 3.27 we find the comparison between the two options, in terms of the signal separation SNR. We can assert that Generalized Gaussian dictionary is really better than Gaussian dictionary, because we can find differences about 2dB in both leads, V1 and Vr (see Table 3.10). This improvement in the SNR is easily observable in Figure 3.28, where we have used a new segment of 1920 samples, to have a general idea of how our system can manage with the VA and AA separation.

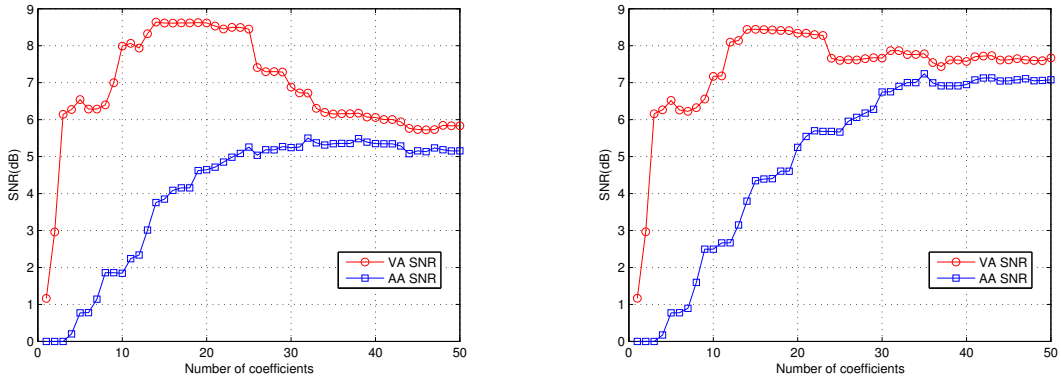


(a) lead V1/D$_{Gaussian}$ (b) lead V1/D$_{GG}$

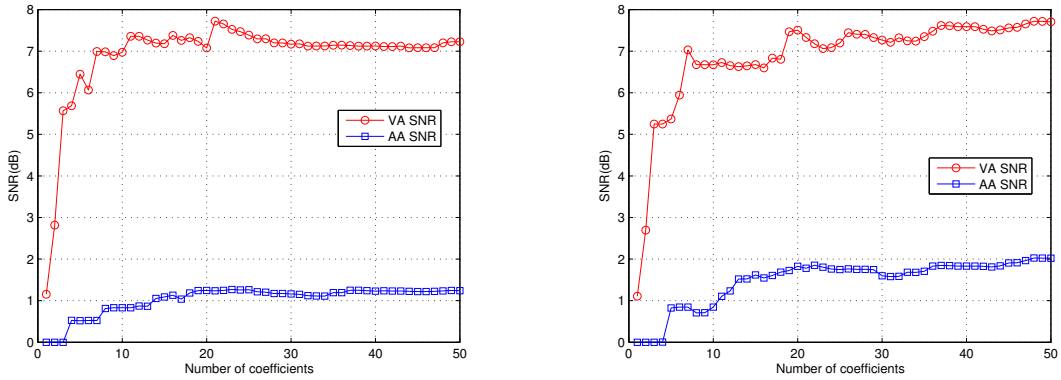


(c) lead Vr/D$_{Gaussian}$ (d) lead Vr/D$_{GG}$

Figure 3.27: Comparison between the Gaussian and the Generalized Gaussian SNR (signal separation) for the leads V1 and Vr

| lead V1 | Gaussian ∪ Gabor | GG ∪ Gabor |
|---|---|---|
| VA SNR(dB) | 5.834 | 7.67 |
| AA SNR(dB) | 5.157 | 7.077 |
| lead Vr | Gaussian ∪ Gabor | GG ∪ Gabor |
| VA SNR(dB) | 7.227 | 7.706 |
| AA SNR(dB) | 1.24 | 2.022 |

Table 3.10: Signal separation SNR comparison with Gabor functions for the AA dictionary (D$_{G_2}$) and two options for the VA dictionary: Gaussian functions and Generalized Gaussian functions (50 coefficients, OMP)

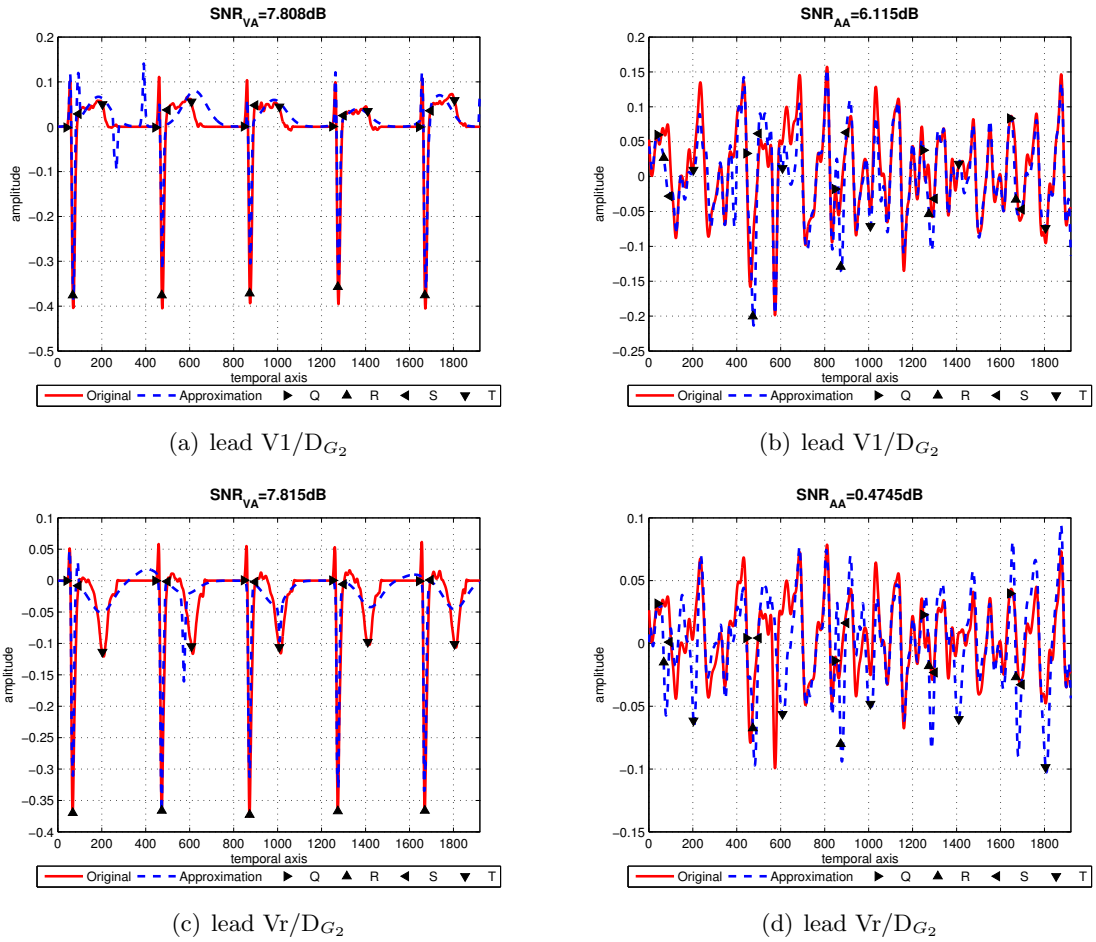


(a) lead V1/$D_{G_2}$

(b) lead V1/$D_{G_2}$

(c) lead Vr/$D_{G_2}$

(d) lead Vr/$D_{G_2}$

Figure 3.28: VA and AA separation for the leads V1 and Vr with $D_{GG}$ for the first and $D_{G_2}$ for the second, using OMP (75 coefficients)

### 3.6.4 Discussion

In summary, we can affirm that Generalized Gaussian has given us more accuracy in our approximations that has lead up to an increase of the signal separation SNR (see Table 3.10).

Moreover, OMP works much better than in the other cases because the SNR grows generally always and, consequently, the presence of basis functions in the approximations (artefacts), which do not belong to these, has decreased (see Figure 3.28).

## 3.7 Conclusions

Eventually, we have achieved good approximations of the VA and the AA signals after doing the signal separation. The use of sparse approximations with a flexible and robust dictionary has born fruit.

Undoubtedly, there are some parts of the VA approximations that can still be improved. The T-waves and the few artefacts present in the VA signal are the mean ones. However, we can say that the error energy introduced in the VA results is pretty low and this allows to obtain good AA approximations.

As regards the dictionary used, we must say that we have been able to find an overcomplete system of many basis functions, that has permitted us to achieve our aim, a good signal separation. It has been done with the union of two dictionaries generating a Multi-Component Dictionary:

- VA dictionary: Generalized Gaussian functions
- AA dictionary: Gabor functions

In the next Table we can see the evolution of the different best SNR values that we have obtained, with 50 coefficients and using OMP, throughout the previous study:

| lead V1 | Gauss $\cup$ CP | Gauss $\cup$ Gabor | GG $\cup$ Gabor |
|---|---|---|---|
| VA SNR(dB) | 2.645 | 7.398 | 7.67 |
| AA SNR(dB) | 1.754 | 6.327 | 7.077 |
| lead Vr | Gauss $\cup$ CP | Gauss $\cup$ Gabor | GG $\cup$ Gabor |
| VA SNR(dB) | 6.061 | 6.686 | 7.706 |
| AA SNR(dB) | 0.867 | 1.103 | 2.022 |

Table 3.11: Signal separation SNR evolution of our thorough study (50 coefficients, OMP)

As a result, we can assert that we have followed an increasing evolution and it proves our dictionary choice, the last one.

# Chapter 4

# Experimental Results

## 4.1 Introduction

Once designed the Multi-component dictionary (MCD), we evaluate two analysis techniques, separating VA and AA signals. Moreover, we test the best MCD found with different real ECG signals.

Firstly, we start by checking how Basis Pursuit Denoising (BPDN) performs as a decomposition algorithm for signal separation. The aim is to compare with the OMP results obtained in Section 3.4, where the Cosine Packet dictionary has been studied. The reason of taking this dictionary and not another is because is the smallest one and BPDN takes more computational complexity than OMP.

Secondly, the overall performance of sparse approximations over redundant dictionaries, for VA and AA separation, is evaluated. For this purpose, real ECG signals from three patients in atrial fibrillation have been used, jointly with our best dictionary (GG functions for VA dictionary and Gabor functions for AA dictionary).

## 4.2 Basis Pursuit Denoising

Similarly to the OMP based source separation approach used in Chapter 3 to achieve the signal sepration, we can use Basis Pursuit Denoising to obtain sparse approximations of our original signal. In order to decide which is the best approach, we compare the source separation results obtained with the dictionary suggested in Section 3.4. This choice is due to the fact that it is the smallest dictionary, among all we have studied, and BPDN has a high computational

complexity. To be able to compare both alternatives, we approximate the signals with the same number of coefficients as for OMP.

Before continuing, we want to remind that Basis Pursuit Denoisign (BPDN) refers to the solution of:

$$\arg\min_{\mathbf{b}} \frac{1}{2}\|f - D\mathbf{b}\|_2^2 + \gamma\|\mathbf{b}\|_1, \tag{4.1}$$

where $\gamma$ is a positive real value employed as a threshold (to limit the maximum $l_1$ norm of $\mathbf{b}$).

BPDN can be solved using classical Quadratic Programming methods and it turned up to adapt BP to the approximation case.

As it is shown in Figures 4.1 and 4.2, none of the approximations are successful, because they do not achieve a good signal separation. Moreover, we cannot say visually which one is better, because in both alternatives, BPDN and OMP, there are lots of artefacts that hinder a good signal separation.

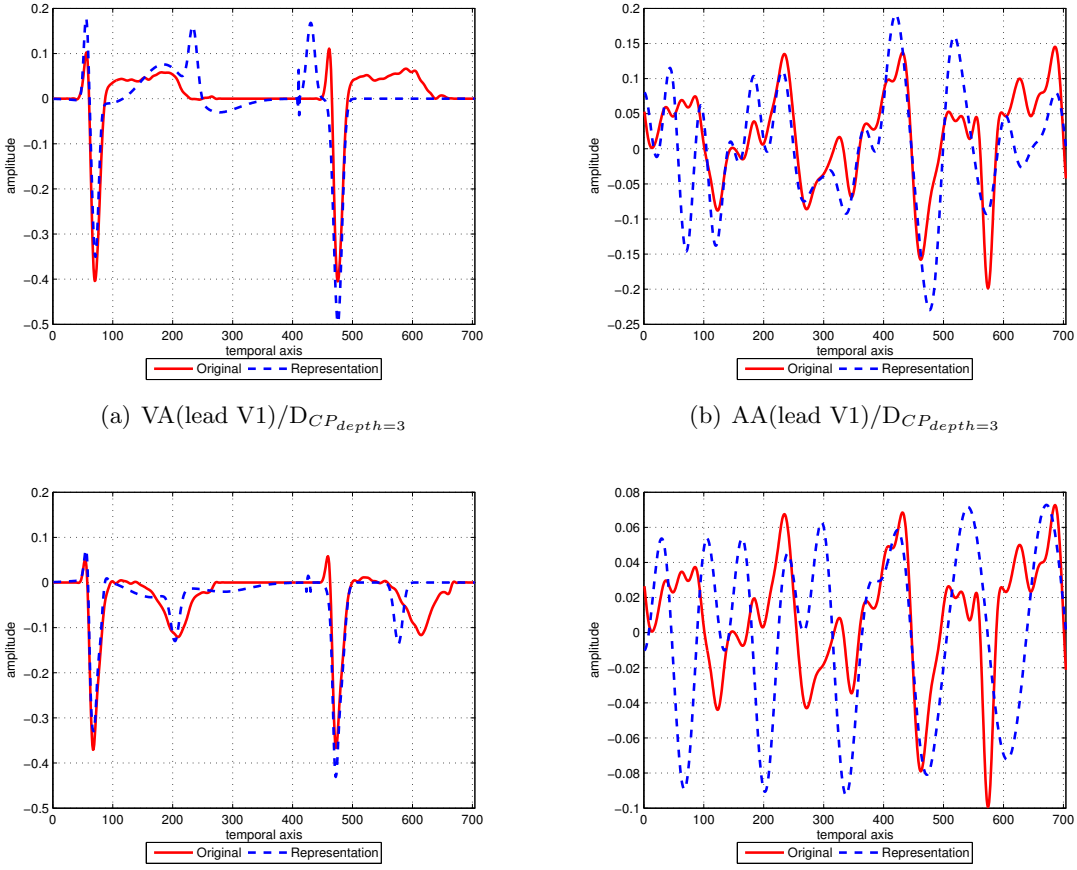


(a) VA(lead V1)/$D_{CP_{depth=3}}$

(b) AA(lead V1)/$D_{CP_{depth=3}}$

(c) VA(lead Vr)/$D_{CP_{depth=1}}$

(d) AA(lead Vr)/$D_{CP_{depth=1}}$

Figure 4.1: VA and AA separation for the leads V1 and Vr with $D_{CP_{depth=3}}$ and BPDN ($\gamma = 0.3$) for the first, $D_{CP_{depth=1}}$ and BPDN ($\gamma = 0.3$) for the second

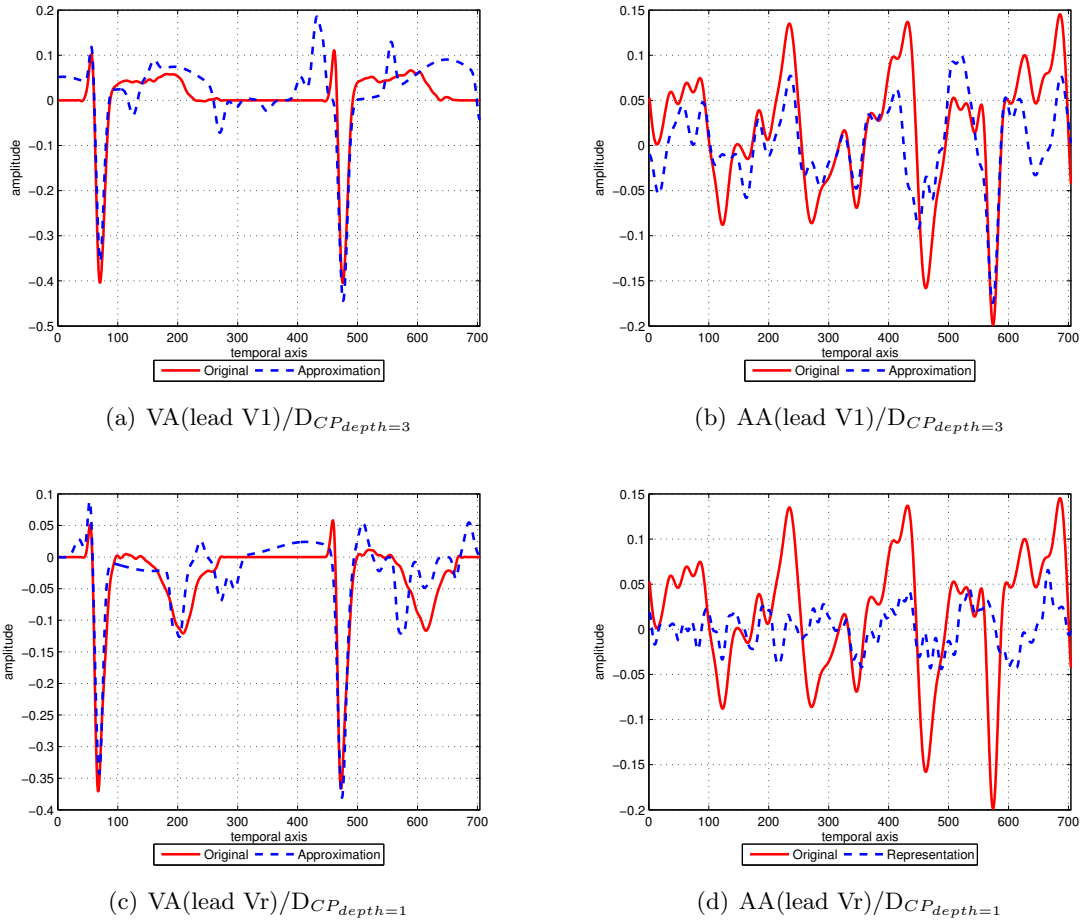


(a) VA(lead V1)/$D_{CP_{depth=3}}$

(b) AA(lead V1)/$D_{CP_{depth=3}}$

(c) VA(lead Vr)/$D_{CP_{depth=1}}$

(d) AA(lead Vr)/$D_{CP_{depth=1}}$

Figure 4.2: VA and AA separation for the leads V1 and Vr with $D_{CP_{depth=3}}$ and OMP for the first and $D_{CP_{depth=1}}$ and OMP for the second

Therefore, to get an idea of which technique is the most appropriate for our goal, a SNR study of the approximations has been done (see Table 4.1).

| Lead V1 | BPDN | OMP |
|---|---|---|
| VA SNR(dB) | 4.07 | 3.6531 |
| AA SNR(dB) | 0.9824 | 2.6305 |

| Lead Vr | BPDN | OMP |
|---|---|---|
| VA SNR(dB) | 7.0176 | 6.5832 |
| AA SNR(dB) | -3.4188 | 0.3372 |

Table 4.1: Signal separation SNR comparison between OMP and BPDN

Although the VA SNR are slightly better for BPDN than for OMP, about 0.4dB, there is not a big difference. Nevertheless, the AA SNR are strongly better for OMP than for BPDN, with differences about 2-4dB. Even, we can find a negative SNR in the VR case, which means that the approximation error has more energy than the original signal.

So, owing to the fact that the BPDN results are worse than the OMP ones and, also, its

computational complexity is really higher than Greedy algorithms, we have dismissed BPDN as a tool to separate the VA and AA signal. We have only used OMP, which is considered to be the most appropriate decomposition algorithm for sparse source separation of VA and AA.

## 4.3 Real ECG

Up to now, we have worked with simulated ECG signals, in order to compare afterwards our approximations and to give a SNR value. The results with the simulated signals are in Section 3.6, using our best dictionary (GG functions for VA dictionary and Gabor functions for AA dictionary), the same that we will use in this case.

In this section, results separating real ECG signals in AF are given. We have taken the ECG signals from three patients with AF and we have separated them, using OMP and 75 coefficients for the sparse decomposition. Due to the fact that the I, II, III and Vf leads are lineal combinations of the others, we have only tested: the Vr, Vl, V1, V2, V3, V4, V5 and V6 leads.

As it can be observed in the Figures 4.3, 4.4 and 4.5, we have achieved good approximations doing the VA and AA separation. However, it is really difficult to assert if they are successful or not. This is because, now, we cannot give a signal separation SNR value by comparing with the original signals. Indeed, original signals are a priori unknown.

Therefore, we can only give some hints about the quality of the results:

- VA approximation: There are really interesting results approximating the VA signal. This is because we always obtain a good approximation of the QRST complexes. Nevertheless, in some leads, we can find small errors in the QRST approximations and, also, some basis functions from the VA dictionary used to represent some parts of the AA signal. These last artefacts can be usually found between two QRST complexes, where there should be only functions from the AA dictionary.

- AA approximation: This is undoubtedly the most difficult to evaluate. Because of its noisy shape, it is impossible to have any structural reference of the signal, unlike the VA one. Thus, we have done a study to check if the frequencies in our AA approximations are inside the theoretical interval: 3Hz - 10Hz [31]. In order to do this, we have calculated the Power Spectrum Density (PSD), using the Welch's averaged periodogram method, with a Hamming window of 426 samples (signal length=1920 samples). Subsequently,

we have looked for the maximum peaks (see it in the $4^{th}$ column of Figures 4.3, 4.4 and 4.5). The results are really encouraging. As we can observe in Table 4.2, most of the found frequencies belong to the 3-10Hz interval. However, we cannot assert that the approximations are correct. This study is only useful to dismiss the results where the maximum frequency is below 3Hz or above 10Hz.

| Patient 0001 | Freq(Hz) | Patient 0002 | Freq(Hz) | Patient 0003 | Freq(Hz) |
|---|---|---|---|---|---|
| Vr | **3.125** | Vr | **3.906** | Vr | 2.148 |
| Vl | **3.906** | Vl | **4.102** | Vl | 2.539 |
| V1 | **7.422** | V1 | **4.102** | V1 | 2.539 |
| V2 | **7.227** | V2 | **3.516** | V2 | **5.078** |
| V3 | **7.422** | V3 | **3.906** | V3 | **5.078** |
| V4 | 2.539 | V4 | **4.102** | V4 | **3.711** |
| V5 | **4.492** | V5 | **3.906** | V5 | **3.125** |
| V6 | **5.469** | V6 | 2.93 | V6 | 2.148 |

Table 4.2: PSD maximums of the AA approximations for the three patients analyzed. In **bold** we find the correct frequencies, it means, the ones belonging to the theoretical interval: 3-10 Hz

- Residues: The mean SNR values for the approximations (not signal separation SNR values) are: 26.2dB, 25.6dB and 23.1dB, for the $1^{st}$, $2^{nd}$ and $3^{rd}$ patients, respectively. So, it means that all the energy of the original signal is placed in the VA and AA approximations.

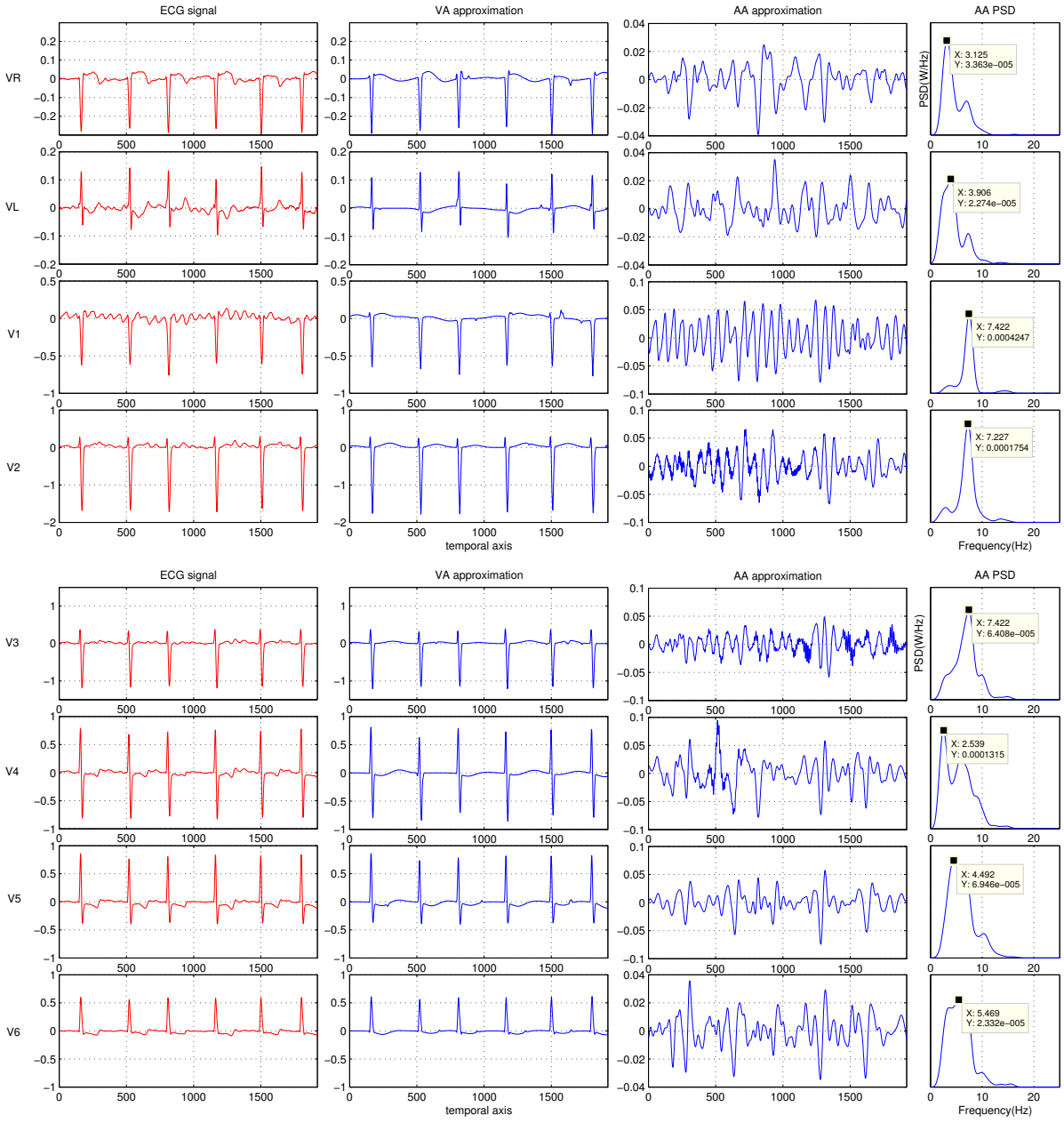


Figure 4.3: Signal separation for the real ECG of the patient 0001 (OMP, 75 coefficients). Left: the separated leads: Vr, Vl, V1, V2, V3, V4, V5 and V6. Middle: VA and AA approximations. Right: AA PSD. In the first three columns, the x-axis units are *samples* and y-axis ones are mV. In this case, we find 7 AF approximations inside the theoretical interval of frequencies

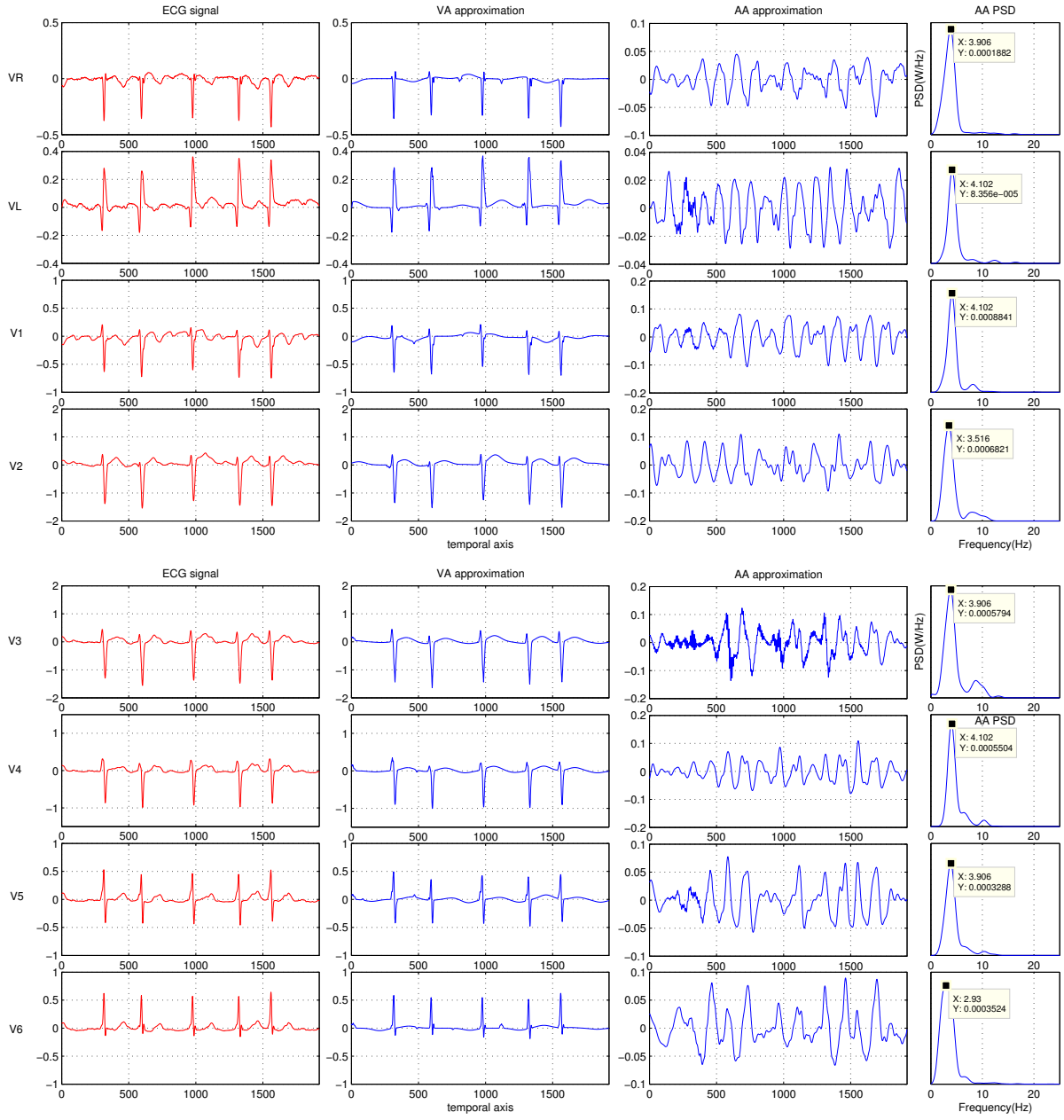


Figure 4.4: Signal separation for the real ECG of the patient 0002 (OMP, 75 coefficients). Left: the separated leads: Vr, Vl, V1, V2, V3, V4, V5 and V6. Middle: VA and AA approximations. Right: AA PSD. In the first three columns, the x-axis units are *samples* and y-axis ones are mV. In this case, we find 7 AF approximations inside the theoretical interval of frequencies

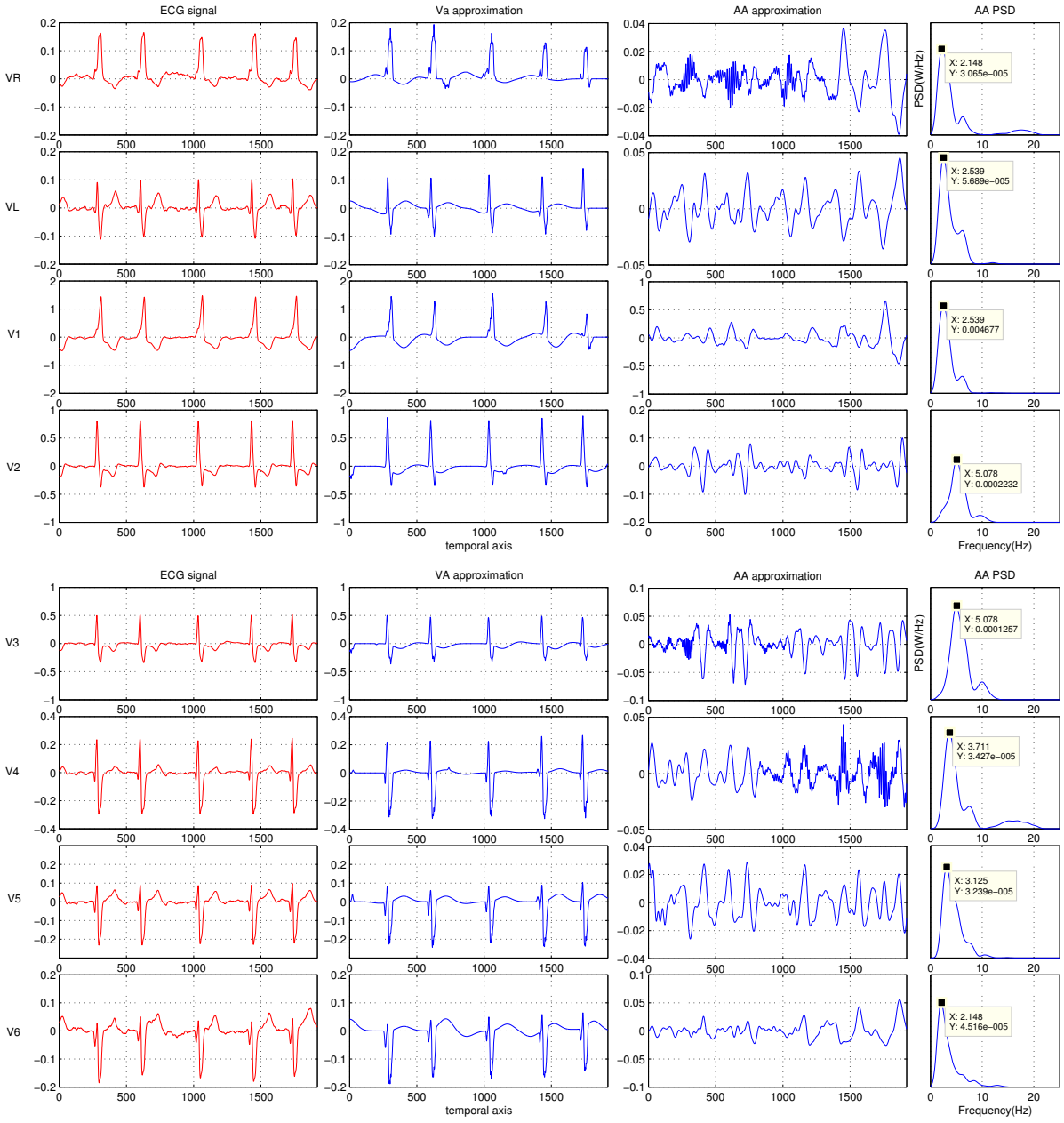


Figure 4.5: Signal separation for the real ECG of the patient 0003 (OMP, 75 coefficients). Left: the separated leads: Vr, Vl, V1, V2, V3, V4, V5 and V6. Middle: VA and AA approximations. Right: AA PSD. In the first three columns, the x-axis units are *samples* and y-axis ones are mV. In this case, we find 4 AF approximations inside the theoretical interval of frequencies

## 4.4 Conclusions

In this chapter different results using the MCD's studied are given. Firstly, after evaluating two different analysis algorithms, OMP and BPDN, we conclude that the first is the most appropriate dictionary, owing to the fact that its approximations and SNR are much better than the BPDN ones. Lastly, different real ECG signals are separated using the OMP approach. The results obtained show that there are some artefacts in both approximations, VA and AA, that make worse the separation. In order to improve it, we propose in the next chapter the use of *a priori* knowledge, helping the OMP principle to avoid these artefacts.

Another conclusion is that the number of coefficients is a value really critic because if it is too high, the approximation starts to have high frequencies destined to represent the residue (see Figures 4.3, 4.4 and 4.5).

# Chapter 5

# A priori knowledge

## 5.1 Introduction

Looking at the results in Chapter 4, we know that they can be improved by taking into account some information about the signals. Although we have this information, the decomposition algorithm (OMP) cannot use it. Therefore, in order to exploit this *a priori* knowledge, we use an algorithm named Weighted-OMP [25]. The new approach is tested afterwards doing the separation of simulated ECG signals and real ECG signals.

## 5.2 Weighted-OMP

As we have previously seen in Chapter 2, MP and OMP iteratively extract vectors, one by one from the dictionary, while optimizing the signal approximation (in terms of energy). Thus, there are two steps at each iteration:

- Firstly, an atom $g_{\gamma_k} \in \mathcal{D}$ is choosen ($k \geq 0$ indicates the number of the iteration).
- Secondly, an approximant $f_m \in span(g_{\gamma_k} : k \in \{0, ..., m-1\})$ and a residual $r_m f = f - f_m$ are generated.

The first step can be formulated as:

$$g_{\gamma_k} = \arg\max_{g_\gamma \in \mathcal{D}} C(r_k f, g_\gamma). \tag{5.1}$$

where $C(r_k f, g_\gamma)$ is a similarity measure between the residual at the $k$th iteration: $r_k f = f - f_k$ and the atoms from the dictionary.

Greedy algorithms use the modulus of the scalar product as this measure, i.e. $C(r_k f, g_\gamma) = |\langle r_k f, g_\gamma \rangle|$. However, if we want to introduce some heuristic measure of *prior* information, we can change it. Hence, we are going to use Weighted-OMP [25]. In this last, the modulus of the scalar product is modified by multiplying a weighting factor $w_\gamma \in [0, 1]$, which represents the *a priori* knowledge and depends on the atom with index $i$, such that:

$$C(r_k f, g_\gamma) = |\langle r_k f, g_\gamma \rangle| \cdot w_\gamma. \tag{5.2}$$

When $w_\gamma$=0, it is the same as deleting $g_\gamma$ from the dictionary. In this work, the *a priori* knowledge is considered independent of the iteration.

## 5.3 Weighting Factors Analysis

In this section, we present our weighting factors analysis, for all the basis functions inside our dictionary. For the choice, we want to make some clarifications about the dictionary and the *a priori* knowledge from the ECG signals.

So, we divide the MCD in three parts (see Figure 5.1):

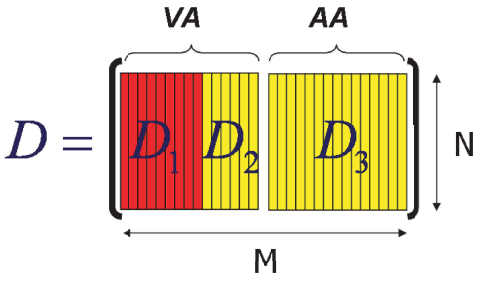


Figure 5.1: Dictionary structure with the 3 kinds of basis functions

- $D_1$: contains the basis functions to approximate the Q, R and S waves,
- $D_2$: contains the basis functions to approximate the T waves,
- $D_3$: contains the basis functions to approximate the atrial fibrillation signal.

In a similar way, we set out our criterion to divide each ECG segment in three areas, understanding segment as the interval between two consecutive Q peaks (see Figure 5.2):

- A: must be approximated with functions from $D_1$ and $D_3$, centred in A,

- B: must be approximated with functions from $D_2$ and $D_3$, centred in B,

- C: must be approximated only with functions from $D_3$.

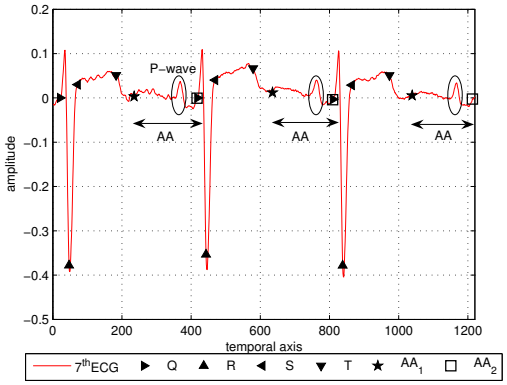


(a) ECG signal in sinus rhythm with the *a priori* knowledge (Q, R, S, T position and AA intervals)

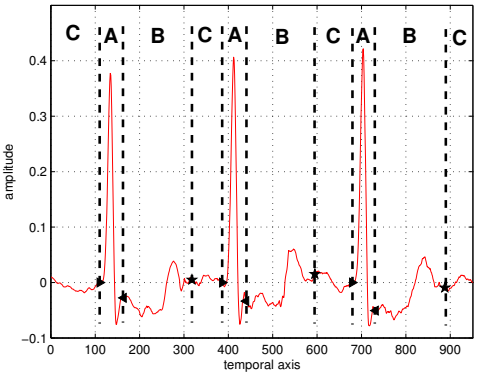


(b) ECG signal in AF with the three areas delimited (A, B and C)

Figure 5.2: *A priori* knowledge (Q, R, S, T position and AA intervals) from the ECG signals and the 3 areas (A, B and C) we establish in the VA signal to design the weights, to use Weighted-OMP as analysis technique

To determine these areas, we have used the *a priori* knowledge, which consists of the positions of the Q, R, S, T waves and the intervals where is only AA.

Once delimited the areas in the ECG signal and the sort of basis functions that can approximate each one, we must establish the weights to help the analysis algorithm to achieve a better signal separation. According to the criterion presented above for each area, we are going to introduce a weight equal to 1 for the correct atoms and another weight in [0,1], for the "wrong" atoms. Figure 5.3 illustrates a block diagram of the selection step in Weighted-OMP. We have put the same weight for the wrong selected atoms in A and B, $w_a$, and another weight, $w_b$, for the incorrect ones in C. Also, we have introduced the notation "in" to say that the atom is inside the interval on the right.

Finally, we are going to do a SNR study of the approximations, obtained after the signal separation, in terms of these weights, $w_a$ and $w_b$. Intuitively, we can think that the best weights for the wrong selected atoms must be ($w_a$,$w_b$)=(0,0) because, in this way, we avoid having them. As we can see in Figure 5.4, the intuition was correct. For the lead Vr, there is a wide area around the ($w_a$,$w_b$)=(0,0) with the maximum SNR, as we have predicted.

However, for the lead V1 (see Figure 5.5), the maximum is not at ($w_a$,$w_b$)=(0,0), it is placed

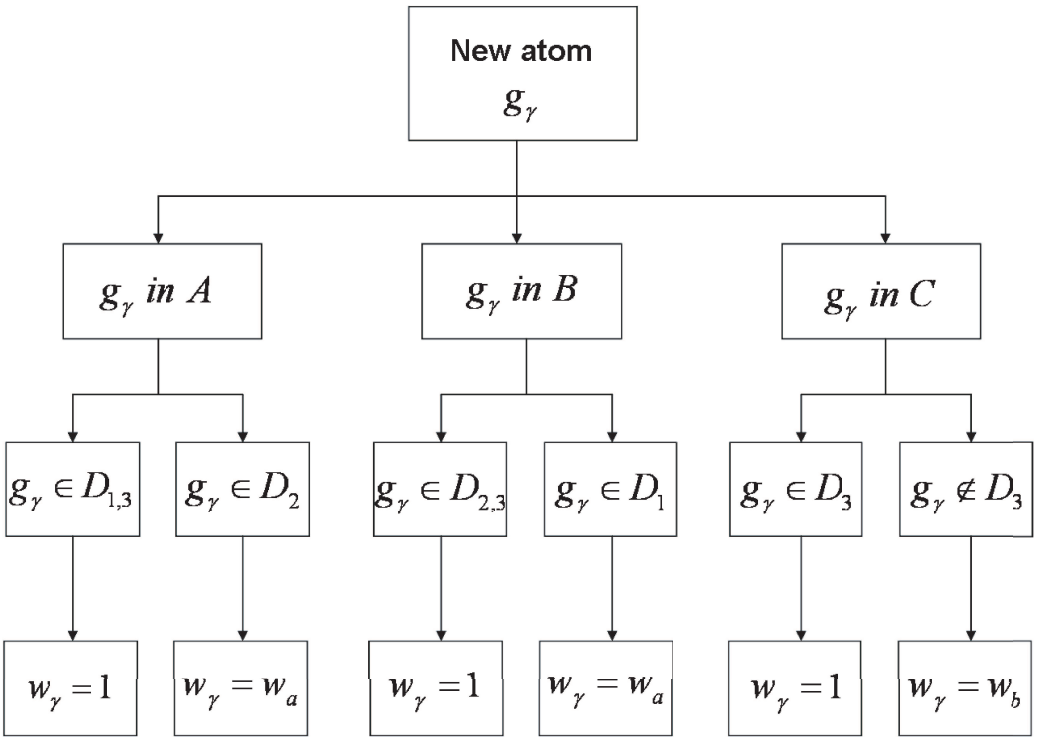


Figure 5.3: Block diagram of the selection step in Weighted-OMP. There are two weights for the incorrect selected atoms: $w_a$ and $w_b$, which will help to achieve a better signal separation

in an area around ($w_a$,$w_b$)=(1,0). But the difference in the SNR values between this two points is really low and we consider this as an outlier. We prefer not to have "wrong" basis functions, understanding "wrong" functions the ones which are centred in some interval which does not correspond to them, in the VA approximations and to get a SNR a little bit lower.

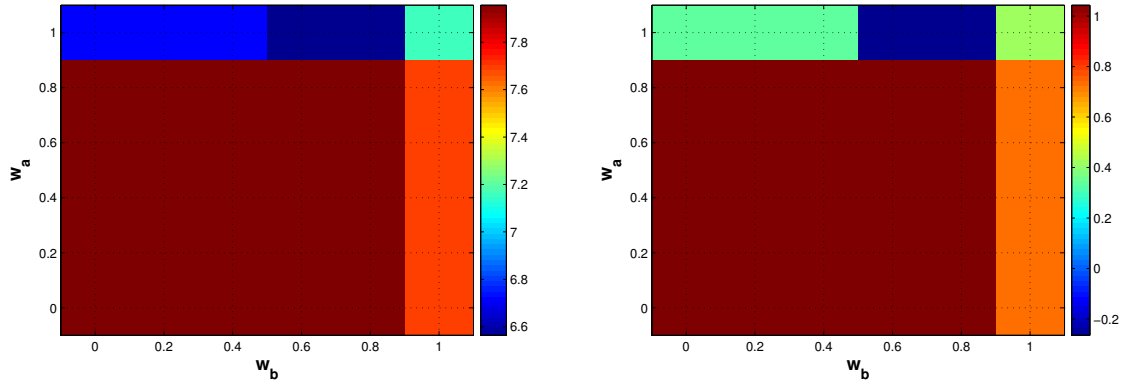


(a) VA(lead Vr) (b) AA(lead Vr)

Figure 5.4: Signal separation SNR in terms of the weights ($w_a$,$w_b$) for the lead Vr. There are 5 levels of SNR and the maximum is placed in (0,0). For the study we have used Weighted-OMP and 50 coefficients.

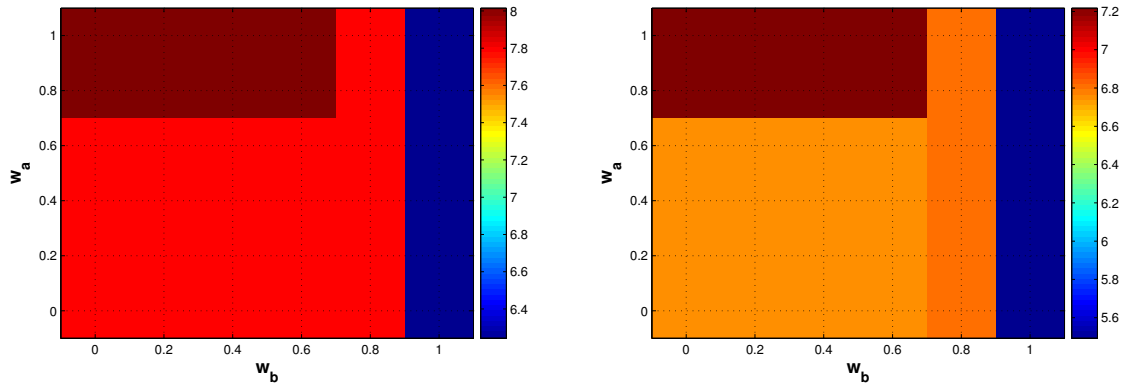


(a) VA(lead V1)

(b) AA(lead V1)

Figure 5.5: Signal separation SNR in terms of the weights ($w_a$,$w_b$) for the lead V1. There are 4 levels of SNR and the maximum is placed in (1,0). Although the SNR is higher in (1,0) than in (0,0), we prefer having the ($w_a$,$w_b$)=(0,0) approximation because we avoid having any artefacts. For the study we have used Weighted-OMP and 50 coefficients.

In conclusion, the most appropriate weights for our purpose are: ($w_a$,$w_b$)=(0,0).

## 5.4 Experiments

The results using Weighted-OMP jointly with the *a priori* knowledge from the ECG signals are presented in this section. For all the experiments, we have taken the best dictionary we have found: GG functions for VA dictionary and Gabor functions for AA dictionary (see Section 3.6).

First of all, we have started separating the simulated ECG signals, to obtain the signal separation SNR that allows to compare with the previous results. To evaluate different amplitudes of the AA signal, we have introduced a new parameter in Eq. 3.3:

$$\hat{f}_{ECG} = \hat{f}_{VA} + \alpha \cdot \hat{f}_{AA} \tag{5.3}$$

where $\alpha$ tunes the AA amplitude ($\alpha$ = 0.5, 1, 1.5).

Figures 5.6, 5.7 and 5.8 show the results for the three values of $\alpha$. As we can see in Table 5.1, the best results approximating the VA signal are for $\alpha$ = 0.5, because the VA energy is higher than the AA one. However, the best ones approximating the AA signal are for $\alpha$ = 1.5, owing to the higher AA amplitude.

Generally, we can affirm that:

- VA approximations are successful because we have eliminated all the artefacts, in charge of representing some parts from the AA signal. Moreover, the Q and R peaks have been improved, although there are still some low errors. With regard to T-waves, we have the best approximation that we can achieve with the dictionary designed. Nevertheless, it is not exact, but this is a task really difficult, due to the different shapes depending on the lead and patient.

- AA approximations suffer the consequences of the poor T-wave approximations. The fact that some SNR are negative is because AA approximations contain errors, which represent the residues from the T-wave approximations, and the energy of AA signal is lower than the error energy.

| Lead Vr | VA+AA | VA+0.5·AA | VA+1.5·AA |
|---|---|---|---|
| VA SNR(dB) | 10.88 | 11.06 | **11.08** |
| AA SNR(dB) | -1.05 | -6.94 | **2.61** |
| Lead V1 | VA+AA | VA+0.5·AA | VA+1.5·AA |
| VA SNR(dB) | 8.69 | **11.13** | 2.41 |
| AA SNR(dB) | **6.81** | 3.61 | 4.28 |
| Lead V4 | VA+AA | VA+0.5·AA | VA+1.5·AA |
| VA SNR(dB) | 11.94 | **12.33** | 11.66 |
| AA SNR(dB) | -0.8 | -6.53 | **2.4** |

Table 5.1: Signal separation SNR for $\alpha = 0.5$, 1, 1.5 and for the leads Vr, V1 and V4. We have used Weighted-OMP ($(w_a,w_b)=(0,0)$) and 75 coefficients. In **bold** the best VA and AA SNR for each lead

If we compare these results with the ones obtained without using the *a priori* knowledge, the VA approximations have become slightly better, about 1dB in terms of SNR, owing to the fact that now, the artefacts have disappeared. However, AA approximations have remained approximately equal (see Table 5.2).

| lead V1 | GG ∪ Gabor (OMP) | GG ∪ Gabor (Weighted-OMP) |
|---|---|---|
| VA SNR(dB) | 7.15 | 7.967 |
| AA SNR(dB) | 0.41 | 1.06 |

Table 5.2: Comparison between the signal separation SNR of the best dictionary found (see Section 3.6) + OMP and the best dictionary found + Weighted-OMP (using the *a priori* knowledge, $(w_a,w_b)=(0,0)$). We have used 30 coefficients (2 QRST complexes in the signals and $\alpha = 1$) for both cases.

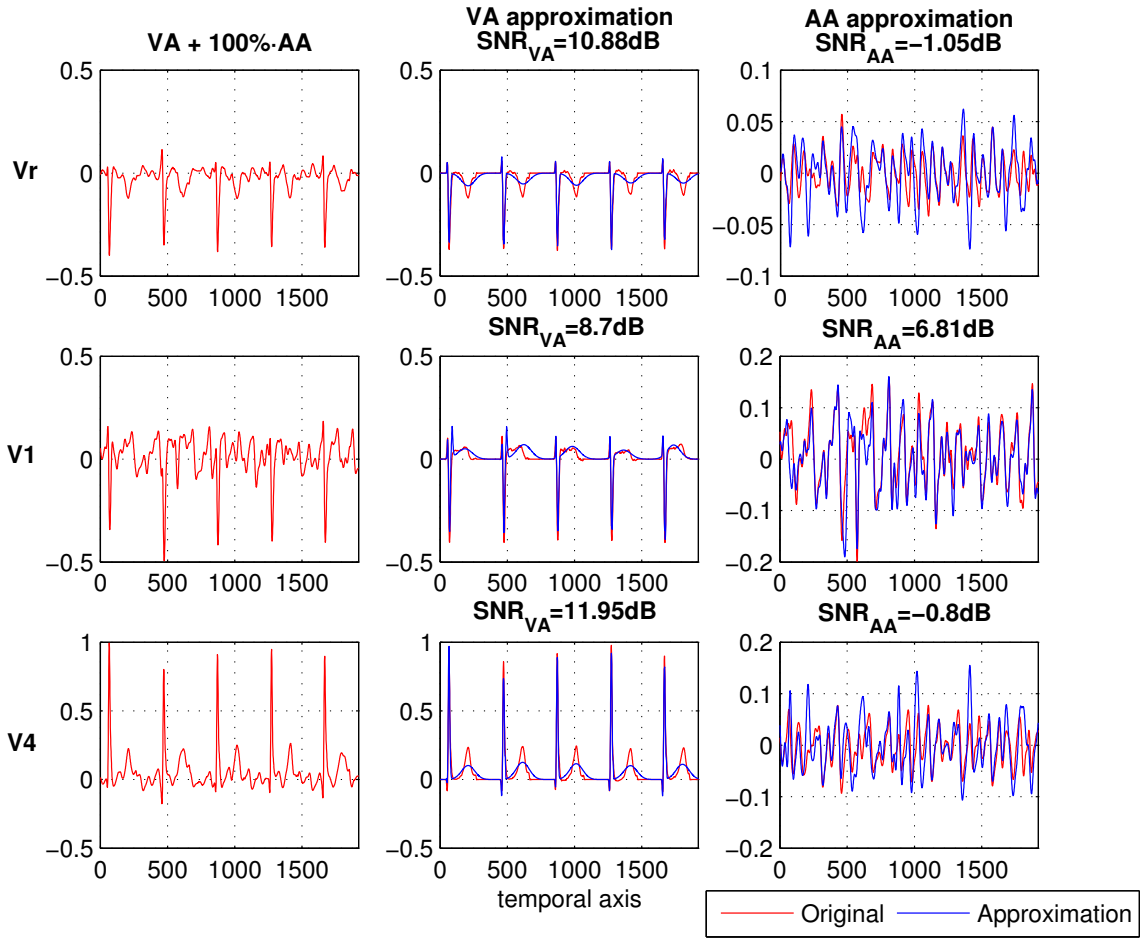


Figure 5.6: Simulated ECG signal ($\alpha$=1) separation using the *a priori* knowledge and Weighted-OMP (50 coefficients, $(w_a,w_b)$=(0,0)). The results are for the leads: Vr, V1 and V4. Left: simulated ECG signal. Middle: VA approximation (with its SNR). Right: AA approximation (with its SNR). In all the columns, the x-axis units are *samples* and y-axis ones are mV

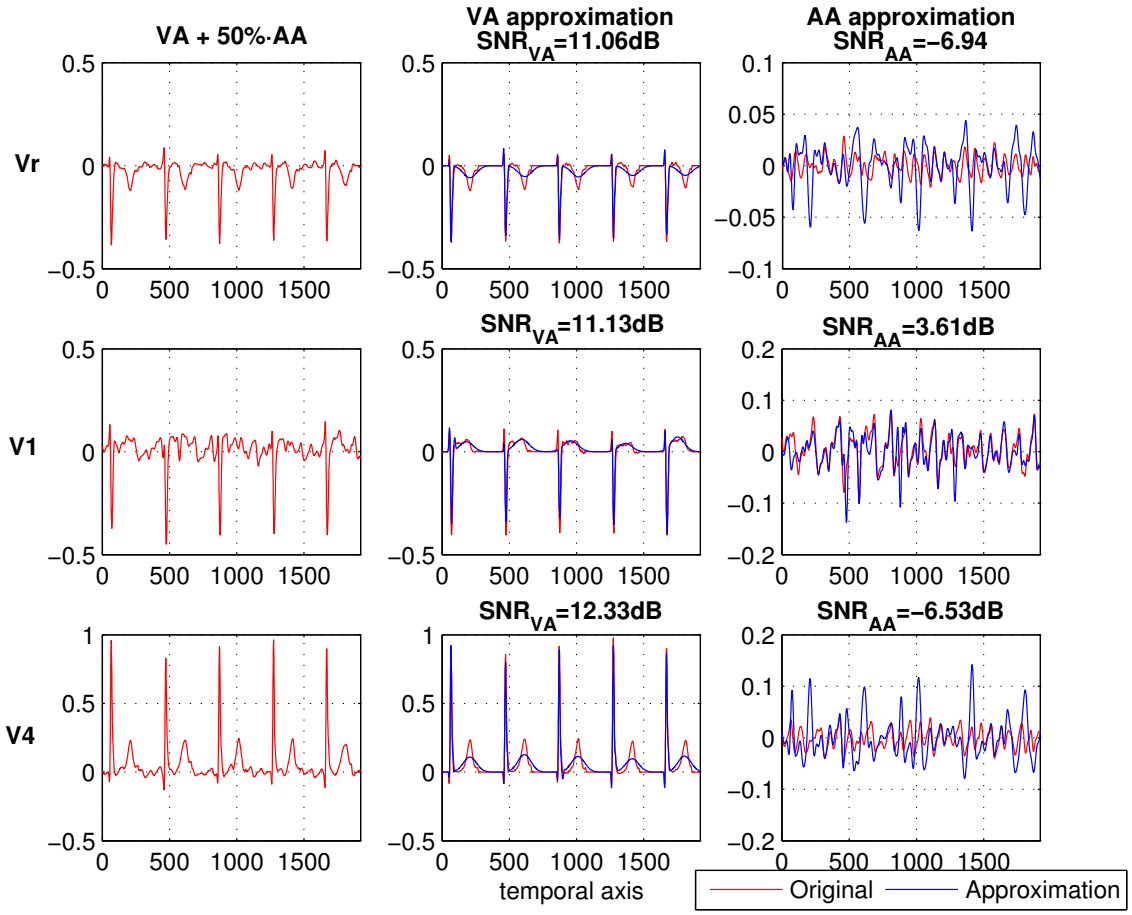


Figure 5.7: Simulated ECG signal ($\alpha$=0.5) separation using the *a priori* knowledge and Weighted-OMP (50 coefficients, $(w_a,w_b)$=(0,0)). The results are for the leads: Vr, V1 and V4. Left: simulated ECG signal. Middle: VA approximation (with its SNR). Right: AA approximation (with its SNR). In all the columns, the x-axis units are *samples* and y-axis ones are mV

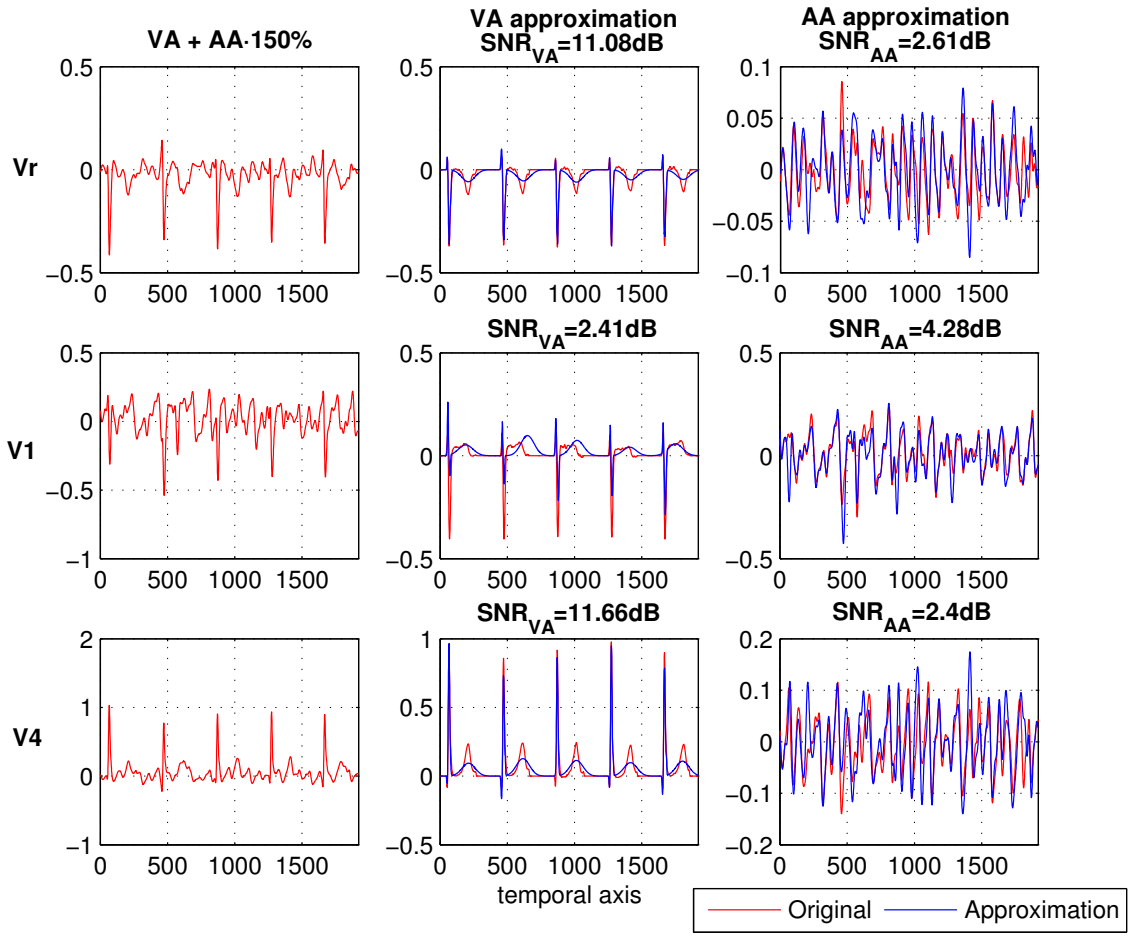


Figure 5.8: Simulated ECG signal ($\alpha$=1.5) separation using the *a priori* knowledge and Weighted-OMP (50 coefficients, $(w_a,w_b)$=(0,0)). The results are for the leads: Vr, V1 and V4. Left: simulated ECG signal. Middle: VA approximation (with its SNR). Right: AA approximation (with its SNR). In all the columns, the x-axis units are *samples* and y-axis ones are mV

To give an example of a long ECG signal, we have studied 10 QRST complexes from the lead V1 ($\alpha = 1$, Weighted-OMP with $((w_a,w_b)=(0,0))$ and 150 coefficients). The results of the VA and AA separation are given in Figures 5.9, 5.10 and 5.11.

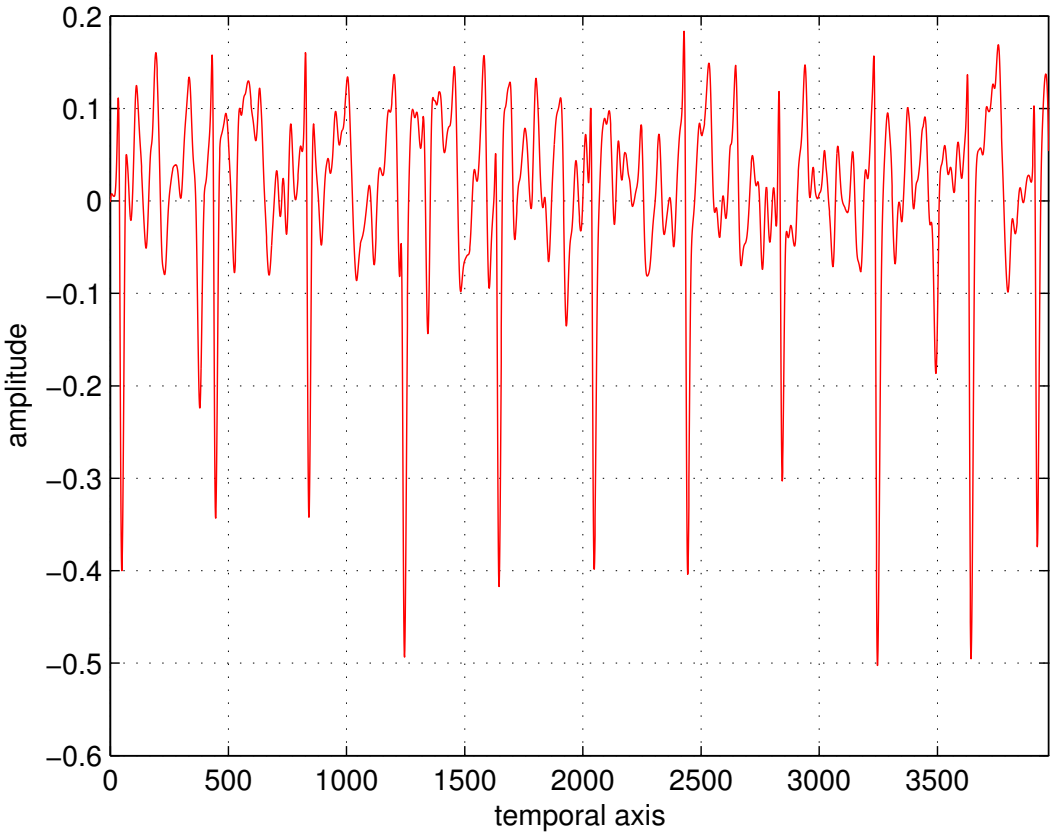


Figure 5.9: Simulated ECG lead V1 with 10 QRST complexes. The x-axis units is *samples* and y-axis ones is mV

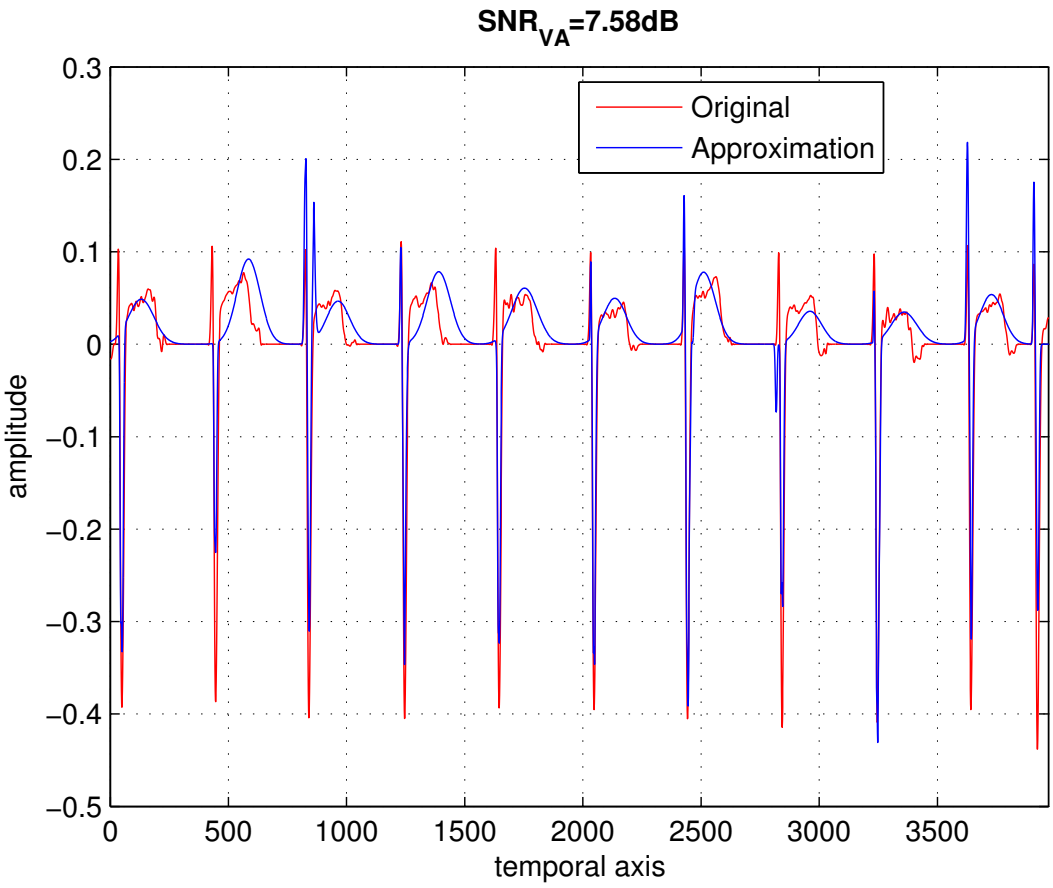


Figure 5.10: VA approximation after the signal separation of the lead V1, with 10 QRST complexes. We have used Weighted-OMP (150 coefficients, $(w_a,w_b)=(0,0)$). The x-axis units is *samples* and y-axis ones is mV

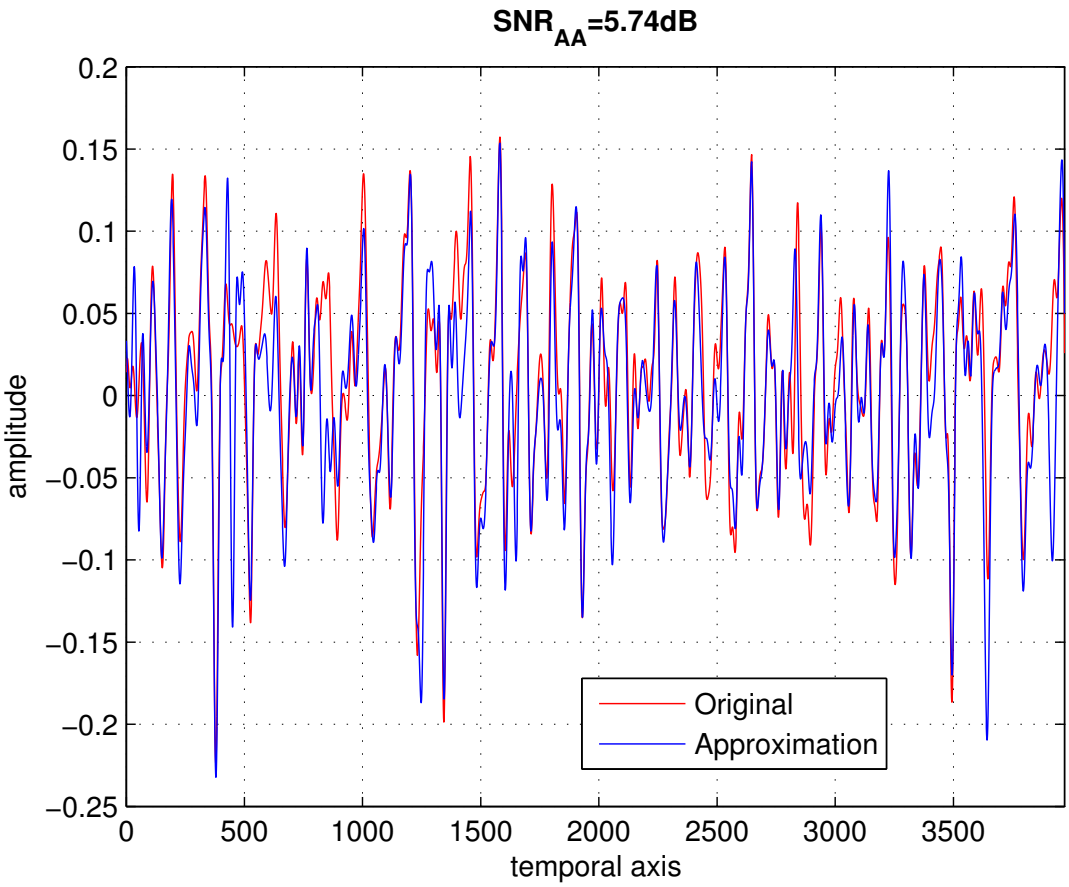


Figure 5.11: AA approximation after the signal separation of the lead V1, with 10 QRST complexes. We have used Weighted-OMP (150 coefficients, $(w_a,w_b)=(0,0)$). The x-axis units is *samples* and y-axis ones is mV

Furthermore, we have tested the system over real ECG signals. In order to do this, we have used the same signals from the three patients in AF as in the previous chapter. Figures 5.12, 5.13 and 5.14 reflect that we have achieved the elimination of the artefacts placed in the last VA approximations.

As occurred in Chapter 4, we can only give some hints about the quality of the results, because we cannot give a signal separation SNR value by comparing with the original signals:

- VA approximation: As we have already mentioned, we have eliminated the artefacts that were in the last VA approximations. However, the T-waves approximations continue being the main problem and, also, the QRS approximations have some errors (see Figures 5.12, 5.13 and 5.14).

- AA approximation: We have done the same study as in the previous chapter to check if the frequencies in our AA approximations are inside the theoretical interval: 3Hz - 10Hz [31]. For this purpose, we have calculated the Power Spectrum Density (PSD), in the same way as in Chapter 4, and we have looked for the maximum peaks. The results are still really encouraging. As we can observe in Table 5.3, most of the frequencies found belong to the interval mentioned.

| Patient 0001 | Freq(Hz) | Patient 0002 | Freq(Hz) | Patient 0003 | Freq(Hz) |
|---|---|---|---|---|---|
| VR | 2.93 | VR | **3.906** | VR | 2.148 |
| VL | 2.73 | VL | **4.102** | VL | **3.32** |
| V1 | **7.422** | V1 | **4.102** | V1 | 2.539 |
| V2 | **7.227** | V2 | 2.93 | V2 | **5.078** |
| V3 | **7.422** | V3 | **4.102** | V3 | 5**.078** |
| V4 | **3.125** | V4 | **3.906** | V4 | **3.32** |
| V5 | **3.125** | V5 | **3.711** | V5 | **3.125** |
| V6 | **7.031** | V6 | **3.516** | V6 | **3.125** |

Table 5.3: PSD maximums of the AA approximations, using *a priori* knowledge, for the three patients analyzed. In **bold** we find the correct frequencies (19 correct values/24 values), it means, the ones belonging to the theoretical interval: 3-10 Hz

- Low residues: The mean SNR values for the approximations (not signal separation SNR values) are: 25.23dB, 22.27dB and 21.17dB, for the $1^{st}$, $2^{nd}$ and $3^{rd}$ patients, respectively. These values are very close to the ones found without using the *a priori* knowledge (26.2dB, 25.6dB and 23.1dB, for the $1^{st}$, $2^{nd}$ and $3^{rd}$ patients). So, it means that all the energy of the original signal is placed in the VA and AA approximations.

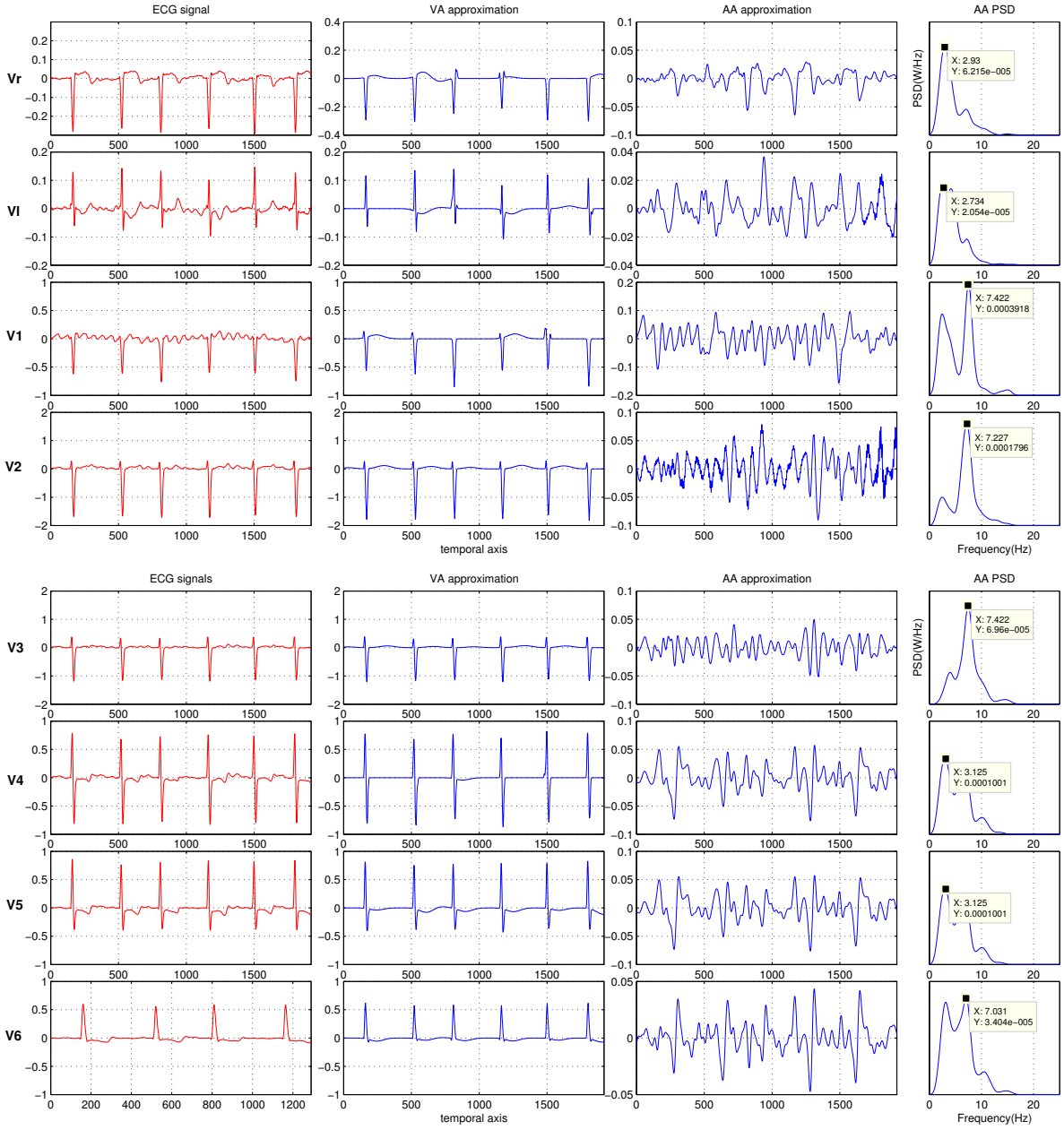


Figure 5.12: Signal separation for the real ECG of the patient 0001 using the *a priori* knowledge (Weighted-OMP, $(w_a,w_b)$=(0,0), 75 coefficients). Left: the separated leads: Vr, Vl, V1, V2, V3, V4, V5 and V6. Middle: VA and AA approximations. Right: AA PSD. In the first three columns, the x-axis units are *samples* and y-axis ones are mV. In this case, we find 6 AF approximations inside the theoretical interval of frequencies of 8 approximation

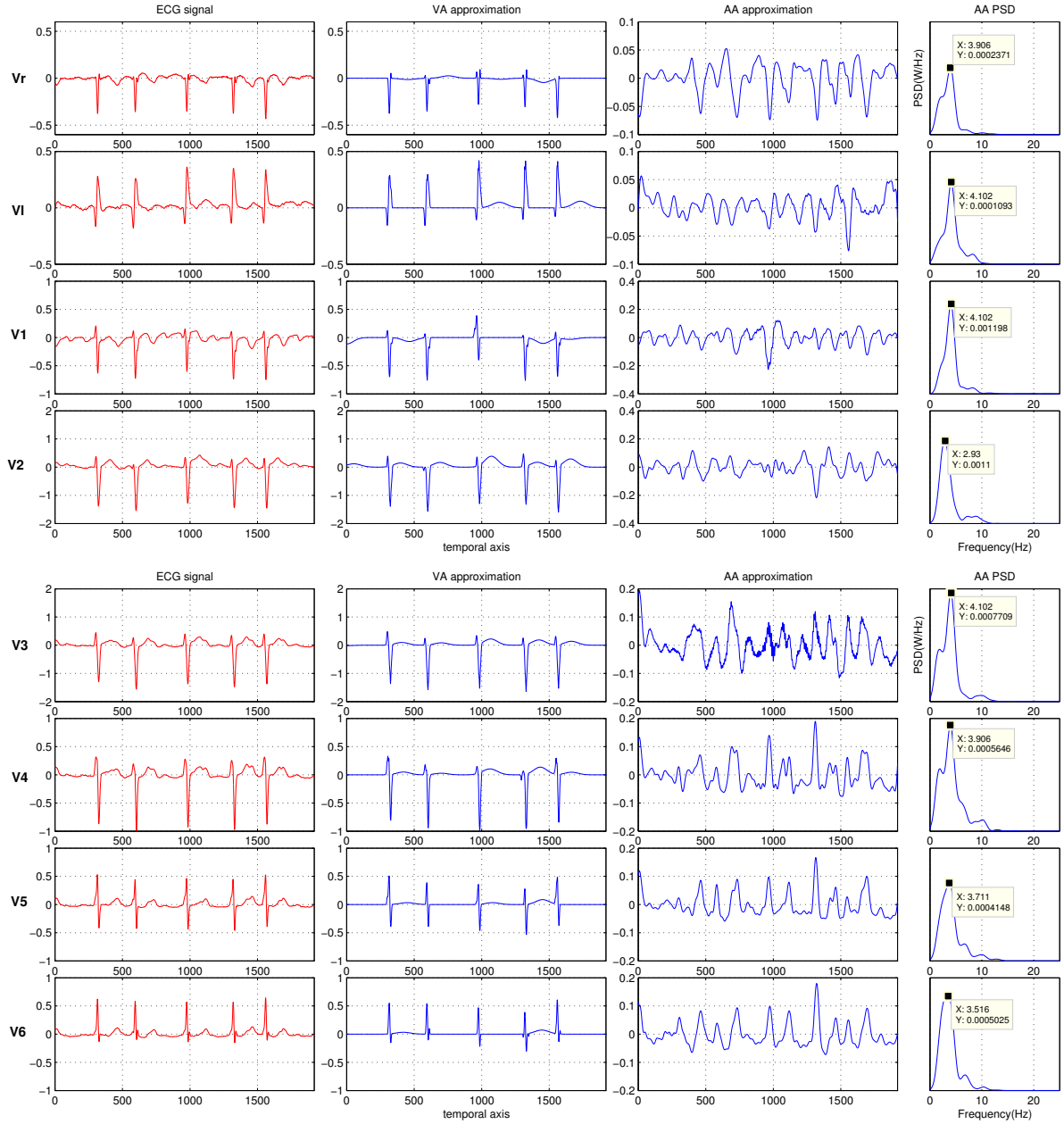


Figure 5.13: Signal separation for the real ECG of the patient 0002 using the *a priori* knowledge (Weighted-OMP, $(w_a,w_b)$=(0,0), 75 coefficients). Left: the separated leads: Vr, Vl, V1, V2, V3, V4, V5 and V6. Middle: VA and AA approximations. Right: AA PSD. In the first three columns, the x-axis units are *samples* and y-axis ones are mV. In this case, we find 7 AF approximations inside the theoretical interval of frequencies of 8 approximations

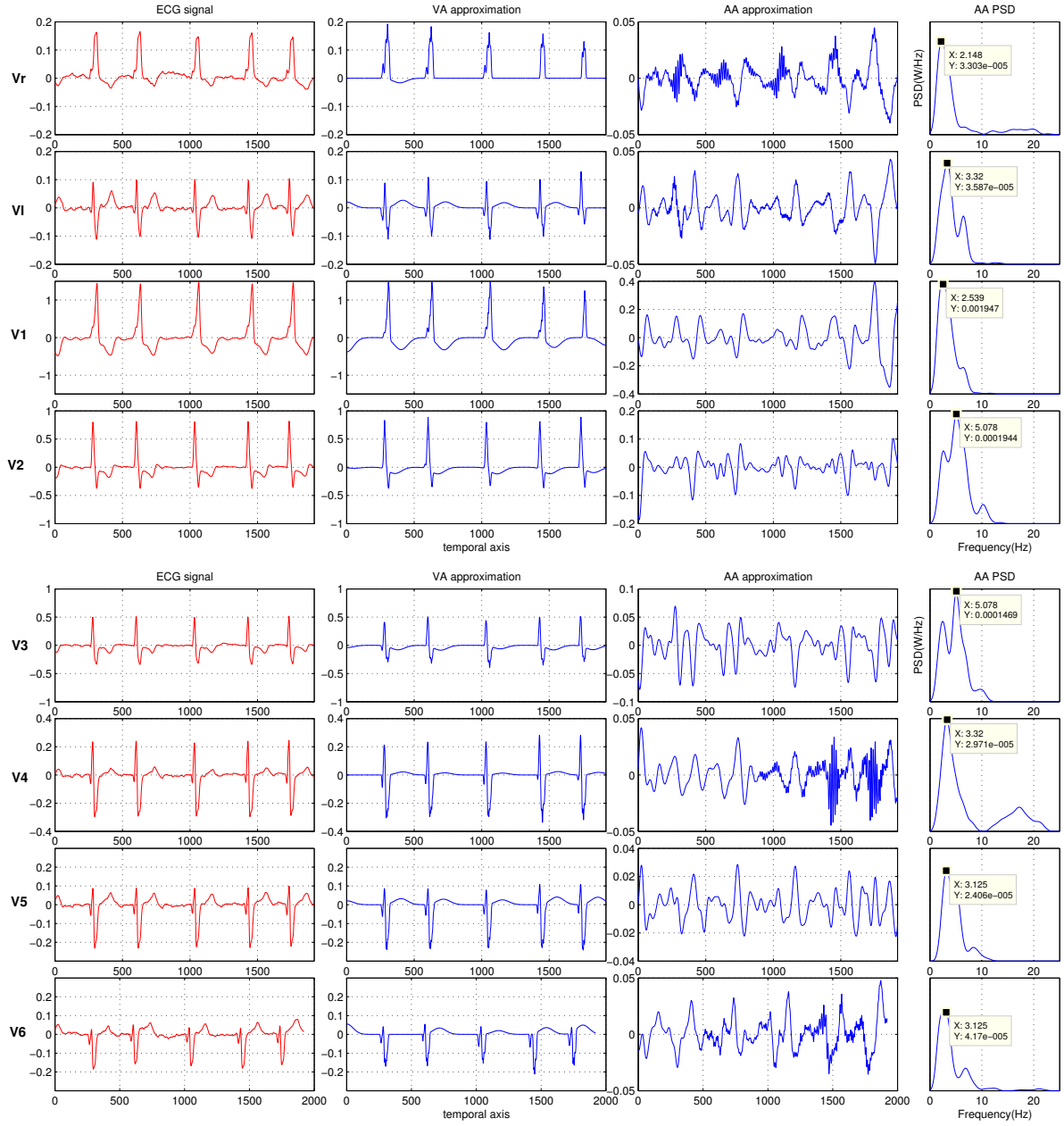


Figure 5.14: Signal separation for the real ECG of the patient 0003 using the *a priori* knowledge (Weighted-OMP, $(w_a,w_b)$=(0,0), 75 coefficients). Left: the separated leads: Vr, Vl, V1, V2, V3, V4, V5 and V6. Middle: VA and AA approximations. Right: AA PSD. In the first three columns, the x-axis units are *samples* and y-axis ones are mV. In this case, we find 6 AF approximations inside the theoretical interval of frequencies of 8 approximations

## 5.5 Conclusions

The use of *a priori* knowledge when recovering the sparse decomposition for signal separation is studied in this chapter.

Although we eliminate the artefacts between QRST complexes, there are still errors in the QRS complex and T-wave approximations, due to the fact that its shape changes depending on the lead and patient. This fact can be observed simultaneously in the simulated ECG approximations and in the real ECG approximations.

The conclusions of the simulated ECG signals results (see Figures 5.6, 5.7 and 5.8) are the following:

- The AA approximations are always better in the lead V1, between 2-10dB, depending on the studied case (changing $\alpha$),
- The best AA approximations are for the case: $\alpha = 1.5$. Furthermore, this fact proves that our AA dictionary, composed of Gabor functions, is strongly good approximating the atrial activity signal,
- The fact that some AA SNR are negative, in cases $\alpha = 0.5, 1$, is due to the VA approximations errors, which have more energy than the AA estimations.

On the other hand, we can see that the number of frequency peaks inside the theoretical interval, observed in the AA power spectrum density (PSD) of the real ECG signals approximations, remains equal, in comparison with the results without using *a priori* knowledge.

Another conclusion is that the number of coefficients is a value really critic because if it is too high, the approximation starts to have high frequencies destined to represent the residue. Figure 5.15 shows how the AA approximation, for the lead Vr of the patient 0003, improves as the number of coefficients decrease from 75, used in Figure 5.14.

Lastly, we want to compare our best source separation results (method 1), using *a priori* knowledge and our best dictionary (see Section 3.6), with the ones obtained by the Beat-to-Beat QRST cancellation method (method 2). This approach does the QRST cancellation in two steps. The first is based on a dominant T-wave approach to cancel the T-wave. The second is based in sinusoids estimations to cancel the QRS complex.

In order to do the comparison, we check both methods with the simulated ECG signals, as in Figures 5.6, 5.7 and 5.8. The results by Beat-to-Beat QRST cancellation method are given in Figures 5.16, 5.17 and 5.18.

The Tables 5.5, 5.4 and 5.6 show that our method achieve 1 better case among 9 cases than the Beat-to-Beat QRST cancellation method. However, there is not a big difference between both results (except for $\alpha$=0.5). We have calculated the average of the difference between the SNR of both methods, for VA and AA signals, and it has given: 6.5, 2.2 and 1.6dB, for the cases $\alpha = 0.5, 1, 1.5$, respectively.

| method 1 | VA SNR (dB) | AA SNR(dB) | method 2 | VA SNR (dB) | AA SNR(dB) |
|---|---|---|---|---|---|
| Vr | 11.06 | -6.94 | Vr | 16.7 | -1.37 |
| V1 | 11.13 | 3.61 | V1 | 11.24 | 3.61 |
| V4 | 12.33 | -6.53 | V4 | 19.58 | 0.6 |

Table 5.4: Comparison between our method and Beat-to-Beat QRST cancellation method. We study the case of $\alpha = 0.5$, in simulated ECG signals, and the results are for the leads: Vr, V1 and V4.

| method 1 | VA SNR (dB) | AA SNR(dB) | method 2 | VA SNR (dB) | AA SNR(dB) |
|---|---|---|---|---|---|
| Vr | 10.88 | -1.05 | Vr | 13.8 | 1.76 |
| V1 | 8.7 | 6.81 | V1 | 6.34 | 4.72 |
| V4 | 11.95 | -0.8 | V4 | 16 | 3.12 |

Table 5.5: Comparison between our method and Beat-to-Beat QRST cancellation method. We study the case of $\alpha = 1$, in simulated ECG signals, and the results are for the leads: Vr, V1 and V4.

| method 1 | VA SNR (dB) | AA SNR(dB) | method 2 | VA SNR (dB) | AA SNR(dB) |
|---|---|---|---|---|---|
| Vr | 11.08 | 2.61 | Vr | 12.2 | 3.59 |
| V1 | 2.41 | 4.28 | V1 | 2.96 | 4.86 |
| V4 | 11.66 | 2.4 | V4 | 13.27 | 3.83 |

Table 5.6: Comparison between our method and Beat-to-Beat QRST cancellation method. We study the case of $\alpha = 1.5$, in simulated ECG signals, and the results are for the leads: Vr, V1 and V4.

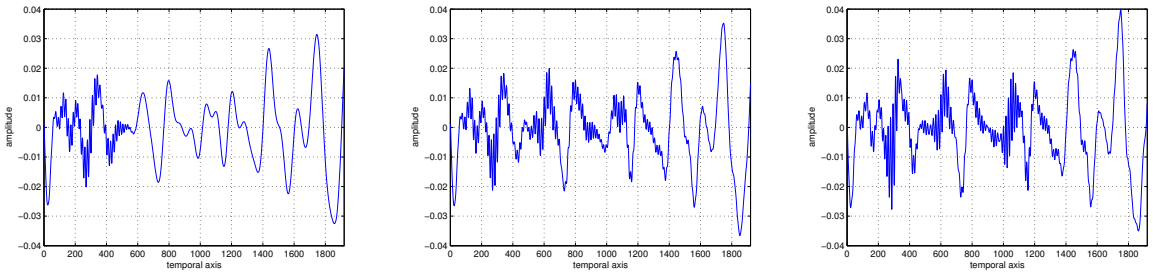


(a) 40 coefficients (b) 50 coefficients (c) 60 coefficients

Figure 5.15: AA approximation, afterwards the signal separation, for the lead Vr of the patient 0003 using the *a priori* knowledge (Weighted-OMP, $(w_a,w_b)=(0,0)$) and changing the number of coefficients. Left: 40 coefficients. Middle: 50 coefficients. Right: 60 coefficients. The x-axis units are *samples* and y-axis ones are mV

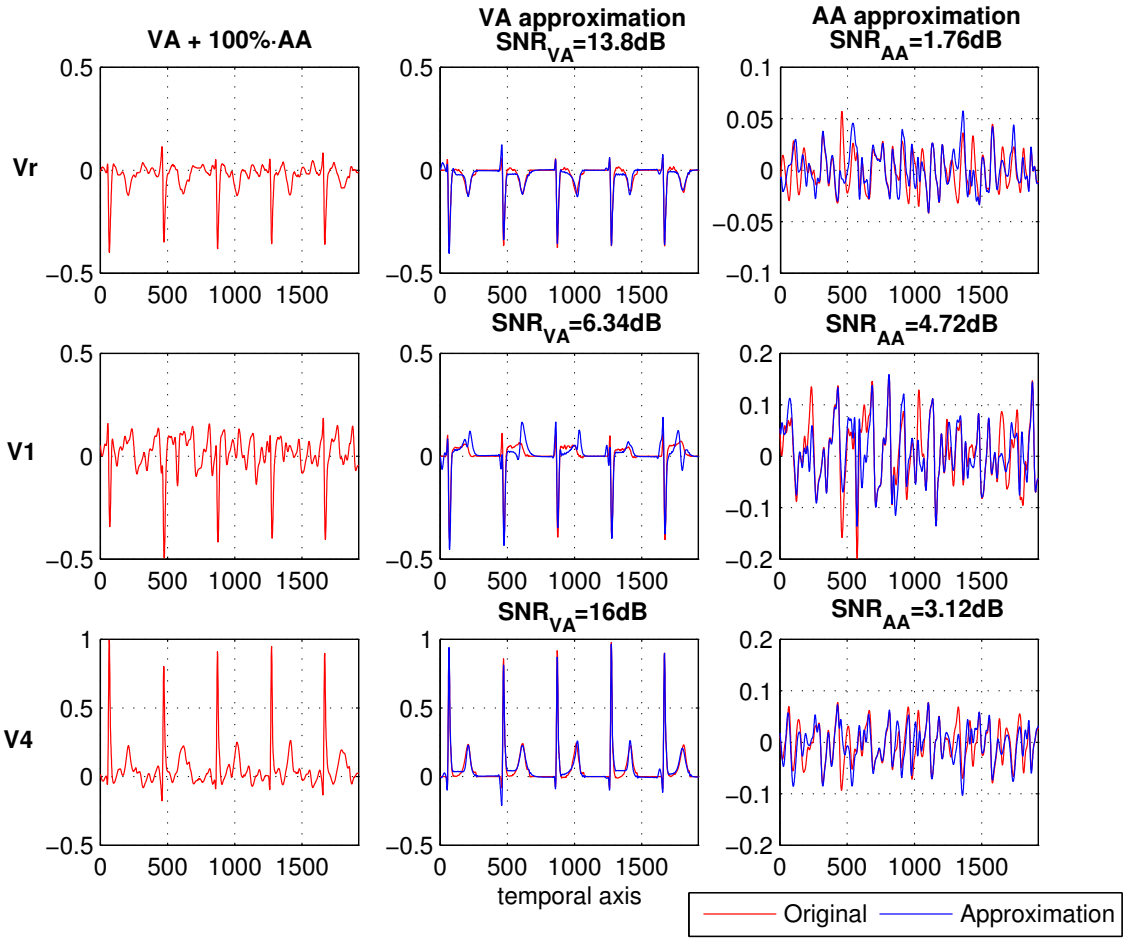


Figure 5.16: Simulated ECG signal ($\alpha$=1) separation using Beat-to-Beat QRST cancellation method. The results are for the leads: Vr, V1 and V4. Left: simulated ECG signal. Middle: VA approximation (with its SNR). Right: AA approximation (with its SNR). In all the columns, the x-axis units are *samples* and y-axis ones are mV

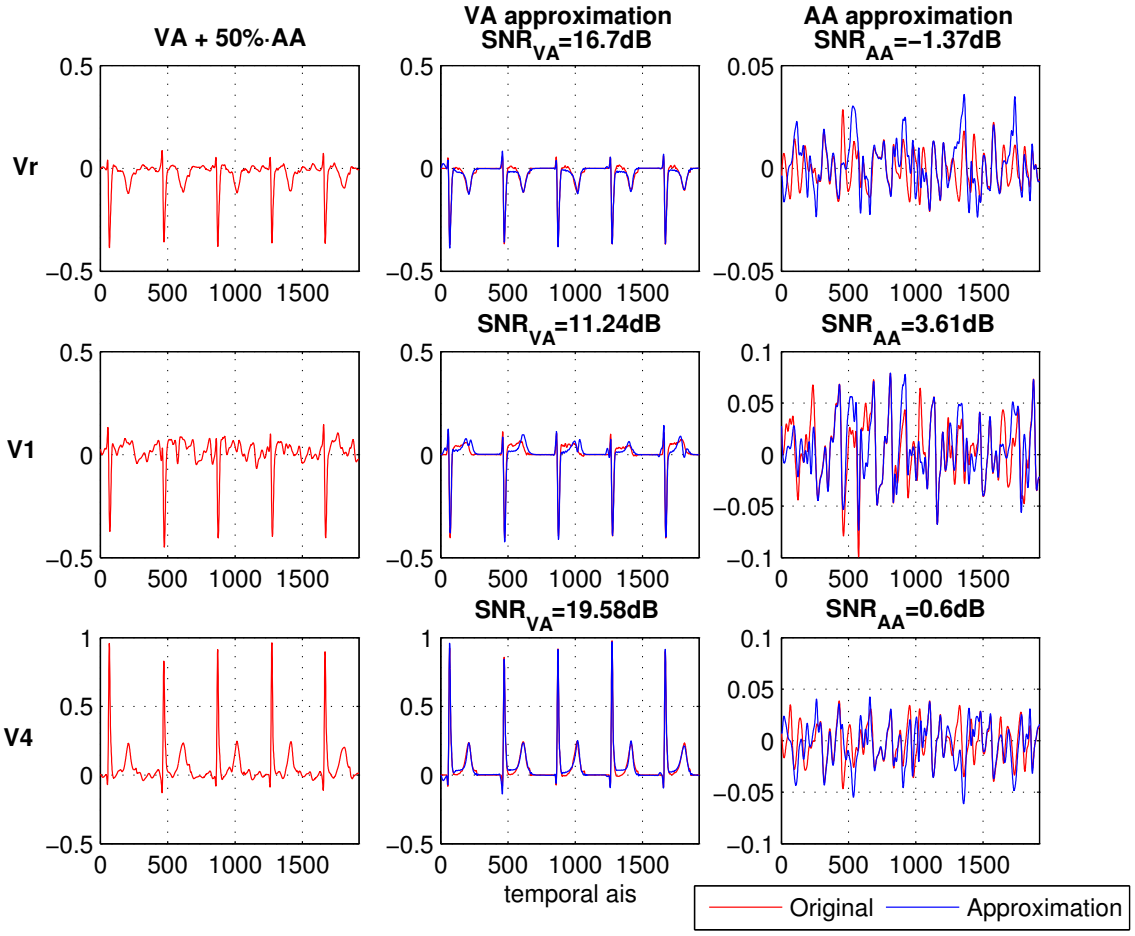


Figure 5.17: Simulated ECG signal ($\alpha$=0.5) separation using Beat-to-Beat QRST cancellation method. The results are for the leads: Vr, V1 and V4. Left: simulated ECG signal. Middle: VA approximation (with its SNR). Right: AA approximation (with its SNR). In all the columns, the x-axis units are *samples* and y-axis ones are mV

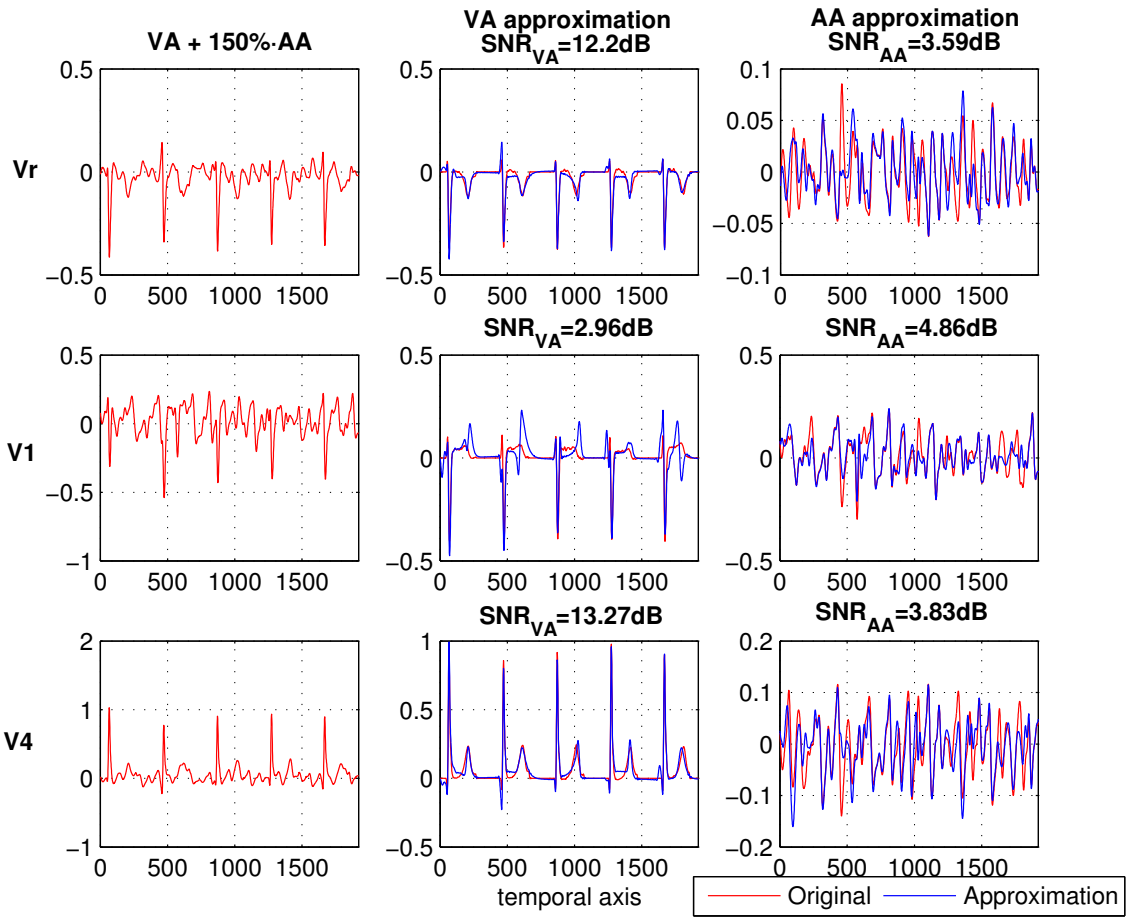


Figure 5.18: Simulated ECG signal ($\alpha$=1.5) separation using Beat-to-Beat QRST cancellation method. The results are for the leads: Vr, V1 and V4. Left: simulated ECG signal. Middle: VA approximation (with its SNR). Right: AA approximation (with its SNR). In all the columns, the x-axis units are *samples* and y-axis ones are mV

Lastly, we have compared our method with other standard methods: the ABS method (method 3), Spatiotemporal QRST cancellation method [2] (method 4) and Spatiotemporal QRST cancellation method using separate QRS and T-waves templates (method 5). In order to do that, we have also used simulated ECG signals.

The comparison is shown in Table 5.7, but only for $\alpha$=0.5. In the other two cases, $\alpha$=1 and 1.5, all the methods mentioned above are unsuccessful. This is due to the fact that, they need large signals to perform their approaches when atrial activity has high amplitudes.

Therefore, the comparison done is not the appropriate one, because it shows only the case where our approach is worse and it should be done for longer and different simulated signals.

| method 1 | VA SNR (dB) | AA SNR(dB) |
|---|---|---|
| Vr | 11.06 | -6.94 |
| V1 | 11.13 | 3.61 |
| V4 | 12.33 | -6.53 |

| method 3 | VA SNR (dB) | AA SNR(dB) |
|---|---|---|
| Vr | 22.2 | 4.4 |
| V1 | 18 | 10.4 |
| V4 | 22.2 | 3.2 |

| method 4 | VA SNR (dB) | AA SNR(dB) |
|---|---|---|
| Vr | 19.4 | 1.24 |
| V1 | 13.25 | 5.61 |
| V4 | 20 | 1.07 |

| method 5 | VA SNR (dB) | AA SNR(dB) |
|---|---|---|
| Vr | 23.14 | 5 |
| V1 | 18.3 | 10.6 |
| V4 | 23 | 4 |

Table 5.7: Comparison of our method with ABS method (method 3), Spatiotemporal QRST cancellation method (method 4) and Spatiotemporal QRST cancellation method using separate QRS and T-waves templates method (method 5). We study the case of $\alpha = 0.5$, in simulated ECG signals, and the results are for the leads: Vr, V1 and V4.

# Chapter 6

# Conclusions and Future Work

## 6.1 Conclusions

The proper analysis and characterization of atrial fibrillation from electrocardiogram recordings requires the extraction of the signal components associated with ventricular activity, that is, the QRST complex. In this work we propose a totally new approach, based on the use of sparse decompositions over redundant dictionaries, for the ventricular and atrial activity separation. The design and implementation of our approach has offered us the opportunity to view the complexity of the VA and AA separation.

Our multi-component dictionary is built by the union of two sub-dictionaries. It has been concluded that if one wants a successful signal separation, the basis functions from one of the dictionaries must be as uncorrelated as much as possible with the functions from the other one. As we have seen in Section 3.4, we cannot take the maximum *coherence parameter* $\mu$ of the dictionary, as a measure of maximum likeness because it is highly pessimistic and it only allows a value of $\mu$ too small. Therefore, we have established our own criterion to know which is the appropriate maximum for a good behavior of the analysis algorithm. Then, we have used it to exclude all the basis functions from the AA dictionary, which have a higher correlation than the designed value, with the functions from the VA dictionary.

The chosen dictionary to achieve the VA and AA signal separation is made up of Generalized Gaussian functions and Gabor functions, respectively. It is huge and with lots of redundant functions (19550 basis functions).

Once designed the MCD, two different analysis algorithms have been tested: Orthogonal Matching Pursuit (OMP) and Basis Pursuit Denoising (BPDN). Either by the features of the

ECG signals or by the dictionary designed, the best results have been obtained with OMP. The comparison between them has shown a wrong behavior in the BPDN approximations. Hence, we have dismissed the BPDN principle as a tool to separate the VA and AA signals.

The simulated and real ECG signals separations have had encouraging results. However, the *a priori* knowledge from the signals (positions of the Q, R, S, T waves and the intervals where is only AA) can still be used to aid OMP to avoid taking "wrong" atoms. In order to do this, a new algorithm has been used, named Weighted-OMP, which puts weigths for each basis function in the MCD. These weights represent the *a priori* information about the ECG signals.

In conclusion, the main limitation of our project is the approximation of the QRST complexes, owing to its different shapes depending on the lead and patient. This hinders to achieve a good AA approximation, since there are several artefacts to represent the error generated by the QRST approximations. Nonetheless, the obtained solution shows really interesting results, which could be improved as follows.

## 6.2 Possible Extensions and Future Work

From this project, much further work can be done in the future:

- the refinement of the basis functions to approximate the T-waves, although it seems really difficult to find some ones able to approximate all sorts of T shapes,
- to give the system some adaptability to the lead in the ECG and to the iteration of the analysis algorithm, changing the weighting factor depending on the iteration,
- to optimize the number of coefficients used in the decomposition, seeing the maximum of SNR in terms of the number of coefficients used,
- to do a learning of the Multi-component dictionary created from a wide set of ECG signals from patients in atrial fibrillation. The consequences will be a reduction of the dictionary size, selecting the appropriate functions,
- to work on all the leads together, considering the ECG as a NxM signal and continuing using Greedy algorithms.

# Bibliography


[1] V. Fuster, L. E. Ryden, R. W. Asinger, D. S. Cannom, H. J. Crijns, R. L. Frye, J. L. Halperin, G. N. Kay, W. W. Klein, S. Levy, R. L. McNamara, E. N. Prystowsky, L. S. Wann, and D. G. Wyse, "ACC/AHA/ESC guidelines for the management of patients with atrial fibrillation: a report of the American College of Cardiology/American Heart Association Task Force on Practice Guidelines and the European Society of Cardiology Committee for Practice Guidelines and Policy Conferences (Committee to Develop Guidelines for the Management of Patients With Atrial Fibrillation)," *J. Amer. Coll. Cardiol*, vol. 38, pp. 1266 i–1266 1xx, 2001.

[2] M. Stridh and L. Sörnmo, "Spatiotemporal QRST cancellation techniques for analysis of atrial fibrillation.," *IEEE Transactions on Biomedical Engineering*, vol. 48, no. 1, pp. 105–111, Jan, 2001.

[3] J. J. Rieta, F. Castells, C. Sánchez, V. Zarzoso, and J. Millet, "Atrial activity extraction for atrial fibrillation analysis using blind source separation.," *IEEE Transactions on Biomedical Engineering*, vol. 51, pp. 1176–1186, July 2004.

[4] F. Castells, J. Igual, V. Zarzoso, J. J. Rieta, and J. Millet, "Exploiting spatiotemporal information for blind atrial activity extraction in atrial arrhythmias.," in *ICA*, pp. 18–25, 2004.

[5] F. Castells, C. Mora, J. Millet, J. J. Rieta, C. Sánchez, and J. M. Sanchis, "Multidimensional ICA for the separation of atrial and ventricular activities from single lead ECGs in paroxysmal atrial fibrillation episodes.," in *ICA*, pp. 1229–1236, 2004.

[6] M. Lemay, J.-M. Vesin, Z. Ihara, and L. Kappenberger, "Suppression of ventricular activity in the surface electrocardiogram of atrial fibrillation.," in *ICA*, pp. 1095–1102, 2004.

[7] B. U. Köhler, C. Henning, and R. Orglmeister, "The Principles of Software QRS Detection.," *IEEE Engineering in medecine and biology*, pp.42-57, 2002.

[8] A. M. Bronstein, M. M. Bronstein, and M. Zibulevsky, "Blind source separation using block-coordinate relative newton method," *Signal Process.*, vol. 84, no. 8, pp. 1447–1459, 2004.

[9] M. Zibulevsky and B. A. Pearlmutter, "Blind source separation by sparse decomposition in a signal dictionary.," *Neural Computation*, vol. 13, no. 4, pp. 863–882, 2001.

[10] P. Bofill and M. Zibulevsky, "Undetermined blind source separation using sparse representations.," in *Eurasip - Signal Processing*, vol. 81(2001), pp. 2353–2362, May, 2001.

[11] R. Gribonval, "Piecewise linear source separation," *In Proc. of Wavelets X, 48th SPIE annual meeting*, vol. 5207, pp. 297–310, San Diego, CA, USA, Nov 2003.

[12] G. Gravier, L. Benaroya, A. Ozerov, R. Gribonval, and F. Bimbot, "Separation de sources á partir d'un seul capteur pour la reconnaissance robuste de la parole," *In Journes d'etude sur la Parole*, February 2004.

[13] R. Gribonval, "Sparse decompositions of stereo signals with matching pursuit and application to blind separation of more than two sources from a stereo mixture.," in *Int. Conf. Acoust. Speech Signal Process. (ICASSP)*, Orlando, Florida, USA, May 2002.

[14] J. L. Starck, M. Elad, and D. L. Donoho, "Image decomposition via the combination of sparse representations and a variational approach," *IEEE Trans. on Image Processing*, September, 2004.

[15] J. J. Rieta, F. Castells, C. Sánchez, and J. Igual, "ICA applied to atrial fibrillation analysis," *International Conference on Independent Component Analysis and Blind Signal Separation (ICA)*, vol. 4, pp. 59–64, Nara, Japan, Apr 2003.

[16] L. Granai and P. Vandergheynst, "Sparse decomposition over multi-component redundant dictionaries," in *Multimedia Signal Processing (MMSP04), Workshop on*, pp. 494–497, IEEE, September 2004.

[17] J. A. Tropp, "Greed is good: algorithmic results for sparse approximation.," *IEEE Transactions on Information Theory*, vol. 50, no. 10, pp. 2231–2242, 2004.

[18] J. A. Tropp, "Just relax: Convex programming methods for subset selection and sparse approximation.," tech. rep., ICES Report 04-04. The University of Texas at Austin, February 2004.

[19] D. L. Donoho and X. Huo, "Uncertainty principles and ideal atomic decomposition.," *IEEE Transactions on Information Theory*, vol. 47, no. 7, pp. 2845–2862, 2001.

[20] S. Mallat, *A wavelet tour of signal processing*. Academic Press, 1998.

[21] S. Mallat and Z. Zhang, "Matching pursuits with time-frequency dictionaries," *IEEE Transactions on Signal Processing*, vol. 41, no. 12, pp. 3397–3415, 1993.

[22] Y. Pati, R. Rezaiifar, and P. Krishnaprasad, "Orthogonal matching pursuit: Recursive function approximation with applications to wavelet decomposition," *Proceedings of the 27 th Annual Asilomar Conference on Signals, Systems, and Computers*, November 1993.

[23] S. S. Chen, D. L. Donoho, and M. A. Saunders, "Atomic decomposition by basis pursuit," *SIAM Journal on Scientific Computing*, vol. 20, no. 1, pp. 33–61, 1998.

[24] D. Donoho and M. Elad, "On the stability of the basis pursuit in the presence of noise," *EURASIP Signal Processing Journal*, April, 2005.

[25] O. Divorra Escoda, L. Granai, and P. Vandergheynst, "On the use of a priori information for sparse signal approximations," Tech. Rep. 23/2004, 1015 Ecublens, November 2004.

[26] N. Virag, V. Jacquemet, C. S. Henriquez, S. Zozor, O. Blanc, J. M. Vesin, E. Pruvot, and L. Kappenberger, "Study of atrial arrhythmias in a computer model based on magnetic resonance images of human atria.," *Chaos*, vol. 12, no. 3, pp. 754–763, 2002.

[27] V. Jacquemet, N. Virag, Z. Ihara, L. Dang, O. Blanc, S. Zozor, J.-M. Vesin, L. Kappenberger, and C. Henriquez, "Study of unipolar electrogram morphology in a computer model of atrial fibrillation.," *J Cardiovasc Electrophysiol*, vol. 14, no. 10(Suppl), pp. S172–9, 2003.

[28] C. S. Henriquez and A. A. Papazoglou, "Using computer models to understand the roles of tissue structure and membrane dynamics in arrhythmogenesis.," *Proc. IEEE*, vol. 84, no. 3, pp. 334–354, 1996.

[29] M. Courtemanche, R. J. Ramirez, and S. Nattel, "Ionic mechanisms underlying human atrial action potential properties: Insights from a mathematical model.," *Am. J. Physiol.*, vol. 275, pp. H301–H321, 1998.

[30] A. van Oosterom and V. Jacquemet, "Genesis of the P wave: atrial signals as generated by the equivalent double layer source model," *Europace*, p. null, 2005. [in press].

[31] V. Jacquemet, M. Lemay, J. M. Vesin, L. Kappenberger, and A. van Oosterom, "Dominant frequency of atrial fibrillation estimated from the surface ECG," Heart Rhythm, 2:302-303, HRS, New Orleans, USA, May 2005.

[32] R. R. Coifman and Y. Meyer, *Remarques sur l'analyze de Fourier à Fenêtre.* Compter Rendus Acad. Sci. Paris (A), 312, pp. 713-718, 1991.

[33] http://www-stat.stanford.edu/ atomizer/.